

# Bifunctional Naphthoquinone Aromatic Amide-Oxime Derivatives Exert Combined Immunotherapeutic and Antitumor Effects through Simultaneous Targeting of Indoleamine-2,3-dioxygenase and Signal Transducer and Activator of Transcription 3

Rizhen Huang,<sup>||</sup> Xiaoteng Jing,<sup>||</sup> Xiaochao Huang, Yingming Pan, Yilin Fang, Guibin Liang, Zhixin Liao, Hengshan Wang,\* Zhenfeng Chen,\* and Ye Zhang\*

Cite This: *J. Med. Chem.* 2020, 63, 1544–1563

Read Online

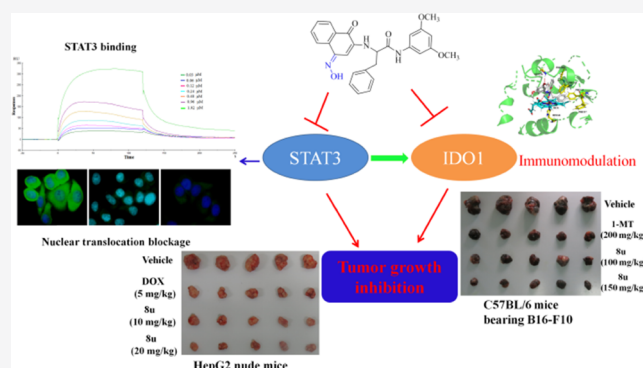
ACCESS |

Metrics & More

Article Recommendations

Supporting Information

**ABSTRACT:** Indoleamine-2,3-dioxygenase 1 (IDO1) and signal transducer and activator of transcription 3 (STAT3) are important targets in the tumor microenvironment for cancer therapy. In the present study, a set of naphthoquinone aromatic amide-oxime derivatives were designed, which stimulated the immune response via IDO1 inhibition and simultaneously displayed powerful antitumor activity against three selected cancer cell lines through suppressing STAT3 signaling. The representative compound **8u** bound effectively to IDO1, with greater inhibitory activity relative to the commercial IDO1 inhibitor 4-amino-*N*-(3-chloro-4-fluorophenyl)-*N'*-hydroxy-1,2,5-oxadiazole-3-carboximidamide (IDOSL) in addition to the efficient suppression of nuclear translocation of STAT3. Consistently, *in vivo* assays demonstrated a higher antiproliferative activity of compound **8u** in both wild-type B16-F10 isograft tumors and an athymic HepG2 xenograft model relative to 1-methyl-*L*-tryptophan (1-MT) and doxorubicin (DOX). This bifunctional compound with dual immunotherapeutic and anticancer efficacy may represent a new generation of highly efficacious drug candidates for cancer therapy.



## INTRODUCTION

Cancer immunotherapy approaches have been a significant focus of interest based on the hypothesis that progression of spontaneous malignancies can be suppressed by the immune system. Immune checkpoint therapy has been documented as a breakthrough in cancer immunotherapy, with remarkable therapeutic effects of anti-PDL1 (programmed death ligand 1), anti-PD1 (programmed cell death protein 1), and anti-CTLA4 (cytotoxic T-lymphocyte-associated protein 4) agents reported in multiple clinical trials as an alternative to conventional chemotherapy following the FDA approval of ipilimumab, pembrolizumab, and nivolumab.<sup>1–3</sup> While immune checkpoint inhibitors have shown clinical success as cancer immunotherapy options, only a fraction of patients with advanced cancers respond effectively to these agents, highlighting the continued requirement for improved therapeutic strategies.<sup>4,5</sup> Recent accumulating evidence suggests that strategies combining immunotherapy and chemotherapy have enormous potential to enhance clinical benefits due to simultaneous targeting of different tumor cell survival pathways, which could aid in overcoming drug resistance in advanced-stage cancers.<sup>6–8</sup> Indeed, a multipronged immune-chemotherapeutic approach would not only facilitate tumor

shrinkage but, more importantly, reactivate the dormant immune response against malignancies to eliminate residual cancer cells. Several immune-chemotherapeutic approaches based on platinum (Pt) drugs incorporating IDO inhibitors have achieved therapeutic synergy to date.<sup>9,10</sup> However, the clinical application of Pt-based drugs is inevitably limited by severe toxicity, acute side effects, and inherent or acquired drug resistance. Accordingly, the design and synthesis of novel immune-chemotherapeutic monomers have attracted considerable research attention in the field of medicinal chemistry.

Indoleamine-2,3-dioxygenase 1 (IDO1) is a heme-containing oxidoreductase that catalyzes tryptophan catabolism to kynurenine through the kynurenine pathway.<sup>11</sup> IDO-mediated rapid consumption of tryptophan results in the suppression of effector T-cell responses and enhancement of immunosuppression-modulated signals by T regulatory cells.<sup>12</sup> IDO1-induced immune tolerance is widely considered as one of the

Received: August 22, 2019

Published: January 30, 2020

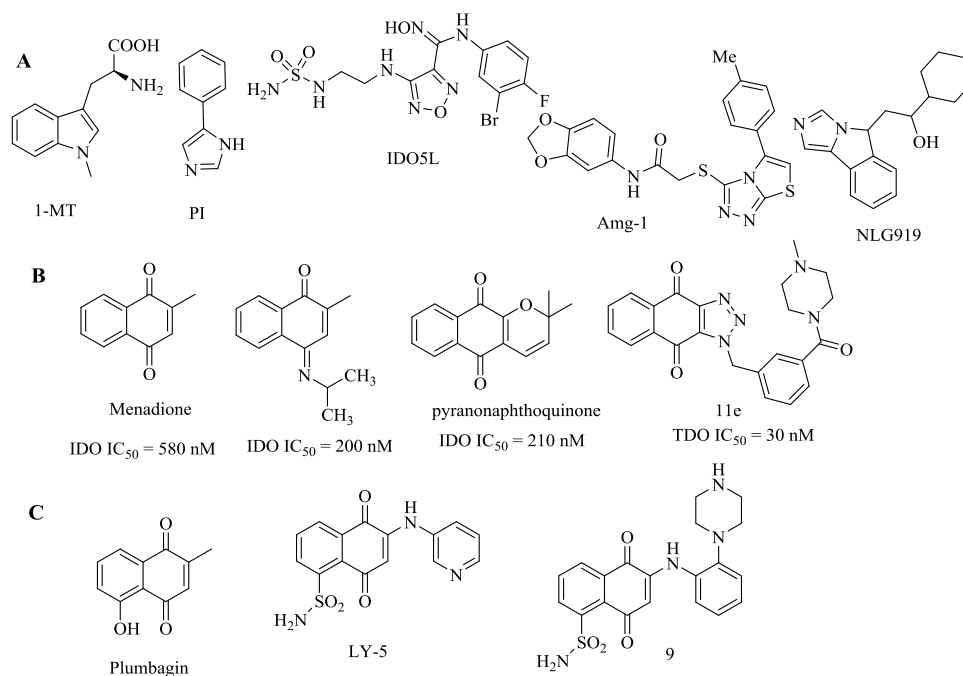


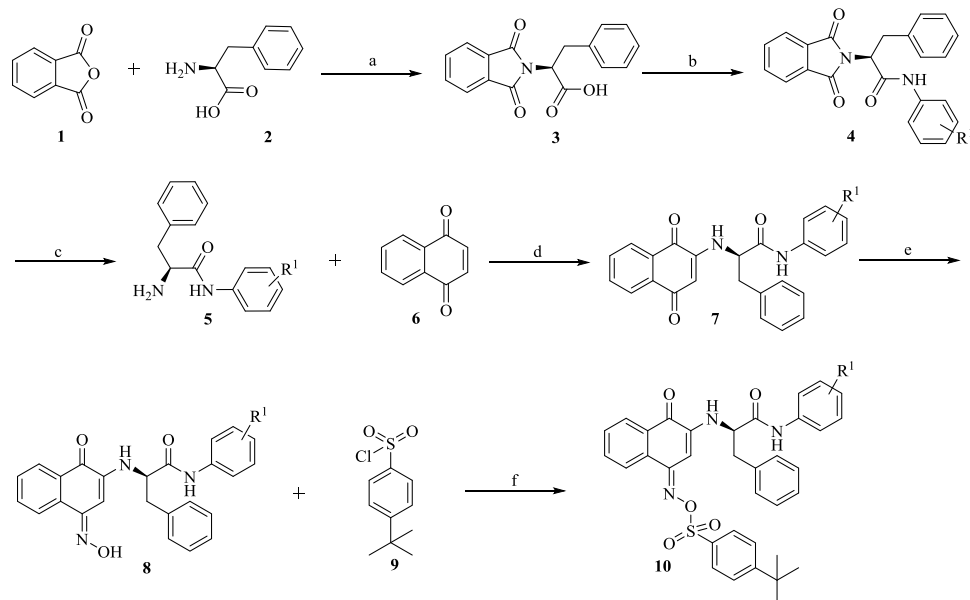
**Figure 1.** Chemical structures of IDO1 and STAT3 inhibitors. (A) Structures of representative IDO1 inhibitors. (B) Naphthoquinone-based IDO1 and tryptophan 2,3-dioxygenase (TDO) inhibitors. (C) Naphthoquinone-based STAT3 inhibitors.

most critical mechanisms evolved by tumors to escape immune surveillance.<sup>13</sup> Furthermore, constitutive overexpression of IDO1 in a variety of human tumors and host antigen-presenting cells has been correlated with different tumor progression parameters and poor prognosis.<sup>14–16</sup> Preclinical studies on mouse tumor models have shown that systemic blockade of IDO1 activity with small-molecule inhibitors successfully impairs outgrowth of tumors, delays metastasis development, prolongs survival, and exerts synergistic therapeutic effects with anticancer drugs to facilitate regression of tumors that are otherwise recalcitrant to treatments. The collective findings in the literature validate the utility of IDO1 as a key target for cancer immunotherapy.<sup>17,18</sup> Several potent small-molecule IDO1 inhibitors that effectively stimulate antitumor immunity have been identified (Figure 1A), but only two of these molecules, 4-amino-*N*-(3-chloro-4-fluorophenyl)-*N'*-hydroxy-1,2,5-oxadiazole-3-carboximidamide (IDO5L) and NLG919, have entered clinical trials to date.<sup>19–23</sup> A key limitation of checkpoint inhibitors is that these molecules narrowly focus on modulating the immune synapse but do not address the critical molecular determinants primarily responsible for immune dysfunction in the tumor microenvironment.<sup>24–26</sup> Signal transducer and activator of transcription 3 (STAT3), a point of convergence for numerous oncogenic signaling pathways and a transcriptional regulator of diverse tumor-promoting factors, is constitutively activated in both tumor and immune cells within the tumor microenvironment and therefore presents an attractive therapeutic target.<sup>27,28</sup> STAT3 regulates multiple genes crucial for tumor cell survival, proliferation, migration, and angiogenesis,<sup>29</sup> and its targeting in tumors with constitutive STAT3 activation has been shown to directly trigger tumor cell death and growth inhibition in vivo.<sup>30</sup> Additionally, constitutively activated STAT3 inhibits the expression of mediators necessary for immune activation and promotes the production of immunosuppressive factors that further stimulate STAT3 activity in

diverse immune cell subsets, altering gene expression programs and thereby suppressing antitumor immune responses. Recent studies have shown that inhibition of STAT3 signaling in the hematopoietic system via ablation of STAT3 or treatment with specific blockers elicits multicomponent antitumor immunity.<sup>31</sup> Intriguingly, antitumor effects are more marked when tumor cells are sensitive to direct killing induced by STAT3 blockade,<sup>31</sup> highlighting the enhanced therapeutic value of approaches targeting both the tumor and its microenvironment. Notably, STAT3 has been shown to maintain the transcriptional expression of IDO and PD-L1 in human cancers.<sup>26,32,33</sup> In the current investigation, we aimed to develop a type of novel small inhibitor molecule targeting both IDO1 and STAT3.

Naphthoquinone structural motifs, such as 1,4-naphthoquinone and its derivatives, exhibit multiple pharmacological activities and have been characterized as enzyme inhibitors.<sup>34–36</sup> A recent study documented that IDO1 is an essential target for naphthoquinone menadione displaying antitumor activity (Figure 1B).<sup>37</sup> Some substituted naphthotriazoleiones were additionally identified as tryptophan 2,3-dioxygenase (TDO) inhibitors using structure-based virtual screening.<sup>38</sup> On the other hand, 1,4-naphthoquinone-based compounds are reported to bind directly to STAT3 and effectively reduce cancer growth in vivo (Figure 1C).<sup>39,40</sup> It is, thus, reasonable to expect that structural modification of the 1,4-naphthoquinone backbone could facilitate both immunomodulatory and antitumor efficacies through simultaneous targeting of IDO1 and STAT3. On the basis of the amide moiety of Amg-1, which is located at the expanded hydrophobic pocket,<sup>41</sup> the aromatic amide was designed and drawn into the naphthoquinone skeleton for binding to the active pocket of IDO1, thus increasing the IDO1 inhibitory activity and antitumor activity. In addition, as inspired by the structure of IDO5L, the oxime moiety was also introduced into the naphthoquinone skeleton for binding to the iron of heme

Scheme 1. Synthetic Pathway to Target Compounds 7(7a–7z), 8(8a–8z), and 10(10a–10c)



<sup>a</sup>Reagents and conditions: (a) phthalic anhydride, CH<sub>3</sub>COOH, 70 °C, 12 h; (b) oxalyl chloride, CH<sub>2</sub>Cl<sub>2</sub>, aromatic primary amines, Et<sub>3</sub>N, room temperature (rt), 12 h; (c) hydrazine hydrate, CH<sub>3</sub>OH, rt, 8 h; (d) DMF, H<sub>2</sub>O, Et<sub>3</sub>N, rt, 18 h; (e) hydroxylamine, CH<sub>3</sub>CH<sub>2</sub>OH, 80 °C, 12 h; (f) CH<sub>2</sub>Cl<sub>2</sub>, Et<sub>3</sub>N, 0 °C, 3 h.

Table 1. Structures and IDO1 Inhibitory Activities of 2-Amino-1,4-Naphthoquinone Derivatives 7a–7z, 8a–8z, and 10a–10c<sup>a</sup>

comps.	R <sup>1</sup>	R <sup>2</sup>	rhIDO1 IC <sub>50</sub> (μM)
7b	3-CF <sub>3</sub>	O	>10
7c	4-CF <sub>3</sub>	O	6.78 ± 0.34
7d	2-F	O	>10
7e	3-F	O	>10
7f	4-F	O	>10
7g	2-Cl	O	>10
7h	3-Cl	O	>10
7i	4-Cl	O	>10
7j	2-Br	O	>10
7k	3-Br	O	>10
7l	4-Br	O	>10
7m	2-OCH <sub>3</sub>	O	>10
7n	3-OCH <sub>3</sub>	O	>10
7o	4-OCH <sub>3</sub>	O	>10
7p	2-CH <sub>3</sub>	O	>10
7q	3-CH <sub>3</sub>	O	>10
7r	4-CH <sub>3</sub>	O	>10
7s	3,5-(CH <sub>3</sub> ) <sub>2</sub>	O	>10
7t	3-Br-4-F	O	>10
7u	3,5-(OCH <sub>3</sub> ) <sub>2</sub>	O	4.84 ± 0.12
7v	3-F-4-Br	O	>10
7w	3,5-(F) <sub>2</sub>	O	>10
7x	3-F-4-CH <sub>3</sub>	O	>10
7y	3-Cl-4-CH <sub>3</sub>	O	>10
7z	2-CH <sub>3</sub> -4-Br	O	>10
10a	3-CF <sub>3</sub>	NOSO <sub>2</sub> Ph	9.60 ± 0.36
10b	3-Br	NOSO <sub>2</sub> Ph	>10
10c	3-OCH <sub>3</sub>	NOSO <sub>2</sub> Ph	>10
6			>10
IDOSL			0.073 ± 0.02

<sup>a</sup>Data are mean ± SD values from three independent experiments.

and expected to act as a donor or acceptor of hydrogen bonds when combined with STAT3. To our knowledge, the combination of the aromatic amide portion, oxime group, and naphthoquinone moiety has not been reported as a dual inhibitor of IDO1 and STAT3 in the literature. Therefore, a series of novel 1,4-naphthoquinone aromatic amide-oxime derivatives co-targeting IDO1 and STAT3 were designed and synthesized, with a view to developing effective anticancer agents that exert synergistic effects through inhibition of STAT3 signaling and simultaneous activation of the antitumor immune response via IDO1 blockage. Our experimental data clearly indicated that the most potent bifunctional inhibitor **8u** showed excellent *in vivo* antitumor efficacy in both wild-type B16-F10 isograft tumors and athymic nude mice, thereby presenting a more proficient immunochemotherapeutic agent against cancers that fail to respond to current immune checkpoint inhibitors or conventional chemotherapeutic agents.

## RESULTS AND DISCUSSION

**Chemistry.** The general procedures for the synthesis of 2-amino-1,4-naphthoquinone aromatic amide-oxime derivatives are described in Scheme 1. First, the reaction of commercially available phthalic anhydride (**1**) with *L*-phenylalanine (**2**) in the presence of acetic acid generating compound **3** was performed as described in the literature.<sup>42</sup> For the synthesis of compound **4**, compound **3** was treated with oxalyl chloride to produce phthalic imide acid chloride, which was substituted with aromatic primary amines to produce phthalic acid amide. Compound **4** reacted with hydrazine hydrate in the presence of ethanol at room temperature, thus generating aromatic amide derivatives (**5**). 2-Amino-1,4-naphthoquinone aromatic amide derivatives (**7**) were prepared, starting from 1,4-naphthoquinone (**6**), which was treated with aromatic amide derivatives (**5**) and triethylamine solution in water at room temperature for 18 h, followed by hydroxylamine hydrochloride in ethyl alcohol at 80 °C for 12 h, to obtain the corresponding 2-amino-1,4-naphthoquinone aromatic amide-oxime derivatives (**8**). These derivatives were converted to 2-amino-1,4-naphthoquinone oxime esters (**10**) through a neutral nucleophilic substitution reaction with 4-*tert*-butylbenzenesulfonyl chloride in dichloromethane in an ice bath. The structures of target compounds **7**, **8**, and **10** were confirmed via <sup>1</sup>H NMR, <sup>13</sup>C NMR, and high-resolution mass spectrometry (HRMS) (Supporting Information).

**Inhibition of IDO1 Activity.** A diverse library of 2-amino-1,4-naphthoquinone aromatic amide-oxime derivatives was synthesized and assayed *in vitro* against activated human IDO1 using a standard enzymatic assay according to previous reports.<sup>43</sup> The potent IDO5L, one of the earliest IDO inhibitors characterized in the literature, was used as a positive control.<sup>19</sup> IC<sub>50</sub> values obtained based on *in vitro* inhibition activities of 2-amino-1,4-naphthoquinone aromatic amide-oxime derivatives are summarized in Table 1.

As shown in Table 1, the newly synthesized 1,4-naphthoquinone aromatic amide-oxime derivative **8** was demonstrated to be a potent IDO1 inhibitor with the IC<sub>50</sub> value mostly in the nanomolar range. The oxime derivative **8** (except for **8m**, **8s**, and **8y**) was significantly more potent than the original lead compound **6** and its derivatives **7** and **10**. Notably, compound **8u** exhibited the best IDO1 inhibition activity relative to that of the commercial IDO1 inhibitor

IDO5L and was, thus, chosen as the representative compound for further investigation as described below.

Structure–activity relationship (SAR) studies were further conducted with the aim of identifying the structural requirements for IDO1 inhibition. The importance of a single substitution at the R<sup>1</sup> position of the phenyl ring was initially investigated. A strong preference for para-substitution was demonstrated by the eightfold improvement in the IDO1 inhibition activity of *p*-fluoro **8f** compared to that of *o*-fluoro **8d**. Similarly, introduction of a fluorine group at the meta-position of the phenyl ring (**8e**) improved the IDO1 inhibitory activity relative to that of **8d**, but the activity was slightly weaker than that of **8f**. Replacement of the fluorine group with a trifluoromethyl group (**8b**, **8c**) resulted in a twofold greater inhibition of IDO1 than those of **8e** and **8f**. After replacement of the fluorine in compound **8f** with a chlorine (**8i**), bromine (**8l**), or methoxy (**8o**) group at the para-position on the phenyl ring, the presence of an electron-donating group on the phenyl ring resulted in a progressive loss of activity. Complete loss of activity was also achieved by introducing a methyl moiety at the ortho-position of the phenyl ring, thus generating compound **8p** (IC<sub>50</sub> > 10 μM). Regarding the effects of the electronic properties of the chemical group at R<sup>1</sup>, the IDO1 inhibitory activity improved in the order methyl < bromine < chlorine < fluorine < trifluoromethyl, thus highlighting an important role of the electron-withdrawing group in the inhibition of IDO1. Variations at R<sup>1</sup> caused substantial differences in inhibitory potency, presumably because of different affinities to the binding pocket.

In addition, we investigated the influence of a second group on the phenyl ring. The compound with a second methyl group at position 2 (**8z**, IC<sub>50</sub> > 50 μM), compared to the 4-Br derivative (**8l**, IC<sub>50</sub> = 0.16 μM), did not show improved activity. In contrast, the addition of an *m*-fluoro substituent to **8l** was tolerated and generated **8v**, which showed strikingly improved potency. Compounds **8w**–**8y** had further substitutions at the 3-position of the phenyl ring. Unfortunately, these compounds displayed poor or retained inhibitory activity against IDO1. The presence of a bromine atom at the 3-position generated **8t** (IC<sub>50</sub> = 0.074 μM), which had a relatively greater inhibitory activity comparable to that of **8f**, but 12-fold more potent than that of **8k**. These results clearly suggested that the electronic and steric properties at the 3-position affect the IDO1 inhibitory activity. Intriguingly, the 3,5-dimethoxy substitution pattern produced the most potent compound, **8u** (IC<sub>50</sub> = 0.046 μM), which was ~11-fold more active than the 3-methoxy derivative **8n** (IC<sub>50</sub> = 0.53 μM). The same compound was 179- and 5-fold more active than the 3,5-dimethyl (**8s**, IC<sub>50</sub> = 8.27 μM) and 3,5-difluoro (**8w**, IC<sub>50</sub> = 0.25 μM) derivatives, respectively.

SAR studies revealed the importance of the unique oxime functional group in binding to IDO1. All modifications of the oxime pharmacophore generated significantly less potent derivatives (Table 1). Further modification of the carbonyl group of **7c** with an oxime group, thus generating **8c**, resulted in a 98-fold increase in the IDO1 inhibitory activity. Esterification of the oxime group in 4-*tert*-butylbenzenesulfonyl oxime esters (compound **10**) revealed the requirement of a free hydroxyl group for binding IDO1. Compounds **10b** and **10c** showed no activity. Only the trifluoromethyl substitution derivative, **10a**, showed measurable activity (albeit 106-fold lower), compared to that of its oxime analogue, **8b**, in the IDO1 assay. This significant loss of activity may be explained

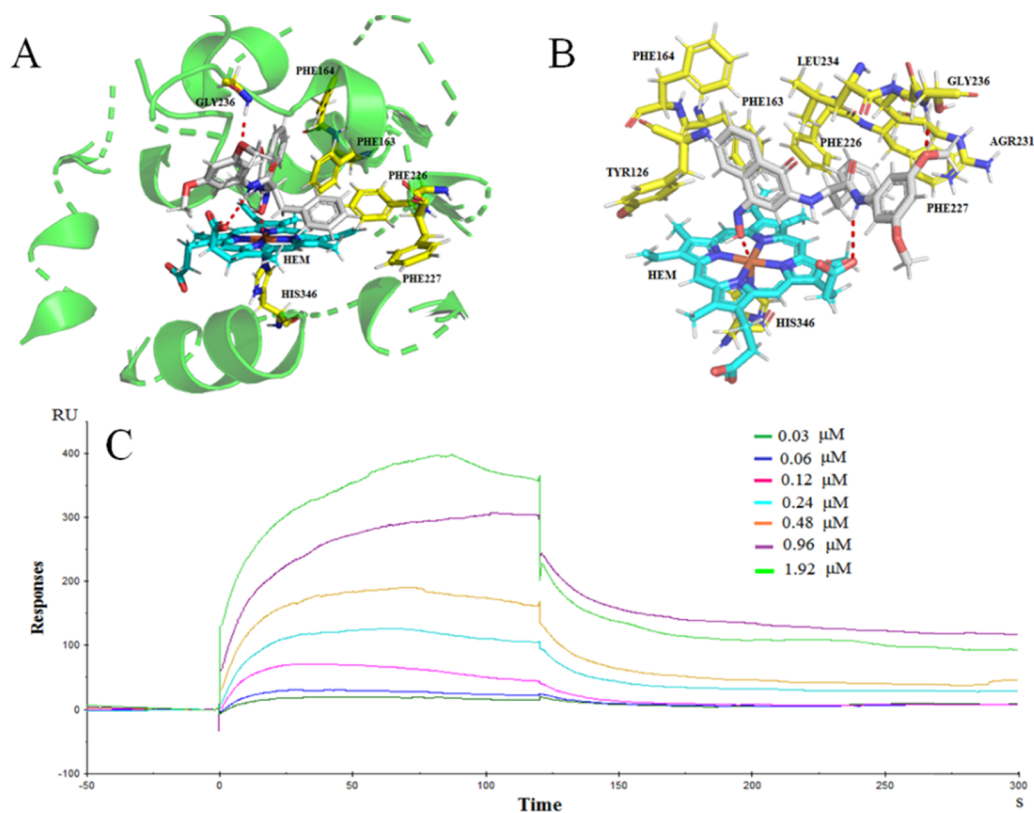


**Figure 2.** (A) Proposed binding mode of compound **8u** in the active site of IDO1 (PDB: 4PK5). Heme is reported as a cyan stick, IDO1 structure is shown as a cartoon. (B) Key hydrogen bond interactions of compound **8u** in the active site of IDO1. Compound **8u**, IDO1 residues, and HEM are shown as gray stick, yellow stick, and cyan stick, respectively. The red dashed lines indicate the H-bond interaction between **8u** and IDO1. (C) Biophysical binding data supports the interaction of compound **8u** with human IDO1 protein. Dose–response curve determined by surface plasmon resonance (SPR) for the binding of IDO1 with **8u** is shown.

by additional esterification of the oxime moiety resulting in a steric clash with the heme group in IDO1, thus preventing the formation of the coordinate covalent bond with heme iron.

On the basis of the established SAR, the known binding affinities of compounds containing the oxime moiety to iron heme<sup>44</sup> and data obtained with IDO1, we surmised that these IDO1 inhibitors may form a dative bond with heme iron in the ferrous state through the oxygen of the oxime moiety.

**Molecular Docking.** As revealed by SAR studies, **8u** exhibited the most potent inhibitory activity against IDO1. To understand the mechanisms underlying the improved potency of **8u** at the molecular level, molecular docking studies of **8u** in the active site of IDO1 were performed using SYBYL-X 2.0 software. The docking scores are summarized in Table S1. The docking model showed that **8u** was strongly bound to the Trp-binding site with its naphthoquinone oxime core almost perpendicular to the heme plane (Figure 2A). The oxygen of the oxime moiety coordinated with heme iron in the catalytically active site, and the quinone part of **8u** located deep into the hydrophobic pocket (Figure 2B), where it was appropriately positioned to facilitate  $\pi$ – $\pi$  interactions with the quinone aromatic core of several aromatic groups (TYR126, PHE163, and PHE164). Additional lipophilic residues were in close contact with the quinone group (VAL130, CYS129, and LEU234). Remarkably, the hydroxyl hydrogen of the oxime moiety formed additional hydrogen bonds with the porphyrin ring of heme, which contributed to its inhibitory activity against IDO1. Furthermore, the phenyl ring of the phenylalanine moiety extended tightly into another hydrophobic

pocket (Figure S1A) and interacted with LEU230, ARG231, PHE226, PHE227, and ILE354 (Figure S1B). Notably,  $\pi$ – $\pi$  interactions between the phenyl ring and side chain of PHE226 were observed, which may be essential for potent IDO1 inhibitory activity, consistent with earlier findings on the role of PHE226.<sup>41</sup> The NH of **8u** was situated in the vicinity of 7-propanoic acid group of the heme ring, where it formed a strong hydrogen bond. Specifically, the methoxy group in the R<sup>1</sup> position as an acceptor established one hydrogen bond with GLY236, which could also contribute to the improved potency of **8u**, and adopted a different rotamer, compared to previous studies.<sup>41,45</sup> The tight packing of the molecule within the IDO1 active site (Figure S1C) clearly explained the lack of activity of the analogues bearing a methyl substituent at the R<sup>1</sup> position as well as the considerable challenges in modifying oxime features.

**UV–Visible Spectroscopy.** UV–visible spectroscopy was performed to further confirm binding of compound **8u** with heme-containing IDO1 protein. The unique UV absorption properties of porphyrins are useful in heme protein studies.<sup>46</sup> Heme is a porphyrin ring with an iron at its center, which absorbs light at the UV–vis spectrum maximally at a wavelength of ~400 nm depending on the oxidation and coordination states of its iron, characterized by the Soret band. Absorbance spectra of the heme group are highly sensitive to changes in the polarity of the heme environment upon ligand/substrate binding, usually resulting in pronounced changes in the spectral properties of heme.<sup>47</sup> Therefore, changes in UV–visible spectra induced by IDO1–ligand interactions could be

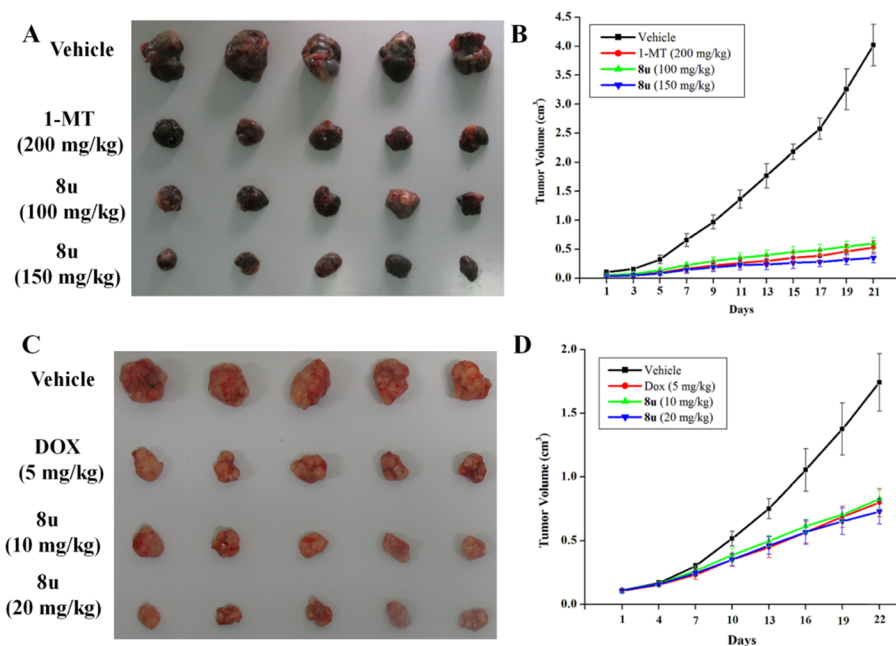


**Figure 3.** In vivo anticancer activity of compound **8u**. (A) Effects of the indicated treatments of **8u** on B16-F10 melanoma tumor xenografts in C57BL/6 mice. The images of the tumors after administering with compound **8u** are also shown. (B) Tumor volumes were detected every 2 days for 21 days of duration. (C) Inhibition of tumor growth for compound **8u** and doxorubicin (DOX) in nude mice bearing HepG2 xenograft model. (D) Tumor volumes were detected every 3 days. Data represent three individual experiments.

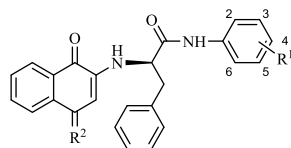
exploited to evaluate binding to IDO1. To obtain a more direct indication of the binding site of compound **8u**, UV–visible spectra of ferric IDO1 were measured in the presence and absence of the compound (Figure S2). In the absence of **8u**, the absorption spectrum of ferric IDO1 exhibited a Soret peak at 403 nm, as described in the literature.<sup>46</sup> The Soret peak shifted to 413 nm in the presence of **8u**, indicative of binding to IDO1 and coordination with the iron of the heme group.<sup>23</sup>

**Surface Plasmon Resonance Assays.** To provide definitive evidence of direct binding to IDO1, a surface plasmon resonance (SPR)-based binding assay was performed using a Biacore T200 instrument. This analytic technique facilitates measurement of the kinetic and thermodynamic parameters of ligand–protein complex formation and is widely utilized to investigate enzyme/inhibitor interactions.<sup>48</sup> Kinetic association and dissociation measurements were obtained, and the binding affinity of compound **8u** for IDO1 was determined with the aid of Biacore evaluation software. Compound **8u** efficiently interacted with the immobilized protein (Figure 2C), as demonstrated by the concentration-dependent responses for association and dissociation, respectively, and the clearly discernible exponential curves, indicative of binding to and dissociation from the IDO1 protein, with an equilibrium dissociation constant ( $K_D$ , representing binding affinity) of 0.08  $\mu$ M. Notably, the kinetic dissociation constant ( $K_d$ ) between compound **8u** and IDO1 was 0.0045 1/s, suggesting that the **8u**-IDO1 complexes formed were extremely stable. Our data provided definitive evidence of direct binding of derivatives of 2-amino-1,4-naphthoquinone aromatic amide-oxime derivatives to IDO1.

**In Vivo Tumor Growth Inhibition.** Compounds that directly interfere with IDO-mediated tryptophan catalysis exert antitumor effects. To establish whether IDO1 inhibition could similarly reverse immune tolerance in vivo, we treated C57BL/6 mice bearing B16-F10 with **8u** or 1-methyl-L-tryptophan (1-MT) for 21 days. IDO is not expressed in B16-F10 tumor cells,

but rather detected in antigen-presenting cells within tumor-draining lymph nodes of the host animal.<sup>49</sup> B16-F10 cells form highly aggressive, poorly immunogenic tumors that are resistant to a variety of immunotherapeutic strategies. Nevertheless, growth of tumor isografts formed by these cells can be suppressed significantly by direct inhibitors of IDO1.<sup>17,37</sup> After 21 days, **8u** exhibited significantly stronger tumor inhibition than the other two groups (Figures 3A and S3A). Comparison of final mean tumor volumes between **8u**-treated and control animals at the 3-week endpoint revealed marked suppression of tumor growth following **8u** treatment of B16-F10 tumor-challenged mice (Figure 3B) equating to a T/C ratio of 29.47% (150 mg/kg). Specifically, **8u** inhibited 70.53% of the tumor volume, while 1-MT reduced the tumor volume by 57.21% (Figure 3B). The mice treated with **8u** showed marked reduction in total tumor weight, whereas the effect on tumor degeneration was smaller in the 1-MT-treated mice (Figure S3B). The body weights of the mice in each group increased gradually, confirming the safety of **8u** (Figure S3C). Although **8u** was incapable of eliciting tumor regression, the compound effectively inhibited tumor growth, supporting its potential as a single agent for tumor therapy.

**Evaluation of Antiproliferative Activity.** Menadione, an anticancer agent with a naphthoquinone core, exhibits low micromolar potency against IDO.<sup>50</sup> Based on the finding that compound **8u** was an inhibitor of IDO1, we evaluated whether **8u** and other naphthoquinone derivatives exerted antitumor effects in Hct-116, SKOV3, A549, and HepG2 cancer cells via the 3-(4,5-dimethylthiazol-2-yl)-2,5-diphenyltetrazolium bromide (MTT) assay. Data are presented in Table 2, showing potent cytotoxicity of several compounds in all of the cell lines examined. Notably, compounds **8** exhibited significantly greater antitumor activity relative to a number of other IDO inhibitors examined, which displayed weak activity when administered as single agents. There is growing consensus that the clinical efficacy of some chemotherapeutic agents addi-

Table 2. Cytotoxic Activity of 2-Amino-1,4-Naphthoquinone Derivatives against Cancer Cell Lines<sup>a</sup>

comps.	IC <sub>50</sub> (μM)					
	R <sup>1</sup>	R <sup>2</sup>	Hct-116	SKOV3	A549	HepG2
8a	H	NOH	1.54 ± 0.43	1.25 ± 0.14	1.47 ± 0.39	1.15 ± 0.17
8b	3-CF <sub>3</sub>	NOH	0.13 ± 0.03	0.10 ± 0.04	0.11 ± 0.09	0.07 ± 0.03
8c	4-CF <sub>3</sub>	NOH	0.083 ± 0.02	0.055 ± 0.01	0.074 ± 0.03	0.068 ± 0.05
8d	2-F	NOH	0.19 ± 0.10	0.14 ± 0.06	0.16 ± 0.08	0.09 ± 0.02
8e	3-F	NOH	0.89 ± 0.28	0.43 ± 0.16	0.81 ± 0.21	0.73 ± 0.08
8f	4-F	NOH	0.11 ± 0.05	0.098 ± 0.02	0.10 ± 0.07	0.05 ± 0.01
8g	2-Cl	NOH	1.09 ± 0.39	1.22 ± 0.31	1.18 ± 0.65	1.03 ± 0.49
8h	3-Cl	NOH	0.56 ± 0.26	0.38 ± 0.09	0.53 ± 0.17	0.28 ± 0.06
8i	4-Cl	NOH	0.071 ± 0.05	0.067 ± 0.03	0.069 ± 0.02	0.042 ± 0.01
8j	2-Br	NOH	3.19 ± 0.47	2.96 ± 0.36	3.05 ± 0.46	1.80 ± 0.31
8k	3-Br	NOH	1.22 ± 0.33	1.08 ± 0.28	1.21 ± 0.23	0.10 ± 0.02
8l	4-Br	NOH	0.31 ± 0.07	0.24 ± 0.09	0.28 ± 0.15	0.11 ± 0.05
8m	2-OCH <sub>3</sub>	NOH	1.41 ± 0.44	1.08 ± 0.33	1.23 ± 0.26	1.07 ± 0.23
8n	3-OCH <sub>3</sub>	NOH	0.66 ± 0.19	0.44 ± 0.15	0.63 ± 0.11	0.06 ± 0.01
8o	4-OCH <sub>3</sub>	NOH	0.58 ± 0.28	0.41 ± 0.22	0.49 ± 0.21	0.04 ± 0.01
8p	2-CH <sub>3</sub>	NOH	9.72 ± 0.70	8.81 ± 0.78	9.08 ± 0.37	8.05 ± 0.37
8q	3-CH <sub>3</sub>	NOH	1.62 ± 0.12	1.15 ± 0.47	1.46 ± 0.36	1.23 ± 0.26
8r	4-CH <sub>3</sub>	NOH	3.86 ± 0.53	2.75 ± 0.37	3.54 ± 0.28	1.29 ± 0.28
8s	3,5-(CH <sub>3</sub> ) <sub>2</sub>	NOH	3.39 ± 0.23	2.84 ± 0.49	3.17 ± 0.34	2.57 ± 0.14
8t	4-F-3-Br	NOH	0.097 ± 0.04	0.073 ± 0.02	0.088 ± 0.03	0.056 ± 0.02
8u	3,5-(OCH <sub>3</sub> ) <sub>2</sub>	NOH	0.037 ± 0.01	0.028 ± 0.01	0.033 ± 0.01	0.012 ± 0.01
8v	3-F-4-Br	NOH	0.16 ± 0.08	0.092 ± 0.06	0.12 ± 0.08	0.07 ± 0.02
8w	3,5-(F) <sub>2</sub>	NOH	0.78 ± 0.13	0.64 ± 0.17	0.69 ± 0.29	0.38 ± 0.11
8x	4-CH <sub>3</sub> -3-F	NOH	2.55 ± 0.41	2.06 ± 0.28	2.34 ± 0.32	1.81 ± 0.22
8y	3-Cl-4-CH <sub>3</sub>	NOH	6.53 ± 0.76	4.68 ± 0.42	6.50 ± 0.62	2.47 ± 0.29
8z	2-CH <sub>3</sub> -4-Br	NOH	9.89 ± 0.55	7.27 ± 0.65	9.48 ± 0.41	4.78 ± 0.44
7a	H	O	>20	>20	>20	>20
7b	3-CF <sub>3</sub>	O	>20	>20	>20	>20
7c	4-CF <sub>3</sub>	O	17.23 ± 0.38	16.52 ± 0.59	18.03 ± 0.51	13.26 ± 0.65
7d	2-F	O	>20	>20	>20	>20
7e	3-F	O	>20	>20	>20	>20
7f	4-F	O	>20	>20	>20	>20
7g	2-Cl	O	>20	>20	>20	>20
7h	3-Cl	O	>20	>20	>20	>20
7i	4-Cl	O	>20	>20	>20	>20
7j	2-Br	O	>20	>20	>20	>20
7k	3-Br	O	>20	>20	>20	>20
7l	4-Br	O	>20	>20	>20	>20
7m	2-OCH <sub>3</sub>	O	>20	>20	>20	>20
7n	3-OCH <sub>3</sub>	O	>20	>20	>20	>20
7o	4-OCH <sub>3</sub>	O	>20	>20	>20	>20
7p	2-CH <sub>3</sub>	O	>20	>20	>20	>20
7q	3-CH <sub>3</sub>	O	>20	>20	>20	>20
7r	4-CH <sub>3</sub>	O	>20	>20	>20	>20
7s	3,5-(CH <sub>3</sub> ) <sub>2</sub>	O	>20	>20	>20	>20
7t	4-F-3-Br	O	>20	>20	>20	>20
7u	3,5-(OCH <sub>3</sub> ) <sub>2</sub>	O	15.38 ± 0.76	13.69 ± 0.83	16.43 ± 0.92	11.44 ± 0.24
7v	3-F-4-Br	O	>20	>20	>20	>20
7w	3,5-(F) <sub>2</sub>	O	>20	>20	>20	>20
7x	4-CH <sub>3</sub> -3-F	O	>20	>20	>20	>20
7y	3-Cl-4-CH <sub>3</sub>	O	>20	>20	>20	>20
7z	2-CH <sub>3</sub> -4-Br	O	>20	>20	>20	>20
10a	3-CF <sub>3</sub>	NOSO <sub>2</sub> Ph	>20	>20	>20	>20
10b	3-Br	NOSO <sub>2</sub> Ph	>20	>20	>20	>20

Table 2. continued

comps.	IC <sub>50</sub> (μM)					
	R <sup>1</sup>	R <sup>2</sup>	Hct-116	SKOV3	A549	HepG2
10c	3-OCH <sub>3</sub>	NOSO <sub>2</sub> Ph	>20	>20	>20	>20
6			17.08 ± 0.58	16.27 ± 0.62	>20	>20
DOX			0.27 ± 0.08	0.16 ± 0.17	0.074 ± 0.05	0.069 ± 0.02

<sup>a</sup>Data are mean ± SD values from three independent experiments.

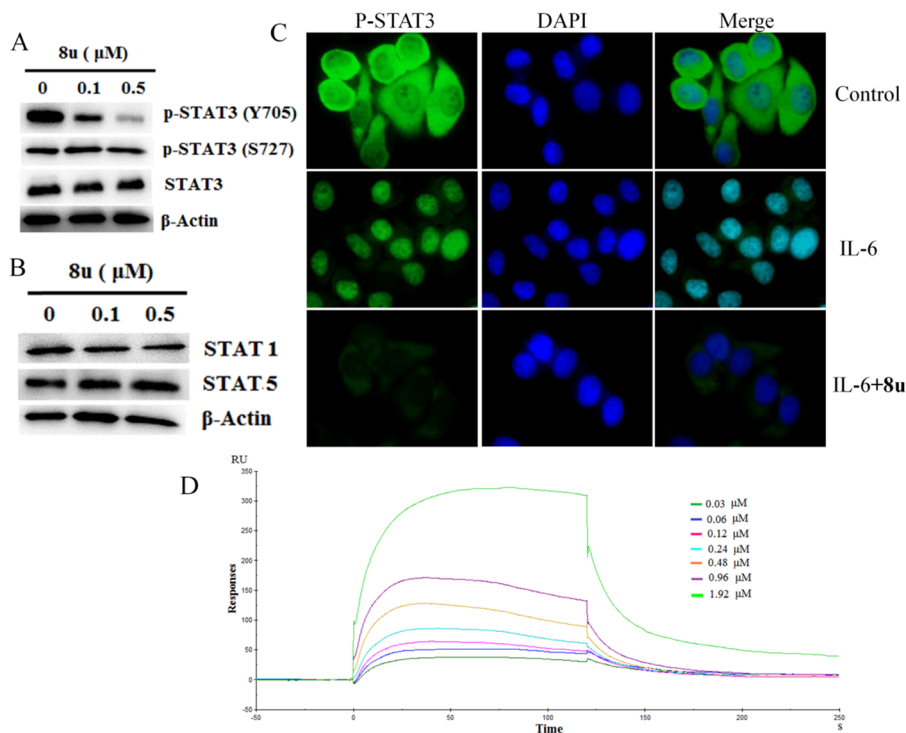


**Figure 4.** Compound **8u** targeted STAT3. (A) Western blot analysis of p-STAT3(Y705), p-STAT3(S727), and total STAT3 after treatment of SKOV3 cells with **8u** at the indicated concentrations and for the indicated times. (B) Western blots of STAT1 and STAT5 from whole-cell lysates from cells were treated with **8u**.  $\beta$ -actin antibody was used as reference control. (C) Effects of compound **8u** (0.5  $\mu$ M) on the nuclear translocation of the p-STAT3 protein induced by cytokine IL-6. After serum-free overnight treatment, SKOV3 cells were pretreated with **8u** for 8 h, followed by IL-6 (50 ng/mL) for 30 min, and then processed for STAT3 nuclear translocation detection by immunofluorescence staining. (D) SPR analysis of compound **8u** with STAT3 protein. The equilibrium dissociation constant (KD) value is 0.53  $\mu$ M.

tionally depends on their off-target immunomodulatory effects.<sup>51,52</sup> Indeed, the newly synthesized naphthoquinone derivatives **8** were potent antitumor agents with IC<sub>50</sub> values mostly in the nanomolar range. Among these, **8u** was the most potent depending on the cell line, with IC<sub>50</sub> values of 0.037 ± 0.01, 0.028 ± 0.01, 0.033 ± 0.01  $\mu$ M, and 0.012 ± 0.01 against Hct-116, SKOV3, A549, and HepG2, respectively. However, the antitumor activity of compounds **7** that induced moderate IDO1 inhibition was relatively weak. Based on the collective kinetic and cell proliferation results, a window between IDO inhibitory activity and general cytotoxicity of compound **7** was hypothesized.

**Antitumor Potency of 8u in Nude Mice in Vivo.** To validate whether IDO1 might present an alternative target for compound **8u**, a xenograft model was prepared by injecting nude mice with human liver cancer HepG2 cells, followed by administration of two doses of **8u** once every 2 days. As depicted in Figures 3C and S4A, intravenous administration of **8u** at 10 or 20 mg/kg every 3 days for 21 consecutive days led to significant suppression of tumor growth (53.4 and 59.0%), compared to the vehicle group (Figure S4B). The antitumor effect of **8u** was additionally evident from the delayed increase

in xenograft volume, compared to doxorubicin (DOX) (Figure 3D). Notably, **8u** was well tolerated and induced no significant loss of body weight (Figure S4C), indicating that its antitumor activity does not require T cell involvement. However, we demonstrated in the previous IDO1 assay that **8u** is a potential IDO1 inhibitor that requires intact T-cell function to suppress tumor outgrowth in wild-type C57BL/6 mice.<sup>17</sup> These findings suggested that **8u**-induced tumor elimination may involve alternative targets. The unique dual action of **8u** was evidently distinct from that of other known IDO1 inhibitors.

To our knowledge, some IDO1 inhibitors also have potential in vitro antitumor activity. For example, menadione is a known anticancer agent that exhibits low micromolar potency against IDO.<sup>50</sup> Moreover, Coluccia et al. reported that IDO1 inhibitors **5** and **21** induce dose-dependent growth inhibition in the IDO1 expressing cancer cell lines HTC116 and HT29.<sup>20</sup>  $\beta$ -lapachone is a naturally occurring 1,2-naphthoquinone-based compound that has advanced into clinical trials, owing to its tumor-selective cytotoxic properties. However, recent studies have shown that IDO1 inhibitory activity is a previously unrecognized attribute of the clinical candidate  $\beta$ -lapachone.<sup>53</sup> The finding that  $\beta$ -lapachone shows IDO1 inhibitory activity

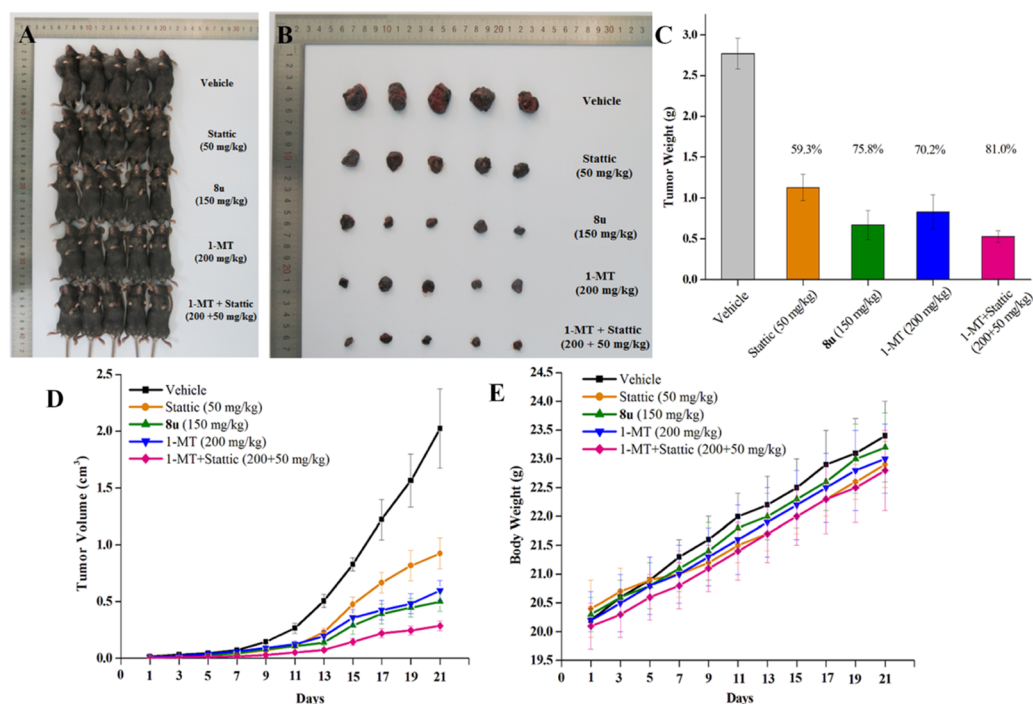


**Figure 5.** Comparative antitumor potency of **8u** and the combination of 1-MT and static in vivo in a B16-F10 tumor-challenged C57BL/6 mice model. (A) Representative images in B16-F10 bearing mice. (B) Representative photos of the tumors at the end of treatment. (C) Average weight of the tumors excised at the end of treatment. (D) Changes in tumor volume in different treatment groups measured every 2 days. (E) Changes in body weight in different treatment groups measured every 2 days.

adds a new dimension distinct from its cytotoxic properties in its potential utility as an anticancer agent, and a synergistic benefit may be achieved through its combined cytotoxic and immunologic effects. Another study has suggested that pyranonaphthoquinone-based compounds possess dual IDO1 and topoisomerase II inhibitory activity, thus inhibiting cell growth of human H460 cells.<sup>54,55</sup> Compounds that integrate tumoricidal activity along with IDO1 inhibitory activity may produce substantially more robust single-agent antitumor responses than IDO1 inhibitors that do not exert a cytotoxic effect. Naphthoquinone-based compounds are reported to act as direct small-molecule inhibitors of signal transducer and activator of transcription 3 (STAT3).<sup>39,56</sup> Recent studies have identified STAT3 as a modulator of tumor-induced immune suppression at many levels in the tumor microenvironment.<sup>57</sup> Furthermore, PD-L1 expression in cancer cells is mediated through the STAT3 pathway.<sup>58,59</sup> Since STAT3 mediates processes of carcinogenesis, such as tumor cell proliferation and survival, angiogenesis, and invasion, the STAT3 pathway may present a direct link between traditional oncogenesis and immune suppression. Many studies have reported constitutive expression of IDO1 and STAT3 in the four tested cancer cell lines, except for IDO1 in HepG2 cells.<sup>12,14,20,60–62</sup> The novel compound **8u** appears to regulate both IDO1 and STAT3 to disrupt the tumor microenvironment, inducing a potent synergistic antitumor effect. If so, this bifunctional inhibitor exerting both immunomodulatory and conventional chemotherapy effects via IDO1 inhibition may hold promise for cancers that respond poorly to conventional chemotherapeutics. The potent immune-chemotherapeutic effects of **8u** prompted us to hypothesize that STAT3 may also be a potential target of **8u**.

**Compound 8u Targets STAT3.** To confirm our theory, STAT3 expression was detected via western blotting. Aberrant

activation of STAT3 is known to contribute to malignant transformation and tumorigenesis, and its activity is ultimately dependent on the phosphorylation of Y705.<sup>39</sup> Treatment of SKOV3 cells with different concentrations of **8u** resulted in a significant decrease in phosphorylated STAT3 (p-STAT3) levels (Figure 4A). Specifically, the p-STAT3 (Y705) level was reduced in a dose-dependent manner while levels of p-STAT3 (S727) were not influenced by **8u** and total STAT3 expression remained unchanged (Figure 4A). We further investigated the levels of other STAT proteins, including STAT1 and STAT5. Pretreatment with compound **8u** had no effect on the levels of other pSTAT proteins, as evident from western blot analyses (Figure 4B). Subsequently, inhibition of STAT3 activation by **8u** was evaluated using a dual luciferase assay. We observed a reduction in luciferase expression in SKOV3 cells treated with **8u** but no changes in STAT1 and STAT5 transcriptional activity (Figure S5).

Mechanistically, STAT3 nuclear translocation was examined via immunofluorescence staining. To this end, SKOV3 cells were treated for 6 h with 0.5  $\mu$ M **8u**, followed by stimulation of STAT3 translocation by adding IL-6 for 30 min. As shown in Figure 4C, in SKOV3 cells treated with IL-6, intense nuclear fluorescence was observed, indicative of nuclear translocation of p-STAT3. Nuclear translocation of STAT3 in **8u**-treated cells was clearly inhibited relative to that in IL-6-stimulated cells. Based on these results, we suggest that inhibition of STAT3 phosphorylation by **8u** may have impaired its transcriptional activity by blocking nuclear translocation.

The SPR binding assay was performed to further examine direct binding between **8u** and STAT3. In the BIAcore sensorgram, resonance curves exhibited strong binding patterns between the two molecules in a dose-dependent manner (Figure 4D). The kinetic parameter, dissociation constant ( $K_D$ ), determined using BIAcore evaluation software,

was 0.53  $\mu\text{M}$ , indicative of a high binding affinity.<sup>63</sup> Our collective data supported the hypothesis that **8u** specifically binds STAT3 protein with high affinity, thus indicating that STAT3 was also the potential target of **8u**.

To further support the favorable in vitro and in vivo data of **8u** and to confirm that the 2-amino-1,4-naphthoquinone derivatives are bifunctional inhibitors, we detected the  $K_D$  values of selected compounds toward STAT3 (**8b–8f**, **8h**, **8q**, **8s**, and **7u**) using SPR assays (Table S2). The 3-trifluoromethyl and 4-trifluoromethyl derivatives **8b** and **8c** both effectively bound STAT3 with an  $\text{IC}_{50}$  value of 0.99 and 0.64  $\mu\text{M}$ , respectively, and were only 1- to 2-fold less active than **8u**. Compound **7u**, in contrast, was 100-fold less active than **8u**, thus indicating that **8u** was the best compound, exhibiting the highest binding affinity toward STAT3 among these derivatives.

We next evaluated the comparative antitumor efficacy of **8u** and the combination of 1-MT and stattic (STAT3 inhibitor) using the B16-F10 tumor-bearing C57BL/6 mice model (Figure SA,B). The efficacy data showed that stattic at a dose of 50 mg/kg had a reduced tumor volume and burden during the treatment period with tumor growth inhibition of 59.3% (Figure SC,D). Treatment of tumor-bearing mice with the combination of 1-MT and stattic was slightly more effective at inhibiting tumor progression compared to **8u** alone. Normal increase of body weight was observed for all mice (Figure SE), indicating that **8u** efficiently suppressed tumor growth in mice without obvious side effects.

## CONCLUSIONS

In summary, we have presented a novel example of organic compounds as multimodal anticancer agents that perform dual targeting of IDO1 and STAT3, inducing greater resistance to immune tolerance of the tumor microenvironment. SAR analyses facilitated the identification of the main pharmacophore groups of this new class of bifunctional inhibitors, among which derivative **8u** was determined as the most active compound. Our SPR analysis provided evidence for the strong binding affinity of **8u** toward IDO1 and STAT3. The quinone oxime core was critical for IDO1 inhibition, and the oxime oxygen acted as the iron-binding group. Remarkably, compound **8u** reduced tumor growth to a significant extent in both immunocompetent and nude mice, signifying dual anticancer and immunomodulatory activity. As elevated STAT3 is a common denominator of immune dysfunction in multiple cancer types, our novel bifunctional small-molecule immune modulator compound **8u** provides an effective cutting-edge immunochemotherapeutic agent for cancers that fail to respond to currently available immune checkpoint inhibitors by simultaneously disabling immune checkpoints and counteracting STAT3-mediated signaling pathways.

## EXPERIMENTAL SECTION

**General Information.** Compound **3** was synthesized according to the literature.<sup>42</sup> All reagents were purchased from commercial sources and were used without further purification unless otherwise noted. Melting points were recorded on a WRS-IA apparatus without correction. Nuclear magnetic resonance (NMR) spectra were recorded in  $\text{DMSO}-d_6$  on Bruker Advance (500 or 400 MHz) with tetramethylsilane (TMS) as an internal standard. HRMS was measured in FTMS EI or electrospray ionization (ESI) mode, and the mass analyzer of the HRMS was time-of-flight (TOF). Flash column chromatography was performed on silica gel (200–300 mesh). All of the compounds submitted for biological studies were at

least of 95% purity by reverse-phase high-performance liquid chromatography (RP-HPLC) on ODS column (250 mm  $\times$  4.6 mm, 5  $\mu\text{m}$ ) with an eluent of methanol/water (80:20, V/V).

**General Procedure for the Preparation of Compounds 7 and 8.** Compound **3** (1 mmol) was added to dry  $\text{CH}_2\text{Cl}_2$  (15 mL) and stirred at 0  $^\circ\text{C}$ . Subsequently, oxalyl chloride (1.5 mmol) was dripped into the mixture and stirred at room temperature for 6 h. After the reaction, the solvent and excess oxalyl chloride were evaporated under reduced pressure. Aromatic primary amines (1 mmol) and triethylamine (0.5 mmol) were added to the mixture and stirred at room temperature for 0.5 h. After the reaction, the solvent was evaporated under reduced pressure and the crude product was purified by chromatography on silica gel eluted with petroleum ether/ethyl acetate (V/V = 6:1), thus yielding compound **4**. Compound **4** (1 mmol) and hydrazine hydrate (3 mmol) were added to ethanol (15 mL), and the mixture was stirred at room temperature for 8 h. After the reaction was completed, the solvent was evaporated under reduced pressure, and the crude product was purified with chromatography on silica gel and eluted with petroleum ether/ethyl acetate (V/V = 3:1) to obtain compound **5**. Compound **5** (2 mmol) and 1,4-naphthoquinone (3 mmol) were added to the mixture containing triethylamine (1 mmol) and stirred at room temperature for 18 h. After the reaction, the solvent was evaporated under reduced pressure and the crude product was purified by chromatography on silica gel and eluted with petroleum ether/ethyl acetate (V/V = 4:1), thus yielding compounds **7a–7z**. The structures were confirmed by  $^1\text{H}$  NMR,  $^{13}\text{C}$  NMR, and HR-MS.

**2-((1,4-Dioxo-1,4-dihydronaphthalen-2-yl)amino)-N,3-diphenylpropanamide (7a).** Yield: 70.2%, yellow solid, mp 101.7–103.2  $^\circ\text{C}$ .  $[\alpha]_D^{20} = -40$  (c 0.1, AcOEt).  $^1\text{H}$  NMR (400 MHz,  $\text{DMSO}-d_6$ )  $\delta$  10.17 (s, 1H, NH), 8.00–7.95 (m, 1H, NH), 7.90 (dd,  $J = 7.6, 0.7$  Hz, 1H, ArH), 7.79 (td,  $J = 7.5, 1.2$  Hz, 1H, ArH), 7.71 (td,  $J = 7.5, 1.2$  Hz, 1H, ArH), 7.55 (d,  $J = 7.7$  Hz, 2H, ArH), 7.36–7.29 (m, 4H, ArH), 7.26 (t,  $J = 7.4$  Hz, 2H, ArH), 7.19 (d,  $J = 7.6$  Hz, 2H, ArH), 7.08 (t,  $J = 7.4$  Hz, 1H, ArH), 5.70 (s, 1H, C=CH), 4.45 (q,  $J = 7.0$  Hz, 1H, CH), 3.27 (d,  $J = 6.8$  Hz, 2H,  $\text{CH}_2$ ).  $^{13}\text{C}$  NMR (101 MHz,  $\text{DMSO}-d_6$ )  $\delta$  181.82, 181.00, 168.55, 147.50, 138.24, 136.92, 134.91, 132.68, 132.46, 130.19, 130.19, 129.24, 128.80, 128.80, 128.28, 128.28, 126.68, 125.98, 125.37, 123.91, 119.74, 119.74, 100.99, 57.55, 37.19. HR-MS ( $m/z$ ) (ESI): calcd for  $\text{C}_{25}\text{H}_{21}\text{N}_2\text{O}_3$  [ $\text{M} + \text{H}$ ] $^+$ : 397.1547; found: 397.1531. Purity: 97.66%.

**2-((1,4-Dioxo-1,4-dihydronaphthalen-2-yl)amino)-3-phenyl-N-(3-(trifluoromethyl)phenyl)propanamide (7b).** Yield: 46.5%, yellow solid, mp 163.1–164.5  $^\circ\text{C}$ .  $[\alpha]_D^{20} = -29$  (c 0.1, AcOEt).  $^1\text{H}$  NMR (400 MHz,  $\text{DMSO}-d_6$ )  $\delta$  10.47 (s, 1H, NH), 8.02–7.96 (m, 2H, NH, ArH), 7.89 (dd,  $J = 7.6, 1.0$  Hz, 1H, ArH), 7.83–7.76 (m, 2H, ArH), 7.71 (dd,  $J = 7.5, 1.3$  Hz, 1H, ArH), 7.57 (t,  $J = 8.0$  Hz, 1H, ArH), 7.44 (d,  $J = 7.8$  Hz, 1H, ArH), 7.34–7.29 (m, 2H, ArH), 7.26 (dd,  $J = 8.1, 6.7$  Hz, 3H, ArH), 7.19 (ddd,  $J = 7.1, 3.8, 1.3$  Hz, 1H, ArH), 5.69 (s, 1H, C=CH), 4.47 (dd,  $J = 14.8, 7.1$  Hz, 1H, CH), 3.30 (d,  $J = 6.9$  Hz, 2H,  $\text{CH}_2$ ).  $^{13}\text{C}$  NMR (101 MHz,  $\text{DMSO}-d_6$ )  $\delta$  181.88, 180.99, 169.21, 147.63, 139.03, 136.91, 134.94, 132.67, 132.53, 130.21, 130.14, 129.24, 129.24, 128.32, 128.32, 126.73, 126.01, 125.39, 123.29, 120.28, 120.25, 115.81, 115.77, 101.07, 57.66, 37.01. HR-MS ( $m/z$ ) (ESI): calcd for  $\text{C}_{26}\text{H}_{19}\text{F}_3\text{N}_2\text{O}_3\text{Na}$  [ $\text{M} + \text{Na}$ ] $^+$ : 465.1421; found: 465.1401. Purity: 99.38%.

**2-((1,4-Dioxo-1,4-dihydronaphthalen-2-yl)amino)-3-phenyl-N-(4-(trifluoromethyl)phenyl)propanamide (7c).** Yield: 45.8%, yellow solid, mp 212.7–213.7  $^\circ\text{C}$ .  $[\alpha]_D^{20} = -32$  (c 0.1, AcOEt).  $^1\text{H}$  NMR (400 MHz,  $\text{DMSO}-d_6$ )  $\delta$  10.50 (s, 1H, NH), 7.98 (d,  $J = 6.9$  Hz, 1H, NH), 7.92–7.86 (m, 1H, ArH), 7.80 (ddd,  $J = 8.6, 6.7, 2.8$  Hz, 3H, ArH), 7.74–7.67 (m, 3H, ArH), 7.35–7.24 (m, 5H, ArH), 7.18 (t,  $J = 7.1$  Hz, 1H, ArH), 5.70 (s, 1H, C=CH), 4.49 (q,  $J = 7.0$  Hz, 1H, CH), 3.30 (d,  $J = 6.8$  Hz, 2H,  $\text{CH}_2$ ).  $^{13}\text{C}$  NMR (101 MHz,  $\text{DMSO}-d_6$ )  $\delta$  181.84, 180.98, 169.27, 147.57, 141.82, 136.83, 134.92, 132.65, 132.50, 130.19, 129.23, 129.23, 128.30, 128.30, 126.72, 126.16, 126.12, 126.00, 125.37, 123.75, 122.93, 119.61, 119.61, 101.06, 57.65, 37.01. HR-MS ( $m/z$ ) (ESI): calcd for  $\text{C}_{26}\text{H}_{19}\text{F}_3\text{N}_2\text{O}_3\text{Na}$  [ $\text{M} + \text{Na}$ ] $^+$ : 487.1240; found: 487.1223. Purity: 96.05%.

2-((1,4-Dioxo-1,4-dihydronaphthalen-2-yl)amino)-N-(2-fluorophenyl)-3-phenylpropanamide (**7d**). Yield: 70.2%, yellow solid, mp 182.5–183.9 °C.  $[\alpha]_D^{20} = -36$  (c 0.1, AcOEt).  $^1\text{H NMR}$  (400 MHz, DMSO- $d_6$ )  $\delta$  10.06 (s, 1H, NH), 7.97 (d,  $J = 7.4$  Hz, 1H, NH), 7.90 (d,  $J = 6.9$  Hz, 1H, ArH), 7.83–7.76 (m, 2H, ArH), 7.72 (td,  $J = 7.5$ , 1.1 Hz, 1H, ArH), 7.34 (d,  $J = 7.2$  Hz, 2H, ArH), 7.27 (dd,  $J = 13.5$ , 6.0 Hz, 4H, ArH), 7.22–7.15 (m, 3H, ArH), 5.73 (s, 1H, C=CH), 4.63 (dd,  $J = 14.0$ , 8.0 Hz, 1H, CH), 3.28 (t,  $J = 6.2$  Hz, 2H, CH $_2$ ).  $^{13}\text{C NMR}$  (101 MHz, DMSO- $d_6$ )  $\delta$  181.86, 181.03, 169.21, 155.17, 152.73, 147.59, 136.93, 134.96, 132.67, 132.52, 130.21, 129.30, 129.30, 128.38, 128.28, 126.69, 126.01, 125.39, 124.53, 124.47, 115.75, 115.56, 101.09, 57.17, 37.18. HR-MS ( $m/z$ ) (ESI): calcd for  $\text{C}_{25}\text{H}_{20}\text{FN}_2\text{O}_3$  [ $\text{M} + \text{H}$ ] $^+$ : 415.1452; found: 415.1437. Purity: 98.24%.

2-((1,4-Dioxo-1,4-dihydronaphthalen-2-yl)amino)-N-(3-fluorophenyl)-3-phenylpropanamide (**7e**). Yield: 61.4%, yellow solid, mp 126.9–128.7 °C.  $[\alpha]_D^{20} = -38$  (c 0.1, AcOEt).  $^1\text{H NMR}$  (400 MHz, DMSO- $d_6$ )  $\delta$  10.42 (s, 1H, NH), 7.97 (d,  $J = 7.5$  Hz, 1H, NH), 7.91–7.85 (m, 1H, ArH), 7.85–7.77 (m, 1H, ArH), 7.72 (td,  $J = 7.5$ , 1.2 Hz, 1H, ArH), 7.54 (dd,  $J = 11.5$ , 1.9 Hz, 1H, ArH), 7.38–7.24 (m, 7H, ArH), 7.18 (t,  $J = 7.1$  Hz, 1H, ArH), 6.92 (td,  $J = 8.4$ , 2.3 Hz, 1H, ArH), 5.67 (s, 1H, C=CH), 4.44 (dd,  $J = 14.7$ , 7.0 Hz, 1H, CH), 3.27 (d,  $J = 6.8$  Hz, 2H, CH $_2$ ).  $^{13}\text{C NMR}$  (101 MHz, DMSO- $d_6$ )  $\delta$  181.99, 181.08, 169.10, 163.37, 160.97, 147.70, 140.09, 139.99, 136.97, 135.08, 132.72, 132.66, 130.70, 130.28, 129.34, 128.42, 126.83, 126.13, 125.49, 115.51, 110.63, 106.67, 101.08, 57.69, 37.10. HR-MS ( $m/z$ ) (ESI): calcd for  $\text{C}_{25}\text{H}_{20}\text{FN}_2\text{O}_3$  [ $\text{M} + \text{H}$ ] $^+$ : 415.1452; found: 415.1437. Purity: 96.84%.

2-((1,4-Dioxo-1,4-dihydronaphthalen-2-yl)amino)-N-(4-fluorophenyl)-3-phenylpropanamide (**7f**). Yield: 76.6%, yellow solid, mp 192.4–194.2 °C.  $[\alpha]_D^{20} = -33$  (c 0.1, AcOEt).  $^1\text{H NMR}$  (400 MHz, DMSO- $d_6$ )  $\delta$  10.22 (s, 1H, NH), 7.97 (dd,  $J = 7.6$ , 1.1 Hz, 1H, NH), 7.89 (dd,  $J = 7.6$ , 1.1 Hz, 1H, ArH), 7.80 (td,  $J = 7.5$ , 1.3 Hz, 1H, ArH), 7.74–7.69 (m, 1H, ArH), 7.59–7.53 (m, 2H, ArH), 7.33–7.22 (m, 5H, ArH), 7.21–7.13 (m, 3H, ArH), 5.69 (s, 1H, C=CH), 4.43 (dd,  $J = 14.8$ , 7.0 Hz, 1H, CH), 3.27 (d,  $J = 6.8$  Hz, 2H, CH $_2$ ).  $^{13}\text{C NMR}$  (101 MHz, DMSO- $d_6$ )  $\delta$  181.83, 181.00, 168.50, 159.57, 157.18, 147.56, 136.96, 134.93, 132.68, 132.49, 130.20, 129.25, 129.25, 128.30, 128.30, 126.69, 126.00, 125.38, 121.64, 121.56, 115.53, 115.31, 100.98, 57.53, 37.13. HR-MS ( $m/z$ ) (ESI): calcd for  $\text{C}_{25}\text{H}_{20}\text{FN}_2\text{O}_3$  [ $\text{M} + \text{H}$ ] $^+$ : 415.1452; found: 415.1436. Purity: 98.52%.

N-(2-Chlorophenyl)-2-((1,4-dioxo-1,4-dihydronaphthalen-2-yl)amino)-3-phenylpropanamide (**7g**). Yield: 71.8%, yellow solid, mp 187.9–189.6 °C.  $[\alpha]_D^{20} = -42$  (c 0.1, AcOEt).  $^1\text{H NMR}$  (400 MHz, DMSO- $d_6$ )  $\delta$  9.88 (s, 1H, NH), 8.00–7.95 (m, 1H, NH), 7.91 (dd,  $J = 7.6$ , 1.0 Hz, 1H, ArH), 7.80 (td,  $J = 7.5$ , 1.3 Hz, 1H, ArH), 7.72 (td,  $J = 7.5$ , 1.3 Hz, 1H, ArH), 7.59 (dd,  $J = 8.0$ , 1.4 Hz, 1H, ArH), 7.49 (dd,  $J = 8.0$ , 1.4 Hz, 1H, ArH), 7.36 (t,  $J = 5.6$  Hz, 2H, ArH), 7.33–7.26 (m, 4H, ArH), 7.25–7.18 (m, 2H, ArH), 5.81 (s, 1H, C=CH), 4.64 (dd,  $J = 14.1$ , 7.9 Hz, 1H, CH), 3.34–3.26 (m, 2H, CH $_2$ ).  $^{13}\text{C NMR}$  (101 MHz, DMSO- $d_6$ )  $\delta$  181.86, 181.03, 169.19, 147.57, 136.94, 134.92, 134.11, 132.66, 132.50, 130.20, 129.55, 129.32, 129.32, 128.32, 128.32, 127.50, 127.11, 126.96, 126.71, 126.53, 125.98, 125.38, 101.41, 57.25, 37.14. HR-MS ( $m/z$ ) (ESI): calcd for  $\text{C}_{25}\text{H}_{20}\text{ClN}_2\text{O}_3$  [ $\text{M} + \text{H}$ ] $^+$ : 431.1157; found: 431.1142. Purity: 96.43%.

N-(3-Chlorophenyl)-2-((1,4-dioxo-1,4-dihydronaphthalen-2-yl)amino)-3-phenylpropanamide (**7h**). Yield: 63.3%, yellow solid, mp 193.0–194.2 °C.  $[\alpha]_D^{20} = -39$  (c 0.1, AcOEt).  $^1\text{H NMR}$  (400 MHz, DMSO- $d_6$ )  $\delta$  10.33 (s, 1H, NH), 7.97 (dd,  $J = 7.6$ , 1.0 Hz, 1H, NH), 7.89 (dd,  $J = 7.6$ , 1.0 Hz, 1H, ArH), 7.80 (td,  $J = 7.5$ , 1.3 Hz, 1H, ArH), 7.75 (t,  $J = 2.0$  Hz, 1H, ArH), 7.72 (td,  $J = 7.5$ , 1.4 Hz, 1H, ArH), 7.44 (ddd,  $J = 8.2$ , 1.9, 1.0 Hz, 1H, ArH), 7.38–7.31 (m, 2H, ArH), 7.31–7.24 (m, 4H, ArH), 7.21–7.12 (m, 2H, ArH), 5.69 (s, 1H, C=CH), 4.44 (q,  $J = 7.0$  Hz, 1H, CH), 3.28 (d,  $J = 6.8$  Hz, 2H, CH $_2$ ).  $^{13}\text{C NMR}$  (101 MHz, DMSO- $d_6$ )  $\delta$  181.85, 180.97, 168.99, 147.58, 139.68, 136.88, 134.92, 133.11, 132.65, 132.50, 130.54, 130.20, 129.23, 129.23, 128.30, 128.30, 126.71, 126.00, 125.38, 123.62, 119.17, 118.07, 101.04, 57.63, 37.02. HR-MS ( $m/z$ ) (ESI): calcd for  $\text{C}_{25}\text{H}_{20}\text{ClN}_2\text{O}_3$  [ $\text{M} + \text{H}$ ] $^+$ : 431.1157; found: 431.1143. Purity: 97.75%.

N-(4-Chlorophenyl)-2-((1,4-dioxo-1,4-dihydronaphthalen-2-yl)amino)-3-phenylpropanamide (**7i**). Yield: 71.3%, yellow solid, mp 196.1–197.5 °C.  $[\alpha]_D^{20} = -38$  (c 0.1, AcOEt).  $^1\text{H NMR}$  (400 MHz, DMSO- $d_6$ )  $\delta$  10.29 (s, 1H, NH), 7.96 (d,  $J = 7.5$  Hz, 1H, NH), 7.89 (d,  $J = 6.9$  Hz, 1H, ArH), 7.79 (dd,  $J = 10.8$ , 4.1 Hz, 1H, ArH), 7.71 (t,  $J = 7.5$  Hz, 1H, ArH), 7.59 (d,  $J = 8.9$  Hz, 2H, ArH), 7.37 (d,  $J = 8.8$  Hz, 2H, ArH), 7.31 (d,  $J = 7.0$  Hz, 2H, ArH), 7.25 (dd,  $J = 12.7$ , 5.0 Hz, 3H, ArH), 7.18 (t,  $J = 7.1$  Hz, 1H, ArH), 5.69 (s, 1H, C=CH), 4.44 (q,  $J = 7.0$  Hz, 1H, CH), 3.27 (d,  $J = 6.8$  Hz, 2H, CH $_2$ ).  $^{13}\text{C NMR}$  (101 MHz, DMSO- $d_6$ )  $\delta$  181.84, 180.98, 168.76, 147.55, 137.20, 136.91, 134.91, 132.66, 132.48, 130.19, 129.24, 129.24, 128.74, 128.74, 128.30, 128.30, 127.54, 126.71, 125.99, 125.38, 121.28, 121.28, 101.01, 57.59, 37.09. HR-MS ( $m/z$ ) (ESI): calcd for  $\text{C}_{25}\text{H}_{19}\text{ClN}_2\text{O}_3\text{Na}$  [ $\text{M} + \text{Na}$ ] $^+$ : 453.0976; found: 453.0958. Purity: 98.24%.

N-(2-Bromophenyl)-2-((1,4-dioxo-1,4-dihydronaphthalen-2-yl)amino)-3-phenylpropanamide (**7j**). Yield: 75.3%, yellow solid, mp 182.4–183.6 °C.  $[\alpha]_D^{20} = -55$  (c 0.1, AcOEt).  $^1\text{H NMR}$  (400 MHz, DMSO- $d_6$ )  $\delta$  9.85 (s, 1H, NH), 7.98 (dd,  $J = 7.6$ , 1.1 Hz, 1H, NH), 7.91 (dd,  $J = 7.6$ , 1.1 Hz, 1H, ArH), 7.82 (td,  $J = 7.5$ , 1.3 Hz, 1H, ArH), 7.76–7.71 (m, 1H, ArH), 7.66 (dd,  $J = 8.0$ , 1.3 Hz, 1H, ArH), 7.51 (dd,  $J = 8.0$ , 1.5 Hz, 1H, ArH), 7.40–7.35 (m, 3H, ArH), 7.32–7.25 (m, 3H, ArH), 7.23–7.19 (m, 1H, ArH), 7.20–7.14 (m, 1H, ArH), 5.81 (s, 1H, C=CH), 4.60 (dd,  $J = 14.3$ , 7.7 Hz, 1H, CH), 3.31 (s, 1H, CH $_2$ ).  $^{13}\text{C NMR}$  (101 MHz, DMSO- $d_6$ )  $\delta$  181.85, 181.02, 169.08, 147.58, 136.99, 135.45, 134.94, 132.73, 132.66, 132.52, 130.20, 129.30, 129.30, 128.33, 128.33, 128.11, 127.58, 127.23, 126.70, 125.99, 125.38, 118.15, 101.47, 57.28, 37.05. HR-MS ( $m/z$ ) (ESI): calcd for  $\text{C}_{25}\text{H}_{20}\text{BrN}_2\text{O}_3$  [ $\text{M} + \text{H}$ ] $^+$ : 475.0652; found: 475.0632. Purity: 98.13%.

N-(3-Bromophenyl)-2-((1,4-dioxo-1,4-dihydronaphthalen-2-yl)amino)-3-phenylpropanamide (**7k**). Yield: 66.9%, yellow solid, mp 186.3–187.7 °C.  $[\alpha]_D^{20} = -57$  (c 0.1, AcOEt).  $^1\text{H NMR}$  (400 MHz, DMSO- $d_6$ )  $\delta$  10.31 (s, 1H, NH), 7.98 (dd,  $J = 7.6$ , 1.0 Hz, 1H, NH), 7.90 (dd,  $J = 8.8$ , 1.3 Hz, 2H, ArH), 7.81 (td,  $J = 7.5$ , 1.4 Hz, 1H, ArH), 7.72 (td,  $J = 7.5$ , 1.4 Hz, 1H, ArH), 7.49 (dt,  $J = 7.1$ , 2.2 Hz, 1H, ArH), 7.32–7.30 (m, 2H, ArH), 7.29–7.24 (m, 4H, ArH), 7.19 (ddd,  $J = 7.1$ , 3.9, 1.4 Hz, 1H, ArH), 5.68 (s, 1H, C=CH), 4.44 (q,  $J = 7.0$  Hz, 1H, CH), 3.28 (d,  $J = 6.8$  Hz, 2H, CH $_2$ ).  $^{13}\text{C NMR}$  (101 MHz, DMSO- $d_6$ )  $\delta$  181.84, 180.97, 168.95, 147.58, 139.81, 136.88, 134.93, 132.65, 132.51, 130.84, 130.19, 129.22, 129.22, 128.30, 128.30, 126.70, 126.51, 126.00, 125.38, 122.02, 121.53, 118.45, 101.03, 57.62, 37.00. HR-MS ( $m/z$ ) (ESI): calcd for  $\text{C}_{25}\text{H}_{20}\text{BrN}_2\text{O}_3$  [ $\text{M} + \text{H}$ ] $^+$ : 475.0652; found: 475.0632. Purity: 98.78%.

N-(4-Bromophenyl)-2-((1,4-dioxo-1,4-dihydronaphthalen-2-yl)amino)-3-phenylpropanamide (**7l**). Yield: 68.5%, yellow solid, mp 210.8–212.1 °C.  $[\alpha]_D^{20} = -46$  (c 0.1, AcOEt).  $^1\text{H NMR}$  (400 MHz, DMSO- $d_6$ )  $\delta$  10.27 (s, 1H, NH), 7.98 (dd,  $J = 7.6$ , 1.0 Hz, 1H, NH), 7.89 (dt,  $J = 8.7$ , 4.4 Hz, 1H, ArH), 7.81 (td,  $J = 7.5$ , 1.3 Hz, 1H, ArH), 7.73 (td,  $J = 7.5$ , 1.3 Hz, 1H, ArH), 7.52 (d,  $J = 2.1$  Hz, 3H, ArH), 7.30 (dd,  $J = 10.4$ , 3.6 Hz, 2H, ArH), 7.27–7.16 (m, 3H, ArH), 5.68 (s, 1H, C=CH), 4.44 (q,  $J = 7.0$  Hz, 1H, CH), 3.27 (d,  $J = 6.8$  Hz, 2H, CH $_2$ ).  $^{13}\text{C NMR}$  (101 MHz, DMSO- $d_6$ )  $\delta$  181.82, 180.99, 168.75, 147.57, 137.60, 136.89, 134.94, 132.66, 132.51, 131.65, 131.65, 130.20, 129.23, 129.23, 128.29, 128.29, 126.69, 126.01, 125.38, 121.64, 121.64, 115.56, 100.98, 57.59, 37.05. HR-MS ( $m/z$ ) (ESI): calcd for  $\text{C}_{25}\text{H}_{20}\text{BrN}_2\text{O}_3$  [ $\text{M} + \text{H}$ ] $^+$ : 475.0652; found: 475.0628. Purity: 98.87%.

2-((1,4-Dioxo-1,4-dihydronaphthalen-2-yl)amino)-N-(2-methoxyphenyl)-3-phenylpropanamide (**7m**). Yield: 72.9%, yellow solid, mp 131.8–133.6 °C.  $[\alpha]_D^{20} = -52$  (c 0.1, AcOEt).  $^1\text{H NMR}$  (400 MHz, DMSO- $d_6$ )  $\delta$  9.54 (s, 1H, NH), 7.96 (d,  $J = 7.0$  Hz, 1H, NH), 7.93–7.82 (m, 2H, ArH), 7.79 (td,  $J = 7.5$ , 1.0 Hz, 1H, ArH), 7.70 (td,  $J = 7.5$ , 1.1 Hz, 1H, ArH), 7.34 (d,  $J = 7.3$  Hz, 2H, ArH), 7.30–7.17 (m, 4H, ArH), 7.09 (dd,  $J = 11.3$ , 4.2 Hz, 1H, ArH), 7.03 (d,  $J = 7.2$  Hz, 1H, ArH), 6.96–6.88 (m, 1H, ArH), 5.79 (s, 1H, C=CH), 4.73 (dd,  $J = 14.0$ , 8.0 Hz, 1H, CH), 3.87–3.67 (m, 3H, CH $_3$ ), 3.25 (t,  $J = 6.1$  Hz, 2H, CH $_2$ ).  $^{13}\text{C NMR}$  (101 MHz, DMSO- $d_6$ )  $\delta$  181.84, 181.07, 168.87, 150.05, 147.47, 137.02, 134.91, 132.68, 132.44, 130.16, 129.31, 129.31, 128.22, 128.22, 126.60, 126.45, 125.96,

125.36, 125.13, 122.37, 120.27, 111.36, 101.26, 57.16, 55.77, 37.31. HR-MS ( $m/z$ ) (ESI): calcd for  $C_{26}H_{23}N_2O_4$  [ $M + H$ ] $^+$ : 427.1652; found: 427.1638. Purity: 95.15%.

2-((1,4-Dioxo-1,4-dihydronaphthalen-2-yl)amino)-*N*-(3-methoxyphenyl)-3-phenylpropanamide (**7n**). Yield: 68.9%, yellow solid, mp 115.3–116.5 °C.  $[\alpha]_D^{20} = -50$  (c 0.1, AcOEt).  $^1H$  NMR (400 MHz, DMSO- $d_6$ )  $\delta$  10.17 (s, 1H, NH), 7.96 (dd,  $J = 7.7$ , 1.1 Hz, 1H, NH), 7.89 (dd,  $J = 7.6$ , 1.0 Hz, 1H, ArH), 7.78 (td,  $J = 7.5$ , 1.3 Hz, 1H, ArH), 7.70 (td,  $J = 7.5$ , 1.4 Hz, 1H, ArH), 7.34–7.30 (m, 2H, ArH), 7.29–7.17 (m, 6H ArH), 7.14–7.10 (m, 1H, ArH), 6.66 (ddd,  $J = 8.2$ , 2.5, 0.7 Hz, 1H, ArH), 5.69 (s, 1H, C=CH), 4.44 (dd,  $J = 14.8$ , 7.1 Hz, 1H, CH), 3.38 (s, 3H, CH $_3$ ), 3.27 (d,  $J = 6.8$  Hz, 2H, CH $_2$ ).  $^{13}C$  NMR (101 MHz, DMSO- $d_6$ )  $\delta$  181.81, 180.98, 168.61, 159.52, 147.50, 139.44, 136.95, 134.89, 132.66, 132.44, 130.17, 129.63, 129.24, 128.28, 126.67, 125.97, 125.36, 111.90, 109.36, 105.43, 100.98, 57.61, 55.00, 37.16. HR-MS ( $m/z$ ) (ESI): calcd for  $C_{26}H_{23}N_2O_4$  [ $M + H$ ] $^+$ : 427.1652; found: 427.1637. Purity: 98.71%.

2-((1,4-Dioxo-1,4-dihydronaphthalen-2-yl)amino)-*N*-(4-methoxyphenyl)-3-phenylpropanamide (**7o**). Yield: 78.9%, yellow solid, mp 149.8–151.7 °C.  $[\alpha]_D^{20} = -45$  (c 0.1, AcOEt).  $^1H$  NMR (400 MHz, DMSO- $d_6$ )  $\delta$  10.06 (s, 1H, NH), 7.94 (dd,  $J = 7.6$ , 1.0 Hz, 1H, NH), 7.88 (dd,  $J = 7.6$ , 0.9 Hz, 1H, ArH), 7.76 (td,  $J = 7.5$ , 1.3 Hz, 1H, ArH), 7.68 (td,  $J = 7.5$ , 1.3 Hz, 1H, ArH), 7.47–7.42 (m, 2H, ArH), 7.30 (dd,  $J = 12.3$ , 5.4 Hz, 2H, ArH), 7.26 (t,  $J = 7.4$  Hz, 2H, ArH), 7.21–7.15 (m, 2H, ArH), 6.92–6.86 (m, 2H, ArH), 5.70 (s, 1H, C=CH), 4.42 (q,  $J = 7.0$  Hz, 1H, CH), 3.70 (d,  $J = 3.7$  Hz, 3H, CH $_3$ ), 3.26 (d,  $J = 6.7$  Hz, 2H, CH $_2$ ).  $^{13}C$  NMR (101 MHz, DMSO- $d_6$ )  $\delta$  181.88, 181.03, 168.11, 155.77, 147.51, 137.00, 134.92, 132.73, 132.47, 131.33, 130.21, 129.31, 129.31, 128.33, 128.33, 126.73, 126.01, 125.41, 121.44, 121.44, 113.98, 113.98, 101.00, 57.50, 55.21, 37.31. HR-MS ( $m/z$ ) (ESI): calcd for  $C_{26}H_{23}N_2O_4$  [ $M + H$ ] $^+$ : 427.1652; found: 427.1637. Purity: 98.91%.

2-((1,4-Dioxo-1,4-dihydronaphthalen-2-yl)amino)-3-phenyl-*N*-(*o*-tolyl)propanamide (**7p**). Yield: 70.5%, yellow solid, mp 119.5–120.7 °C.  $[\alpha]_D^{20} = -61$  (c 0.1, AcOEt).  $^1H$  NMR (400 MHz, DMSO- $d_6$ )  $\delta$  9.54 (s, 1H, NH), 7.98 (d,  $J = 7.1$  Hz, 1H, NH), 7.90 (d,  $J = 7.0$  Hz, 1H, ArH), 7.86–7.78 (m, 2H, ArH), 7.72 (td,  $J = 7.6$ , 1.1 Hz, 1H, ArH), 7.34 (d,  $J = 7.3$  Hz, 2H, ArH), 7.26 (dd,  $J = 15.8$ , 8.0 Hz, 3H, ArH), 7.18 (t,  $J = 7.2$  Hz, 1H, ArH), 7.14–7.07 (m, 1H, ArH), 7.04 (d,  $J = 7.3$  Hz, 1H, ArH), 6.91 (t,  $J = 7.6$  Hz, 1H, ArH), 5.76 (d,  $J = 9.3$  Hz, 1H, C=CH), 4.72 (dd,  $J = 13.9$ , 8.1 Hz, 1H, CH), 3.81 (d,  $J = 4.0$  Hz, 3H, CH $_3$ ), 3.32–3.18 (m, 2H, CH $_2$ ).  $^{13}C$  NMR (101 MHz, DMSO- $d_6$ )  $\delta$  181.85, 181.09, 168.88, 150.05, 147.51, 137.05, 134.97, 132.68, 132.50, 130.18, 129.32, 129.32, 128.23, 128.23, 126.61, 126.42, 126.00, 125.37, 125.15, 122.39, 120.28, 111.37, 101.22, 57.15, 55.78, 37.27. HR-MS ( $m/z$ ) (ESI): calcd for  $C_{26}H_{22}N_2O_3Na$  [ $M + Na$ ] $^+$ : 433.1523; found: 433.150. Purity: 99.77%.

2-((1,4-Dioxo-1,4-dihydronaphthalen-2-yl)amino)-3-phenyl-*N*-(*m*-tolyl)propanamide (**7q**). Yield: 60.2%, yellow solid, mp 147.5–149.0 °C.  $[\alpha]_D^{20} = -59$  (c 0.1, AcOEt).  $^1H$  NMR (400 MHz, DMSO- $d_6$ )  $\delta$  10.12 (s, 1H, NH), 7.98–7.92 (m, 1H, NH), 7.88 (d,  $J = 7.0$  Hz, 1H, ArH), 7.76 (td,  $J = 7.5$ , 1.1 Hz, 1H, ArH), 7.67 (td,  $J = 7.5$ , 1.1 Hz, 1H, ArH), 7.43–7.36 (m, 2H, ArH), 7.33 (d,  $J = 7.2$  Hz, 2H, ArH), 7.30–7.16 (m, 5H, ArH), 6.89 (d,  $J = 7.5$  Hz, 1H, ArH), 5.70 (s, 1H, C=CH), 4.45 (dd,  $J = 14.4$ , 7.3 Hz, 1H, CH), 3.28 (d,  $J = 6.0$  Hz, 2H, CH $_2$ ), 2.26 (s, 3H, CH $_3$ ).  $^{13}C$  NMR (101 MHz, DMSO- $d_6$ )  $\delta$  181.82, 180.99, 168.53, 147.52, 138.22, 138.06, 137.00, 134.87, 132.68, 132.42, 130.17, 129.27, 129.27, 128.66, 128.30, 128.30, 126.69, 125.96, 125.37, 124.59, 120.22, 116.88, 101.01, 57.65, 37.21, 21.12. HR-MS ( $m/z$ ) (ESI): calcd for  $C_{26}H_{23}N_2O_3$  [ $M + H$ ] $^+$ : 411.1703; found: 411.1688. Purity: 98.92%.

2-((1,4-Dioxo-1,4-dihydronaphthalen-2-yl)amino)-3-phenyl-*N*-(*p*-tolyl)propanamide (**7r**). Yield: 70.5%, yellow solid, mp 97.2–99.1 °C.  $[\alpha]_D^{20} = -54$  (c 0.1, AcOEt).  $^1H$  NMR (400 MHz, DMSO- $d_6$ )  $\delta$  10.10 (s, 1H, NH), 7.94 (dd,  $J = 7.6$ , 0.9 Hz, 1H, NH), 7.88 (dd,  $J = 7.6$ , 0.8 Hz, 1H, ArH), 7.76 (td,  $J = 7.5$ , 1.3 Hz, 1H, ArH), 7.67 (td,  $J = 7.5$ , 1.3 Hz, 1H, ArH), 7.45 (d,  $J = 8.4$  Hz, 2H, ArH), 7.32 (d,  $J = 7.1$  Hz, 2H, ArH), 7.26 (t,  $J = 7.5$  Hz, 2H, ArH), 7.18 (dt,  $J = 9.6$ , 6.5 Hz, 2H, ArH), 7.11 (d,  $J = 8.3$  Hz, 2H, ArH), 5.70 (s, 1H, C=CH), 4.44 (dd,  $J = 14.7$ , 7.1 Hz, 1H, CH), 3.27 (d,  $J = 6.8$  Hz, 2H, CH $_2$ ),

2.23 (s, 3H, CH $_3$ ).  $^{13}C$  NMR (101 MHz, DMSO- $d_6$ )  $\delta$  181.79, 180.96, 168.31, 147.46, 136.97, 135.73, 134.84, 132.90, 132.67, 132.39, 130.16, 129.25, 129.25, 129.16, 129.16, 128.27, 128.27, 126.66, 125.94, 125.34, 119.75, 119.75, 100.97, 57.54, 37.25, 20.44. HR-MS ( $m/z$ ) (ESI): calcd for  $C_{26}H_{22}N_2O_3Na$  [ $M + Na$ ] $^+$ : 433.1523; found: 433.1505. Purity: 99.46%.

*N*-(3,5-Dimethylphenyl)-2-((1,4-dioxo-1,4-dihydronaphthalen-2-yl)amino)-3-phenylpropanamide (**7s**). Yield: 63.7%, yellow solid, mp 122.0–123.8 °C.  $[\alpha]_D^{20} = -48$  (c 0.1, AcOEt).  $^1H$  NMR (400 MHz, DMSO- $d_6$ )  $\delta$  10.03 (s, 1H, NH), 7.96 (dd,  $J = 7.6$ , 0.9 Hz, 1H, NH), 7.89 (dd,  $J = 7.6$ , 1.0 Hz, 1H, ArH), 7.79 (td,  $J = 7.5$ , 1.2 Hz, 1H, ArH), 7.70 (td,  $J = 7.5$ , 1.3 Hz, 1H, ArH), 7.34–7.30 (m, 2H, ArH), 7.27 (t,  $J = 7.5$  Hz, 2H, ArH), 7.20 (q,  $J = 7.7$  Hz, 4H, ArH), 6.71 (s, 1H, ArH), 5.68 (s, 1H, C=CH), 4.42 (dd,  $J = 14.2$ , 7.6 Hz, 1H, CH), 3.30–3.17 (m, 2H, CH $_2$ ), 2.22 (s, 6H, 2CH $_3$ ).  $^{13}C$  NMR (101 MHz, DMSO- $d_6$ )  $\delta$  181.80, 180.99, 168.43, 147.53, 138.14, 137.81, 137.81, 137.01, 134.90, 132.67, 132.45, 130.18, 130.18, 129.24, 129.24, 128.29, 128.29, 126.66, 125.97, 125.37, 125.37, 117.40, 100.97, 57.66, 37.17, 21.02, 21.02. HR-MS ( $m/z$ ) (ESI): calcd for  $C_{27}H_{25}N_2O_3$  [ $M + H$ ] $^+$ : 425.1860; found: 425.1843. Purity: 98.52%.

*N*-(4-Bromo-3-fluorophenyl)-2-((1,4-dioxo-1,4-dihydronaphthalen-2-yl)amino)-3-phenylpropanamide (**7t**). Yield: 69.9%, yellow solid, mp 242.5–244.2 °C.  $[\alpha]_D^{20} = -39$  (c 0.1, AcOEt).  $^1H$  NMR (400 MHz, DMSO- $d_6$ )  $\delta$  10.45 (s, 1H, NH), 7.96 (dd,  $J = 7.6$ , 1.0 Hz, 1H, NH), 7.89 (dd,  $J = 7.6$ , 1.0 Hz, 1H, ArH), 7.79 (td,  $J = 7.5$ , 1.3 Hz, 1H, ArH), 7.71 (ddd,  $J = 9.4$ , 5.8, 1.7 Hz, 2H, ArH), 7.64 (t,  $J = 8.4$  Hz, 1H, ArH), 7.29 (ddd,  $J = 18.4$ , 11.7, 4.6 Hz, 6H, ArH), 7.21–7.15 (m, 1H, ArH), 5.68 (s, 1H, C=CH), 4.45 (q,  $J = 7.0$  Hz, 1H, CH), 3.28 (d,  $J = 6.8$  Hz, 2H, CH $_2$ ).  $^{13}C$  NMR (101 MHz, DMSO- $d_6$ )  $\delta$  181.83, 180.94, 169.15, 159.21, 156.79, 147.57, 139.45, 136.84, 134.90, 133.43, 132.62, 132.48, 130.17, 129.21, 129.21, 128.29, 128.29, 126.71, 125.98, 125.36, 116.99, 116.96, 107.79, 101.05, 57.63, 36.95. HR-MS ( $m/z$ ) (ESI): calcd for  $C_{25}H_{17}BrFN_2O_3$  [ $M - H$ ] $^-$ : 491.0412; found: 491.0414. Purity: 97.99%.

*N*-(3,5-Dimethoxyphenyl)-2-((1,4-dioxo-1,4-dihydronaphthalen-2-yl)amino)-3-phenylpropanamide (**7u**). Yield: 73.0%, yellow solid, mp 197.0–198.5 °C.  $[\alpha]_D^{20} = -43$  (c 0.1, AcOEt).  $^1H$  NMR (400 MHz, DMSO- $d_6$ )  $\delta$  10.04 (s, 1H, NH), 7.97 (dd,  $J = 7.6$ , 0.9 Hz, 1H, NH), 7.90 (dd,  $J = 7.6$ , 1.0 Hz, 1H, ArH), 7.81 (td,  $J = 7.5$ , 1.3 Hz, 1H, ArH), 7.72 (td,  $J = 7.5$ , 1.3 Hz, 1H, ArH), 7.29 (dt,  $J = 14.9$ , 4.6 Hz, 4H, ArH), 7.23–7.16 (m, 3H, ArH), 7.08 (dd,  $J = 8.7$ , 2.3 Hz, 1H, ArH), 6.90 (d,  $J = 8.8$  Hz, 1H, ArH), 5.68 (s, 1H, C=CH), 4.41 (dd,  $J = 14.7$ , 7.0 Hz, 1H, CH), 3.72 (d,  $J = 4.7$  Hz, 6H, 2CH $_3$ ), 3.26 (d,  $J = 6.8$  Hz, 2H, CH $_2$ ).  $^{13}C$  NMR (101 MHz, DMSO- $d_6$ )  $\delta$  179.89, 169.77, 160.55, 160.55, 145.26, 140.46, 140.12, 137.17, 133.88, 132.95, 129.23, 129.23, 129.01, 128.45, 128.35, 128.35, 126.68, 125.86, 122.35, 97.89, 97.89, 95.82, 91.41, 57.89, 55.16, 55.16, 37.62. HR-MS ( $m/z$ ) (ESI): calcd for  $C_{27}H_{25}N_2O_5$  [ $M + H$ ] $^+$ : 457.1758; found: 457.1740. Purity: 96.71%.

*N*-(4-Bromo-3-fluorophenyl)-2-((1,4-dioxo-1,4-dihydronaphthalen-2-yl)amino)-3-phenylpropanamide (**7v**). Yield: 55.3%, yellow solid, mp 228.9–230.5 °C.  $[\alpha]_D^{20} = -36$  (c 0.1, AcOEt).  $^1H$  NMR (400 MHz, DMSO- $d_6$ )  $\delta$  10.47 (s, 1H, NH), 7.96 (dd,  $J = 7.6$ , 1.0 Hz, 1H, NH), 7.89 (dd,  $J = 7.6$ , 1.0 Hz, 1H, ArH), 7.79 (td,  $J = 7.5$ , 1.3 Hz, 1H, ArH), 7.71 (ddd,  $J = 8.6$ , 4.9, 1.9 Hz, 2H, ArH), 7.63 (t,  $J = 8.4$  Hz, 1H, ArH), 7.34–7.22 (m, 6H, ArH), 7.21–7.14 (m, 1H, ArH), 5.68 (s, 1H, C=CH), 4.45 (q,  $J = 7.0$  Hz, 1H, CH), 3.28 (d,  $J = 6.8$  Hz, 2H, CH $_2$ ).  $^{13}C$  NMR (101 MHz, DMSO- $d_6$ )  $\delta$  181.84, 180.95, 169.15, 159.21, 156.80, 147.55, 139.35, 136.81, 134.90, 133.42, 132.63, 132.48, 130.17, 129.22, 129.22, 128.30, 128.30, 126.72, 125.98, 125.37, 116.97, 107.54, 101.07, 57.62, 36.98. HR-MS ( $m/z$ ) (ESI): calcd for  $C_{25}H_{19}BrFN_2O_3$  [ $M + H$ ] $^+$ : 493.0558; found: 493.0592. Purity: 96.68%.

*N*-(3,5-Difluorophenyl)-2-((1,4-dioxo-1,4-dihydronaphthalen-2-yl)amino)-3-phenylpropanamide (**7w**). Yield: 65.8%, yellow solid, mp 171.2–173.5 °C.  $[\alpha]_D^{20} = -35$  (c 0.1, AcOEt).  $^1H$  NMR (400 MHz, DMSO- $d_6$ )  $\delta$  10.50 (s, 1H, NH), 7.98–7.94 (m, 1H, NH), 7.89 (dd,  $J = 7.6$ , 1.0 Hz, 1H, ArH), 7.78 (td,  $J = 7.5$ , 1.3 Hz, 1H, ArH), 7.70 (td,  $J = 7.5$ , 1.3 Hz, 1H, ArH), 7.33–7.24 (m, 7H, ArH), 7.22–

7.16 (m, 1H, ArH), 6.96–6.89 (m, 1H, ArH), 5.68 (s, 1H, C=CH), 4.45 (q,  $J = 7.0$  Hz, 1H, CH), 3.28 (d,  $J = 6.8$  Hz, 2H, CH<sub>2</sub>). <sup>13</sup>C NMR (101 MHz, DMSO-*d*<sub>6</sub>)  $\delta$  181.88, 180.95, 169.34, 163.56, 161.14, 147.57, 140.74, 136.80, 134.91, 132.63, 132.50, 130.18, 129.23, 129.23, 128.32, 128.32, 126.74, 125.99, 125.38, 102.69, 102.40, 101.12, 99.05, 57.67, 36.94. HR-MS ( $m/z$ ) (ESI): calcd for C<sub>25</sub>H<sub>19</sub>F<sub>2</sub>N<sub>2</sub>O<sub>3</sub> [M + H]<sup>+</sup>: 433.1358; found: 433.1345. Purity: 98.99%.

**2-((1,4-Dioxo-1,4-dihydronaphthalen-2-yl)amino)-N-(2-fluoro-4-methylphenyl)-3-phenylpropanamide (7x).** Yield: 70.5%, yellow solid, mp 158.2–160.7 °C. [ $\alpha$ ]<sub>D</sub><sup>20</sup> = –41 (c 0.1, AcOEt). <sup>1</sup>H NMR (400 MHz, DMSO-*d*<sub>6</sub>)  $\delta$  9.95 (s, 1H, NH), 7.96 (dd,  $J = 7.7, 1.0$  Hz, 1H, NH), 7.90 (dd,  $J = 7.7, 1.0$  Hz, 1H, ArH), 7.79 (td,  $J = 7.5, 1.3$  Hz, 1H, ArH), 7.70 (td,  $J = 7.5, 1.3$  Hz, 1H, ArH), 7.60 (t,  $J = 8.3$  Hz, 1H, ArH), 7.39–7.32 (m, 2H, ArH), 7.27 (t,  $J = 7.5$  Hz, 2H, ArH), 7.19 (ddd,  $J = 7.2, 6.6, 3.4$  Hz, 2H, ArH), 7.08 (dd,  $J = 11.8, 1.1$  Hz, 1H, ArH), 6.96 (d,  $J = 8.1$  Hz, 1H, ArH), 5.73 (s, 1H, C=CH), 4.60 (dt,  $J = 14.0, 7.1$  Hz, 1H, CH), 3.34–3.20 (m, 2H, CH<sub>2</sub>), 2.27 (s, 3H, CH<sub>3</sub>). <sup>13</sup>C NMR (101 MHz, DMSO-*d*<sub>6</sub>)  $\delta$  181.83, 181.00, 169.03, 155.13, 152.70, 147.51, 136.92, 134.89, 132.67, 132.45, 130.18, 129.29, 129.29, 128.25, 128.25, 126.66, 125.96, 125.36, 124.80, 124.49, 122.55, 122.43, 101.07, 57.11, 37.22, 20.35. HR-MS ( $m/z$ ) (ESI): calcd for C<sub>26</sub>H<sub>22</sub>FN<sub>2</sub>O<sub>3</sub>Na [M + Na]<sup>+</sup>: 451.1428; found: 451.1410. Purity: 98.63%.

**N-(3-Chloro-4-methylphenyl)-2-((1,4-dioxo-1,4-dihydronaphthalen-2-yl)amino)-3-phenylpropanamide (7y).** Yield: 71.2%, yellow solid, mp 99.8–101.4 °C. [ $\alpha$ ]<sub>D</sub><sup>20</sup> = –70 (c 0.1, AcOEt). <sup>1</sup>H NMR (400 MHz, DMSO-*d*<sub>6</sub>)  $\delta$  10.22 (s, 1H, NH), 7.97 (dd,  $J = 7.6, 0.9$  Hz, 1H, NH), 7.89 (dd,  $J = 7.6, 1.0$  Hz, 1H, ArH), 7.80 (td,  $J = 7.5, 1.3$  Hz, 1H, ArH), 7.72 (ddd,  $J = 8.9, 5.6, 1.3$  Hz, 2H, ArH), 7.29 (tdd,  $J = 16.3, 8.6, 3.7$  Hz, 7H, ArH), 7.18 (ddd,  $J = 7.0, 3.8, 1.4$  Hz, 1H, ArH), 5.68 (s, 1H, C=CH), 4.43 (q,  $J = 7.0$  Hz, 1H, CH), 3.27 (d,  $J = 6.8$  Hz, 2H, CH<sub>2</sub>), 2.26 (s, 3H, CH<sub>3</sub>). <sup>13</sup>C NMR (101 MHz, DMSO-*d*<sub>6</sub>)  $\delta$  181.80, 180.95, 168.70, 147.56, 137.34, 136.91, 134.90, 132.99, 132.64, 132.47, 131.24, 130.58, 130.18, 129.22, 129.22, 128.28, 128.28, 126.67, 125.97, 125.36, 119.66, 118.30, 100.98, 57.57, 37.03, 18.94. HR-MS ( $m/z$ ) (ESI): calcd for C<sub>26</sub>H<sub>22</sub>ClN<sub>2</sub>O<sub>3</sub> [M + H]<sup>+</sup>: 445.1313; found: 475.1306. Purity: 98.19%.

**N-(4-Bromo-2-methylphenyl)-2-((1,4-dioxo-1,4-dihydronaphthalen-2-yl)amino)-3-phenylpropanamide (7z).** Yield: 69.8%, yellow solid, mp 78.5–80.3 °C. [ $\alpha$ ]<sub>D</sub><sup>20</sup> = –85 (c 0.1, AcOEt). <sup>1</sup>H NMR (400 MHz, DMSO-*d*<sub>6</sub>)  $\delta$  9.66 (s, 1H, NH), 8.18 (d,  $J = 8.0$  Hz, 1H, NH), 8.05 (d,  $J = 7.3$  Hz, 1H, ArH), 7.73–7.64 (m, 1H, ArH), 7.62–7.53 (m, 1H, ArH), 7.41 (d,  $J = 2.0$  Hz, 1H, ArH), 7.32 (dt,  $J = 14.9, 4.9$  Hz, 5H, ArH), 7.27–7.19 (m, 2H, ArH), 6.69 (s, 1H, C=CH), 6.30 (d,  $J = 7.9$  Hz, 1H, ArH), 4.49 (q,  $J = 7.2$  Hz, 1H, CH), 3.28–3.19 (m, 2H, CH<sub>2</sub>), 2.08 (s, 3H, CH<sub>3</sub>). <sup>13</sup>C NMR (101 MHz, DMSO-*d*<sub>6</sub>)  $\delta$  179.91, 169.88, 145.28, 140.51, 137.17, 135.14, 134.91, 133.92, 132.94, 132.80, 129.34, 129.34, 129.01, 128.82, 128.48, 128.40, 128.40, 127.06, 126.73, 125.86, 122.38, 117.80, 91.77, 57.44, 37.72, 17.46. HR-MS ( $m/z$ ) (ESI): calcd for C<sub>26</sub>H<sub>21</sub>BrN<sub>2</sub>O<sub>3</sub>Na [M + Na]<sup>+</sup>: 511.0628; found: 511.0607. Purity: 97.39%.

**General Procedure for the Preparation of Compounds 8.** To a solution of 1,4-naphthoquinone-2-aminoacylation-substituted anilines (1 mmol) in absolute ethanol (25 mL) was added hydroxylamine hydrochloride (1 mmol). The resulting mixture was refluxed at 80 °C for 12 h. Water (15 mL) was added, and the reaction mixture was extracted with dichloromethane (3 × 20 mL), dried (Na<sub>2</sub>SO<sub>4</sub>), filtered, and concentrated. The residue was purified by flash chromatography (light petroleum/ethyl acetate, V/V = 4:1) to give compounds **8** as a yellow-green solid.

**(Z)-2-((4-(Hydroxyimino)-1-oxo-1,4-dihydronaphthalen-2-yl)amino)-N,3-diphenylpropanamide (8a).** Yield: 50.6%, yellow-green solid, mp 230.0–231.2 °C. [ $\alpha$ ]<sub>D</sub><sup>20</sup> = –36 (c 0.1, AcOEt). <sup>1</sup>H NMR (400 MHz, DMSO-*d*<sub>6</sub>)  $\delta$  10.27 (s, 1H, OH), 8.12 (d,  $J = 7.9$  Hz, 1H, NH), 8.05–7.97 (m, 1H, ArH), 7.70–7.60 (m, 1H, ArH), 7.61–7.52 (m, 1H, ArH), 7.50 (d,  $J = 7.7$  Hz, 2H, ArH), 7.34–7.22 (m, 7H, ArH), 7.18 (td,  $J = 5.7, 2.5$  Hz, 1H, ArH), 7.06 (t,  $J = 7.4$  Hz, 1H, ArH), 6.58 (s, 1H, C=CH), 6.25 (d,  $J = 8.0$  Hz, 1H, NH), 4.35 (dd,  $J = 13.6, 7.8$  Hz, 1H, CH), 3.23–3.12 (m, 2H, CH<sub>2</sub>). <sup>13</sup>C NMR (101

MHz, DMSO-*d*<sub>6</sub>)  $\delta$  180.44, 170.28, 145.80, 140.88, 138.63, 137.39, 134.21, 133.59, 129.67, 129.67, 129.63, 129.38, 129.38, 128.89, 128.79, 128.79, 127.28, 126.36, 124.56, 122.83, 120.28, 120.28, 91.85, 58.27, 38.02. HR-MS ( $m/z$ ) (ESI): calcd for C<sub>25</sub>H<sub>21</sub>N<sub>3</sub>O<sub>3</sub>Na [M + Na]<sup>+</sup>: 434.1475; found: 434.1469. Purity: 98.13%.

**(Z)-2-((4-(Hydroxyimino)-1-oxo-1,4-dihydronaphthalen-2-yl)amino)-3-phenyl-N-(3-(trifluoromethyl)phenyl)propanamide (8b).** Yield: 38.9%, yellow-green solid, mp 122.2–123.5 °C. [ $\alpha$ ]<sub>D</sub><sup>20</sup> = –26 (c 0.1, AcOEt). <sup>1</sup>H NMR (400 MHz, DMSO-*d*<sub>6</sub>)  $\delta$  12.35 (s, 1H, OH), 10.54 (s, 1H, NH), 8.16 (d,  $J = 7.8$  Hz, 1H, NH), 8.10–7.98 (m, 2H, ArH), 7.78 (d,  $J = 8.3$  Hz, 1H, ArH), 7.71–7.64 (m, 1H, ArH), 7.60–7.53 (m, 2H, ArH), 7.43 (d,  $J = 8.2$  Hz, 1H, ArH), 7.35–7.25 (m, 4H, ArH), 7.20 (t,  $J = 7.0$  Hz, 1H, ArH), 6.60 (s, 1H, C=CH), 6.36 (d,  $J = 8.1$  Hz, 1H, NH), 4.40 (dd,  $J = 14.4, 7.1$  Hz, 1H, CH), 3.24 (d,  $J = 6.8$  Hz, 2H, CH<sub>2</sub>). <sup>13</sup>C NMR (101 MHz, DMSO-*d*<sub>6</sub>)  $\delta$  179.85, 170.32, 145.23, 140.48, 139.19, 137.08, 133.86, 132.95, 130.16, 129.23, 129.23, 129.01, 128.45, 128.37, 128.37, 126.72, 125.85, 125.42, 123.18, 122.34, 120.18, 115.69, 115.65, 91.42, 57.95, 37.50. HR-MS ( $m/z$ ) (ESI): calcd for C<sub>26</sub>H<sub>20</sub>F<sub>3</sub>N<sub>3</sub>O<sub>3</sub>Na [M + Na]<sup>+</sup>: 502.1349; found: 502.1341. Purity: 95.55%.

**(Z)-2-((4-(Hydroxyimino)-1-oxo-1,4-dihydronaphthalen-2-yl)amino)-3-phenyl-N-(4-(trifluoromethyl)phenyl)propanamide (8c).** Yield: 48.2%, yellow-green solid, mp 197.1–198.7 °C. [ $\alpha$ ]<sub>D</sub><sup>20</sup> = –28 (c 0.1, AcOEt). <sup>1</sup>H NMR (400 MHz, DMSO-*d*<sub>6</sub>)  $\delta$  12.33 (s, 1H, OH), 10.57 (s, 1H, NH), 8.16 (dd,  $J = 8.0, 0.6$  Hz, 1H, ArH), 8.06 (dd,  $J = 7.9, 1.0$  Hz, 1H, ArH), 7.78 (d,  $J = 8.6$  Hz, 2H, ArH), 7.67 (dd,  $J = 11.2, 5.2$  Hz, 3H, ArH), 7.60–7.54 (m, 1H, ArH), 7.35–7.24 (m, 4H, ArH), 7.20 (ddd,  $J = 6.7, 3.9, 1.7$  Hz, 1H, ArH), 6.60 (s, 1H, C=CH), 6.36 (d,  $J = 8.2$  Hz, 1H, NH), 4.43 (q,  $J = 7.0$  Hz, 1H, CH), 3.24 (d,  $J = 6.7$  Hz, 2H, CH<sub>2</sub>). <sup>13</sup>C NMR (101 MHz, DMSO-*d*<sub>6</sub>)  $\delta$  179.84, 170.34, 145.21, 141.99, 140.42, 136.99, 133.85, 132.93, 129.21, 129.21, 128.99, 128.42, 128.33, 128.33, 126.69, 126.18, 126.14, 125.83, 123.94, 123.62, 122.32, 119.49, 119.49, 91.42, 57.88, 37.46. HR-MS ( $m/z$ ) (ESI): calcd for C<sub>26</sub>H<sub>21</sub>F<sub>3</sub>N<sub>3</sub>O<sub>3</sub> [M + H]<sup>+</sup>: 480.1530; found: 480.1521. Purity: 98.05%.

**(Z)-N-(2-Fluorophenyl)-2-((4-(hydroxyimino)-1-oxo-1,4-dihydronaphthalen-2-yl)amino)-3-phenylpropanamide (8d).** Yield: 55.3%, yellow-green solid, mp 226.5–228.2 °C. [ $\alpha$ ]<sub>D</sub><sup>20</sup> = –33 (c 0.1, AcOEt). <sup>1</sup>H NMR (400 MHz, DMSO-*d*<sub>6</sub>)  $\delta$  12.38 (s, 1H, OH), 10.09 (s, 1H, NH), 8.16 (d,  $J = 7.8$  Hz, 1H, ArH), 8.04 (d,  $J = 7.1$  Hz, 1H, ArH), 7.77 (td,  $J = 7.8, 2.9$  Hz, 1H, ArH), 7.70–7.65 (m, 1H, ArH), 7.60–7.53 (m, 1H, ArH), 7.28 (dt,  $J = 9.5, 4.4$  Hz, 5H, ArH), 7.18 (ddd,  $J = 9.7, 8.9, 3.2$  Hz, 3H, ArH), 6.64 (s, 1H, C=CH), 6.33 (d,  $J = 8.3$  Hz, 1H, NH), 4.57 (dd,  $J = 14.6, 7.1$  Hz, 1H, CH), 3.21 (d,  $J = 6.8$  Hz, 2H, CH<sub>2</sub>). <sup>13</sup>C NMR (101 MHz, DMSO-*d*<sub>6</sub>)  $\delta$  180.05, 170.36, 155.27, 152.83, 145.41, 140.57, 137.21, 133.99, 133.11, 129.41, 129.41, 129.16, 128.54, 128.45, 128.45, 126.82, 125.97, 125.50, 124.59, 122.48, 115.87, 115.68, 91.65, 57.42, 37.71. HR-MS ( $m/z$ ) (ESI): calcd for C<sub>25</sub>H<sub>20</sub>FN<sub>3</sub>O<sub>3</sub>Na [M + Na]<sup>+</sup>: 452.1381; found: 452.1380. Purity: 99.66%.

**(Z)-N-(3-Fluorophenyl)-2-((4-(hydroxyimino)-1-oxo-1,4-dihydronaphthalen-2-yl)amino)-3-phenylpropanamide (8e).** Yield: 49.9%, yellow-green solid, mp 201.8–203.5 °C. [ $\alpha$ ]<sub>D</sub><sup>20</sup> = –30 (c 0.1, AcOEt). <sup>1</sup>H NMR (400 MHz, DMSO-*d*<sub>6</sub>)  $\delta$  12.37 (s, 1H, OH), 10.45 (s, 1H, NH), 8.19–8.14 (m, 1H, ArH), 8.05 (dd,  $J = 7.9, 0.8$  Hz, 1H, ArH), 7.71–7.63 (m, 1H, ArH), 7.60–7.52 (m, 2H, ArH), 7.36 (dd,  $J = 11.4, 4.7$  Hz, 1H, ArH), 7.33–7.25 (m, 6H, ArH), 7.23–7.16 (m, 1H, ArH), 6.90 (td,  $J = 8.2, 1.8$  Hz, 1H, ArH), 6.60 (s, 1H, C=CH), 6.35 (d,  $J = 8.2$  Hz, 1H, NH), 4.40 (q,  $J = 7.0$  Hz, 1H, CH), 3.22 (d,  $J = 6.7$  Hz, 2H, CH<sub>2</sub>). <sup>13</sup>C NMR (101 MHz, DMSO-*d*<sub>6</sub>)  $\delta$  179.89, 170.13, 163.36, 160.96, 145.27, 140.48, 140.23, 140.12, 137.11, 133.89, 132.98, 130.61, 129.26, 129.03, 128.47, 128.39, 126.74, 125.89, 122.37, 115.38, 110.42, 106.55, 91.44, 57.90, 37.55. HR-MS ( $m/z$ ) (ESI): calcd for C<sub>25</sub>H<sub>20</sub>FN<sub>3</sub>O<sub>3</sub>Na [M + Na]<sup>+</sup>: 452.1381; found: 452.1377. Purity: 96.24%.

**(Z)-N-(4-Fluorophenyl)-2-((4-(hydroxyimino)-1-oxo-1,4-dihydronaphthalen-2-yl)amino)-3-phenylpropanamide (8f).** Yield: 56.6%, yellow-green solid, mp 181.7–182.9 °C. [ $\alpha$ ]<sub>D</sub><sup>20</sup> = –29 (c 0.1, AcOEt). <sup>1</sup>H NMR (400 MHz, DMSO-*d*<sub>6</sub>)  $\delta$  12.36 (s, 1H, OH), 10.35 (s, 1H, NH), 8.16 (d,  $J = 7.8$  Hz, 1H, ArH), 8.05 (d,  $J = 7.1$  Hz, 1H, ArH),

7.74–7.64 (m, 1H, ArH), 7.61–7.51 (m, 4H, ArH), 7.34–7.25 (m, 5H, ArH), 7.17 (dt,  $J = 17.7, 7.9$  Hz, 4H, ArH), 6.61 (s, 1H, C=CH), 6.32 (d,  $J = 5.4$  Hz, 1H, NH), 4.39 (d,  $J = 4.7$  Hz, 1H, CH), 3.22 (d,  $J = 6.8$  Hz, 2H, CH<sub>2</sub>). <sup>13</sup>C NMR (101 MHz, DMSO-*d*<sub>6</sub>)  $\delta$  179.93, 169.64, 159.56, 157.17, 145.30, 140.48, 137.19, 134.88, 134.85, 133.93, 132.96, 129.29, 129.02, 128.49, 128.38, 126.72, 125.89, 122.39, 121.58, 121.50, 115.56, 115.34, 91.43, 57.79, 37.66. HR-MS (*m/z*) (ESI): calcd for C<sub>25</sub>H<sub>20</sub>FN<sub>3</sub>O<sub>3</sub> Na [M + Na]<sup>+</sup>: 452.1381; found: 452.1381. Purity: 98.42%.

(*Z*)-*N*-(2-Chlorophenyl)-2-((4-(hydroxyimino)-1-oxo-1,4-dihydronaphthalen-2-yl)amino)-3-phenylpropanamide (**8g**). Yield: 55.9%, yellow-green solid, mp 133.7–134.6 °C. [ $\alpha$ ]<sub>D</sub><sup>20</sup> = –37 (c 0.1, AcOEt). <sup>1</sup>H NMR (400 MHz, DMSO-*d*<sub>6</sub>)  $\delta$  12.36 (s, 1H, OH), 9.86 (s, 1H, NH), 8.17 (d,  $J = 8.0$  Hz, 1H, ArH), 8.05 (dd,  $J = 7.9, 0.9$  Hz, 1H, ArH), 7.71–7.65 (m, 1H, ArH), 7.62 (dd,  $J = 8.0, 1.4$  Hz, 1H, ArH), 7.59–7.54 (m, 1H, ArH), 7.48 (dd,  $J = 8.0, 1.3$  Hz, 1H, ArH), 7.32 (ddd,  $J = 9.9, 7.3, 5.4$  Hz, 5H, ArH), 7.20 (ddd,  $J = 9.2, 3.5, 1.5$  Hz, 2H, ArH), 6.68 (s, 1H, C=CH), 6.39 (d,  $J = 8.1$  Hz, 1H, NH), 4.55 (dd,  $J = 14.5, 7.1$  Hz, 1H, CH), 3.27 (d,  $J = 6.8$  Hz, 2H, CH<sub>2</sub>). <sup>13</sup>C NMR (101 MHz, DMSO-*d*<sub>6</sub>)  $\delta$  179.92, 170.18, 145.28, 140.51, 137.21, 134.30, 133.92, 132.97, 129.57, 129.33, 129.33, 129.03, 128.47, 128.39, 128.39, 127.54, 126.96, 126.83, 126.72, 126.29, 125.86, 122.38, 91.89, 57.52, 37.54. HR-MS (*m/z*) (ESI): calcd for C<sub>25</sub>H<sub>21</sub>ClN<sub>3</sub>O<sub>3</sub> Na [M + H]<sup>+</sup>: 446.1266; found: 446.1267. Purity: 95.24%.

(*Z*)-*N*-(3-Chlorophenyl)-2-((4-(hydroxyimino)-1-oxo-1,4-dihydronaphthalen-2-yl)amino)-3-phenylpropanamide (**8h**). Yield: 48.6%, yellow-green solid, mp 160.2–161.9 °C. [ $\alpha$ ]<sub>D</sub><sup>20</sup> = –35 (c 0.1, AcOEt). <sup>1</sup>H NMR (400 MHz, DMSO-*d*<sub>6</sub>)  $\delta$  12.36 (s, 1H, OH), 10.42 (s, 1H, NH), 8.16 (d,  $J = 7.9$  Hz, 1H, ArH), 8.05 (d,  $J = 7.6$  Hz, 1H, ArH), 7.75 (s, 1H, ArH), 7.67 (dd,  $J = 11.2, 4.0$  Hz, 1H, ArH), 7.57 (t,  $J = 7.3$  Hz, 1H, ArH), 7.43 (d,  $J = 8.5$  Hz, 1H, ArH), 7.37–7.25 (m, 5H, ArH), 7.19 (t,  $J = 6.6$  Hz, 1H, ArH), 7.13 (dd,  $J = 7.9, 0.9$  Hz, 1H, ArH), 6.59 (s, 1H, C=CH), 6.33 (d,  $J = 8.1$  Hz, 1H, NH), 4.39 (dd,  $J = 14.4, 7.0$  Hz, 1H, CH), 3.22 (d,  $J = 6.7$  Hz, 2H, CH<sub>2</sub>). <sup>13</sup>C NMR (101 MHz, DMSO-*d*<sub>6</sub>)  $\delta$  179.87, 170.11, 145.24, 140.45, 139.87, 137.06, 133.87, 133.14, 132.96, 130.59, 129.24, 129.24, 129.02, 128.45, 128.37, 128.37, 126.72, 125.86, 123.53, 122.35, 119.10, 118.02, 91.44, 57.89, 37.50. HR-MS (*m/z*) (ESI): calcd for C<sub>25</sub>H<sub>21</sub>ClN<sub>3</sub>O<sub>3</sub> [M + H]<sup>+</sup>: 446.1266; found: 446.1252. Purity: 95.42%.

(*Z*)-*N*-(4-Chlorophenyl)-2-((4-(hydroxyimino)-1-oxo-1,4-dihydronaphthalen-2-yl)amino)-3-phenylpropanamide (**8i**). Yield: 53.2%, yellow-green solid, mp 194.5–196.0 °C. [ $\alpha$ ]<sub>D</sub><sup>20</sup> = –33 (c 0.1, AcOEt). <sup>1</sup>H NMR (400 MHz, DMSO-*d*<sub>6</sub>)  $\delta$  12.35 (s, 1H, OH), 10.36 (s, 1H, NH), 8.17 (d,  $J = 7.9$  Hz, 1H, ArH), 8.05 (dd,  $J = 7.9, 0.9$  Hz, 1H, ArH), 7.70–7.63 (m, 1H, ArH), 7.61–7.54 (m, 3H, ArH), 7.40–7.34 (m, 2H, ArH), 7.32–7.24 (m, 4H, ArH), 7.19 (dt,  $J = 9.2, 4.2$  Hz, 1H, ArH), 6.61 (s, 1H, C=CH), 6.33 (d,  $J = 8.1$  Hz, 1H, NH), 4.40 (dd,  $J = 14.5, 7.0$  Hz, 1H, CH), 3.22 (d,  $J = 6.7$  Hz, 2H, CH<sub>2</sub>). <sup>13</sup>C NMR (101 MHz, DMSO-*d*<sub>6</sub>)  $\delta$  179.89, 169.85, 145.27, 140.45, 137.39, 137.09, 133.89, 132.92, 129.24, 129.24, 128.98, 128.75, 128.75, 128.46, 128.35, 128.35, 127.43, 126.69, 125.85, 122.35, 121.21, 121.21, 91.43, 57.83, 37.60. HR-MS (*m/z*) (ESI): calcd for C<sub>25</sub>H<sub>20</sub>ClN<sub>3</sub>O<sub>3</sub> Na [M + Na]<sup>+</sup>: 468.1085; found: 468.1084. Purity: 6.41%.

(*Z*)-*N*-(2-Bromophenyl)-2-((4-(hydroxyimino)-1-oxo-1,4-dihydronaphthalen-2-yl)amino)-3-phenylpropanamide (**8j**). Yield: 57.2%, yellow-green solid, mp 160.6–162.3 °C. [ $\alpha$ ]<sub>D</sub><sup>20</sup> = –49 (c 0.1, AcOEt). <sup>1</sup>H NMR (400 MHz, DMSO-*d*<sub>6</sub>)  $\delta$  12.30 (s, 1H, OH), 9.75 (s, 1H, NH), 8.11 (dd,  $J = 8.0, 0.6$  Hz, 1H, ArH), 7.99 (dd,  $J = 7.9, 1.0$  Hz, 1H, ArH), 7.65–7.56 (m, 2H, ArH), 7.50 (ddd,  $J = 9.6, 7.0, 1.4$  Hz, 2H, ArH), 7.32–7.27 (m, 3H, ArH), 7.23 (t,  $J = 7.5$  Hz, 2H, ArH), 7.18–7.12 (m, 1H, ArH), 7.08 (td,  $J = 7.8, 1.6$  Hz, 1H, ArH), 6.61 (s, 1H, C=CH), 6.33 (d,  $J = 8.1$  Hz, 1H, NH), 4.44 (dd,  $J = 13.8, 7.8$  Hz, 1H, CH), 3.25–3.19 (m, 2H, CH<sub>2</sub>). <sup>13</sup>C NMR (101 MHz, DMSO-*d*<sub>6</sub>)  $\delta$  179.91, 170.10, 145.28, 140.55, 137.27, 135.63, 133.92, 132.98, 132.76, 129.32, 129.32, 129.04, 128.47, 128.42, 128.42, 128.17, 127.45, 126.94, 126.73, 125.86, 122.39, 117.95, 91.96, 57.60,

37.48. HR-MS (*m/z*) (ESI): calcd for C<sub>25</sub>H<sub>21</sub>BrN<sub>3</sub>O<sub>3</sub> [M + H]<sup>+</sup>: 490.0761; found: 490.0744. Purity: 98.33%.

(*Z*)-*N*-(3-Bromophenyl)-2-((4-(hydroxyimino)-1-oxo-1,4-dihydronaphthalen-2-yl)amino)-3-phenylpropanamide (**8k**). Yield: 51.1%, yellow-green solid, mp 137.1–138.3 °C. [ $\alpha$ ]<sub>D</sub><sup>20</sup> = –46 (c 0.1, AcOEt). <sup>1</sup>H NMR (400 MHz, DMSO-*d*<sub>6</sub>)  $\delta$  12.35 (s, 1H, OH), 10.38 (s, 1H, NH), 8.16 (d,  $J = 7.5$  Hz, 1H, ArH), 8.05 (dd,  $J = 7.9, 1.0$  Hz, 1H, ArH), 7.88 (d,  $J = 1.8$  Hz, 1H, ArH), 7.68 (td,  $J = 7.8, 1.4$  Hz, 1H, ArH), 7.62–7.53 (m, 1H, ArH), 7.47 (dt,  $J = 7.1, 2.1$  Hz, 1H, ArH), 7.34–7.25 (m, 6H, ArH), 7.20 (ddt,  $J = 8.5, 5.5, 2.9$  Hz, 1H, ArH), 6.58 (s, 1H, C=CH), 6.33 (d,  $J = 8.1$  Hz, 1H, NH), 4.37 (dd,  $J = 14.5, 7.1$  Hz, 1H, CH), 3.22 (d,  $J = 6.8$  Hz, 2H, CH<sub>2</sub>). <sup>13</sup>C NMR (101 MHz, DMSO-*d*<sub>6</sub>)  $\delta$  179.88, 170.10, 145.25, 140.47, 140.01, 137.06, 133.87, 132.99, 130.91, 129.24, 129.24, 129.05, 128.45, 128.39, 128.39, 126.74, 126.45, 125.88, 122.36, 121.96, 121.60, 118.41, 91.44, 57.91, 37.51. HR-MS (*m/z*) (ESI): calcd for C<sub>25</sub>H<sub>21</sub>BrN<sub>3</sub>O<sub>3</sub> [M + H]<sup>+</sup>: 490.0761; found: 490.0760. Purity: 97.18%.

(*Z*)-*N*-(4-Bromophenyl)-2-((4-(hydroxyimino)-1-oxo-1,4-dihydronaphthalen-2-yl)amino)-3-phenylpropanamide (**8l**). Yield: 54.1%, yellow-green solid, mp 180.9–182.4 °C. [ $\alpha$ ]<sub>D</sub><sup>20</sup> = –42 (c 0.1, AcOEt). <sup>1</sup>H NMR (400 MHz, DMSO-*d*<sub>6</sub>)  $\delta$  12.35 (s, 1H, OH), 10.35 (s, 1H, NH), 8.16 (d,  $J = 7.9$  Hz, 1H, ArH), 8.09–8.01 (m, 1H, ArH), 7.73–7.61 (m, 1H, ArH), 7.62–7.47 (m, 5H, ArH), 7.28 (t,  $J = 7.3$  Hz, 4H, ArH), 7.19 (dt,  $J = 9.2, 4.2$  Hz, 1H, ArH), 6.60 (s, 1H, C=CH), 6.33 (d,  $J = 8.1$  Hz, 1H, NH), 4.39 (q,  $J = 7.0$  Hz, 1H, CH), 3.22 (d,  $J = 6.7$  Hz, 2H, CH<sub>2</sub>). <sup>13</sup>C NMR (101 MHz, DMSO-*d*<sub>6</sub>)  $\delta$  179.91, 169.90, 145.29, 140.46, 137.82, 137.09, 133.90, 132.97, 131.69, 131.69, 129.26, 129.26, 129.03, 128.47, 128.38, 128.38, 126.73, 125.89, 122.37, 121.60, 121.60, 115.49, 91.43, 57.88, 37.59. HR-MS (*m/z*) (ESI): calcd for C<sub>25</sub>H<sub>20</sub>BrN<sub>3</sub>O<sub>3</sub> Na [M + Na]<sup>+</sup>: 512.0580; found: 512.0580. Purity: 96.35%.

(*Z*)-2-((4-(Hydroxyimino)-1-oxo-1,4-dihydronaphthalen-2-yl)amino)-*N*-(2-methoxyphenyl)-3-phenylpropanamide (**8m**). Yield: 54.8%, yellow solid, mp 183.3–184.4 °C. [ $\alpha$ ]<sub>D</sub><sup>20</sup> = –47 (c 0.1, AcOEt). <sup>1</sup>H NMR (400 MHz, DMSO-*d*<sub>6</sub>)  $\delta$  12.35 (s, 1H, OH), 9.49 (s, 1H, NH), 8.17 (dd,  $J = 8.0, 0.6$  Hz, 1H, ArH), 8.06 (dd,  $J = 7.9, 1.0$  Hz, 1H, ArH), 7.88 (dd,  $J = 8.0, 1.5$  Hz, 1H, ArH), 7.71–7.64 (m, 1H, ArH), 7.61–7.51 (m, 1H, ArH), 7.34–7.31 (m, 2H, ArH), 7.26 (t,  $J = 7.4$  Hz, 2H, ArH), 7.21–7.16 (m, 1H, ArH), 7.11–7.05 (m, 1H, ArH), 7.02 (dd,  $J = 8.2, 1.3$  Hz, 1H, ArH), 6.93–6.88 (m, 1H, ArH), 6.65 (s, 1H, C=CH), 6.41 (d,  $J = 8.3$  Hz, 1H, NH), 4.63 (dd,  $J = 14.3, 7.4$  Hz, 1H, CH), 3.76 (s, 3H, CH<sub>3</sub>), 3.21 (d,  $J = 6.9$  Hz, 2H, CH<sub>2</sub>). <sup>13</sup>C NMR (101 MHz, DMSO-*d*<sub>6</sub>)  $\delta$  179.92, 169.74, 149.85, 145.27, 140.48, 137.34, 133.91, 132.92, 129.30, 129.30, 128.98, 128.44, 128.25, 128.25, 126.65, 126.56, 125.82, 124.91, 122.35, 122.00, 120.33, 111.38, 91.65, 57.43, 55.80, 37.58. HR-MS (*m/z*) (ESI): calcd for C<sub>26</sub>H<sub>24</sub>N<sub>3</sub>O<sub>4</sub> [M + H]<sup>+</sup>: 442.1761; found: 442.1748. Purity: 98.43%.

(*Z*)-2-((4-(Hydroxyimino)-1-oxo-1,4-dihydronaphthalen-2-yl)amino)-*N*-(3-methoxyphenyl)-3-phenylpropanamide (**8n**). Yield: 50.6%, yellow-green solid, mp 115.4–117.2 °C. [ $\alpha$ ]<sub>D</sub><sup>20</sup> = –45 (c 0.1, AcOEt). <sup>1</sup>H NMR (400 MHz, DMSO-*d*<sub>6</sub>)  $\delta$  12.34 (s, 1H, OH), 10.21 (s, 1H, NH), 8.16 (d,  $J = 7.5$  Hz, 1H, ArH), 8.05 (dd,  $J = 7.9, 1.0$  Hz, 1H, ArH), 7.71–7.65 (m, 1H, ArH), 7.60–7.54 (m, 1H, ArH), 7.32–7.18 (m, 7H, ArH), 7.12–7.07 (m, 1H, ArH), 6.65 (dd,  $J = 8.2, 1.9$  Hz, 1H, ArH), 6.60 (s, 1H, C=CH), 6.30 (d,  $J = 8.2$  Hz, 1H, NH), 4.38 (dd,  $J = 14.3, 7.3$  Hz, 1H, CH), 3.72 (s, 3H, CH<sub>3</sub>), 3.20 (d,  $J = 6.8$  Hz, 2H, CH<sub>2</sub>). <sup>13</sup>C NMR (101 MHz, DMSO-*d*<sub>6</sub>)  $\delta$  179.90, 169.71, 159.56, 145.26, 140.45, 139.62, 137.17, 133.88, 132.96, 129.67, 129.24, 129.24, 129.02, 128.45, 128.35, 128.35, 126.68, 125.86, 122.35, 111.89, 109.29, 105.38, 91.40, 57.83, 55.05, 37.63. HR-MS (*m/z*) (ESI): calcd for C<sub>26</sub>H<sub>24</sub>N<sub>3</sub>O<sub>4</sub> [M + H]<sup>+</sup>: 442.1761; found: 442.1760. Purity: 97.69%.

(*Z*)-2-((4-(Hydroxyimino)-1-oxo-1,4-dihydronaphthalen-2-yl)amino)-*N*-(4-methoxyphenyl)-3-phenylpropanamide (**8o**). Yield: 55.7%, yellow-green solid, mp 93.3–94.5 °C. [ $\alpha$ ]<sub>D</sub><sup>20</sup> = –41 (c 0.1, AcOEt). <sup>1</sup>H NMR (400 MHz, DMSO-*d*<sub>6</sub>)  $\delta$  12.33 (s, 1H, OH), 10.06 (s, 1H, NH), 8.16 (d,  $J = 7.6$  Hz, 1H, ArH), 8.05 (dd,  $J = 7.9, 1.0$  Hz, 1H, ArH), 7.73–7.64 (m, 1H, ArH), 7.62–7.53 (m, 1H, ArH), 7.51–7.38 (m, 2H, ArH), 7.33–7.26 (m, 4H, ArH), 7.20 (dd,  $J = 5.8, 2.8$

Hz, 1H, ArH), 6.97–6.82 (m, 2H, ArH), 6.59 (s, 1H, C=CH), 6.28 (d,  $J = 8.1$  Hz, 1H, NH), 4.35 (dd,  $J = 14.4, 7.0$  Hz, 1H, CH), 3.19 (d,  $J = 6.7$  Hz, 2H, CH<sub>2</sub>). <sup>13</sup>C NMR (101 MHz, DMSO-*d*<sub>6</sub>)  $\delta$  179.91, 169.12, 155.64, 145.28, 140.44, 137.22, 133.90, 132.95, 131.50, 129.25, 129.25, 129.01, 128.46, 128.34, 128.34, 126.66, 125.86, 122.35, 121.30, 121.30, 113.96, 113.96, 91.35, 57.67, 55.23, 37.69. HR-MS ( $m/z$ ) (ESI): calcd for C<sub>26</sub>H<sub>24</sub>N<sub>3</sub>O<sub>4</sub> [M + H]<sup>+</sup>: 442.1761; found: 442.1761. Purity: 98.51%.

(*Z*)-2-((4-(Hydroxyimino)-1-oxo-1,4-dihydronaphthalen-2-yl)amino)-3-phenyl-*N*-(*o*-tolyl)propanamide (**8p**). Yield: 50.1%, yellow-green solid, mp 230.4–231.7 °C. [ $\alpha$ ]<sub>D</sub><sup>20</sup> = –56 (c 0.1, AcOEt). <sup>1</sup>H NMR (400 MHz, DMSO-*d*<sub>6</sub>)  $\delta$  12.37 (s, 1H, OH), 9.62 (s, 1H, NH), 8.18 (d,  $J = 7.9$  Hz, 1H, ArH), 8.06 (d,  $J = 7.1$  Hz, 1H, ArH), 7.72–7.66 (m, 1H, ArH), 7.60–7.54 (m, 1H, ArH), 7.38–7.22 (m, 6H, ArH), 7.20–7.06 (m, 3H, ArH), 6.71 (s, 1H, C=CH), 6.32 (d,  $J = 8.0$  Hz, 1H, NH), 4.53–4.43 (m, 1H, CH), 3.28–3.21 (m, 2H, CH<sub>2</sub>), 2.09 (s, 3H, CH<sub>3</sub>). <sup>13</sup>C NMR (101 MHz, DMSO-*d*<sub>6</sub>)  $\delta$  179.93, 169.68, 145.28, 140.53, 137.28, 135.68, 133.92, 132.94, 132.19, 130.37, 129.34, 129.34, 129.01, 128.49, 128.39, 128.39, 126.70, 126.00, 125.85, 125.65, 125.28, 122.37, 91.72, 57.46, 37.76, 17.76. HR-MS ( $m/z$ ) (ESI): calcd for C<sub>26</sub>H<sub>23</sub>N<sub>3</sub>O<sub>3</sub> Na [M + Na]<sup>+</sup>: 448.1632; found: 448.1628. Purity: 99.28%.

(*Z*)-2-((4-(Hydroxyimino)-1-oxo-1,4-dihydronaphthalen-2-yl)amino)-3-phenyl-*N*-(*m*-tolyl)propanamide (**8q**). Yield: 49.0%, yellow-green solid, mp 124.5–125.6 °C. [ $\alpha$ ]<sub>D</sub><sup>20</sup> = –54 (c 0.1, AcOEt). <sup>1</sup>H NMR (400 MHz, DMSO-*d*<sub>6</sub>)  $\delta$  12.35 (s, 1H, OH), 10.15 (s, 1H, NH), 8.16 (d,  $J = 7.6$  Hz, 1H, ArH), 8.05 (dd,  $J = 7.9, 0.9$  Hz, 1H, ArH), 7.73–7.63 (m, 1H, ArH), 7.64–7.48 (m, 1H, ArH), 7.42–7.25 (m, 6H, ArH), 7.24–7.14 (m, 2H, ArH), 6.88 (d,  $J = 7.5$  Hz, 1H, ArH), 6.60 (s, 1H, C=CH), 6.31 (d,  $J = 8.2$  Hz, 1H, NH), 4.38 (dd,  $J = 14.5, 7.2$  Hz, 1H, CH), 3.20 (d,  $J = 6.9$  Hz, 2H, CH<sub>2</sub>), 2.26 (s, 3H, CH<sub>3</sub>). <sup>13</sup>C NMR (101 MHz, DMSO-*d*<sub>6</sub>)  $\delta$  179.94, 169.64, 145.31, 140.50, 138.42, 138.11, 137.23, 133.92, 133.00, 129.28, 129.28, 129.05, 128.73, 128.48, 128.39, 128.39, 126.71, 125.90, 124.53, 122.39, 120.19, 116.84, 91.41, 57.86, 37.67, 21.20. HR-MS ( $m/z$ ) (ESI): calcd for C<sub>26</sub>H<sub>24</sub>N<sub>3</sub>O<sub>3</sub> [M + H]<sup>+</sup>: 426.1812; found: 426.1810. Purity: 99.23%.

(*Z*)-2-((4-(Hydroxyimino)-1-oxo-1,4-dihydronaphthalen-2-yl)amino)-3-phenyl-*N*-(*p*-tolyl)propanamide (**8r**). Yield: 50.5%, yellow-green solid, mp 138.9–140.4 °C. [ $\alpha$ ]<sub>D</sub><sup>20</sup> = –50 (c 0.1, AcOEt). <sup>1</sup>H NMR (400 MHz, DMSO-*d*<sub>6</sub>)  $\delta$  12.36 (s, 1H, OH), 10.24 (s, 1H, NH), 8.16 (d,  $J = 7.6$  Hz, 1H, ArH), 8.05 (dd,  $J = 7.9, 0.9$  Hz, 1H, ArH), 7.70–7.64 (m, 1H, ArH), 7.59–7.53 (m, 1H, ArH), 7.44 (d,  $J = 8.4$  Hz, 2H, ArH), 7.33–7.23 (m, 5H, ArH), 7.21–7.16 (m, 1H, ArH), 7.10 (d,  $J = 8.3$  Hz, 2H, ArH), 6.60 (s, 1H, C=CH), 6.29 (d,  $J = 8.2$  Hz, 1H, NH), 4.40 (dd,  $J = 14.1, 7.4$  Hz, 1H, CH), 3.29–3.12 (d, 2H, CH<sub>2</sub>), 2.24 (s, 3H, CH<sub>3</sub>). <sup>13</sup>C NMR (101 MHz, DMSO-*d*<sub>6</sub>)  $\delta$  179.90, 169.39, 145.24, 140.41, 137.22, 135.98, 133.91, 132.92, 132.74, 129.26, 129.26, 129.17, 129.17, 128.97, 128.44, 128.31, 126.63, 125.84, 122.35, 119.67, 119.67, 91.36, 57.68, 37.67, 20.50. HR-MS ( $m/z$ ) (ESI): calcd for C<sub>26</sub>H<sub>23</sub>N<sub>3</sub>O<sub>3</sub> Na [M + Na]<sup>+</sup>: 448.1632; found: 448.1619. Purity: 99.08%.

(*Z*)-*N*-(3,5-Dimethylphenyl)-2-((4-(hydroxyimino)-1-oxo-1,4-dihydronaphthalen-2-yl)amino)-3-phenylpropanamide (**8s**). Yield: 52.5%, yellow-green solid, mp 131.4–133.2 °C. [ $\alpha$ ]<sub>D</sub><sup>20</sup> = –44 (c 0.1, AcOEt). <sup>1</sup>H NMR (400 MHz, DMSO-*d*<sub>6</sub>)  $\delta$  12.34 (s, 1H, OH), 10.06 (s, 1H, NH), 8.16 (d,  $J = 7.6$  Hz, 1H, ArH), 8.05 (dd,  $J = 7.9, 1.0$  Hz, 1H, ArH), 7.72–7.64 (m, 1H, ArH), 7.60–7.54 (m, 1H, ArH), 7.31–7.25 (m, 4H, ArH), 7.21–7.17 (m, 3H, ArH), 6.64 (d,  $J = 49.4$  Hz, 2H, ArH, C=CH), 6.30 (d,  $J = 8.2$  Hz, 1H, NH), 4.36 (dd,  $J = 14.2, 7.4$  Hz, 1H, CH), 3.20–3.16 (m, 2H, CH<sub>2</sub>), 2.22 (s, 6H, 2CH<sub>3</sub>). <sup>13</sup>C NMR (101 MHz, DMSO-*d*<sub>6</sub>)  $\delta$  179.94, 169.58, 145.30, 140.50, 138.35, 137.89, 137.89, 137.24, 133.91, 133.00, 129.27, 129.27, 129.06, 128.47, 128.39, 128.39, 126.71, 125.89, 125.33, 122.39, 117.37, 117.37, 91.40, 57.90, 37.67, 21.11, 21.11. HR-MS ( $m/z$ ) (ESI): calcd for C<sub>27</sub>H<sub>23</sub>N<sub>3</sub>O<sub>3</sub> Na [M + Na]<sup>+</sup>: 462.1788; found: 462.1788. Purity: 97.32%.

(*Z*)-*N*-(3-Bromo-4-fluorophenyl)-2-((4-(hydroxyimino)-1-oxo-1,4-dihydronaphthalen-2-yl)amino)-3-phenylpropanamide (**8t**). Yield: 55.5%, yellow-green solid, mp 170.2–171.6 °C. [ $\alpha$ ]<sub>D</sub><sup>20</sup> = –34 (c 0.1,

AcOEt). <sup>1</sup>H NMR (400 MHz, DMSO-*d*<sub>6</sub>)  $\delta$  12.35 (s, 1H, OH), 10.53 (s, 1H, NH), 8.16 (d,  $J = 7.8$  Hz, 1H, ArH), 8.05 (d,  $J = 7.0$  Hz, 1H, ArH), 7.72–7.55 (m, 4H, ArH), 7.28 (d,  $J = 6.8$  Hz, 5H, ArH), 7.20 (dd,  $J = 5.9, 2.6$  Hz, 1H, ArH), 6.58 (s, 1H, C=CH), 6.35 (d,  $J = 8.1$  Hz, 1H, NH), 4.38 (q,  $J = 7.0$  Hz, 1H, CH), 3.22 (d,  $J = 6.7$  Hz, 2H, CH<sub>2</sub>). <sup>13</sup>C NMR (101 MHz, DMSO-*d*<sub>6</sub>)  $\delta$  179.82, 170.25, 159.24, 156.83, 145.20, 140.42, 139.61, 136.98, 133.83, 133.46, 132.94, 129.21, 129.21, 129.00, 128.42, 128.35, 126.71, 125.84, 122.32, 116.92, 107.68, 101.47, 91.41, 57.90, 37.44. HR-MS ( $m/z$ ) (ESI): calcd for C<sub>25</sub>H<sub>19</sub>BrFN<sub>3</sub>O<sub>3</sub> Na [M + Na]<sup>+</sup>: 530.0486; found: 530.0488. Purity: 99.87%.

(*Z*)-*N*-(3,5-Dimethoxyphenyl)-2-((4-(hydroxyimino)-1-oxo-1,4-dihydronaphthalen-2-yl)amino)-3-phenylpropanamide (**8u**). Yield: 50.5%, yellow-green solid, mp 122.5–123.6 °C. [ $\alpha$ ]<sub>D</sub><sup>20</sup> = –39 (c 0.1, AcOEt). <sup>1</sup>H NMR (400 MHz, DMSO-*d*<sub>6</sub>)  $\delta$  12.35 (s, 1H, OH), 10.19 (s, 1H, NH), 8.16 (d,  $J = 7.9$  Hz, 1H, ArH), 8.10–8.02 (m, 1H, ArH), 7.72–7.63 (m, 1H, ArH), 7.56 (dd,  $J = 11.1, 4.0$  Hz, 1H, ArH), 7.38–7.25 (m, 4H, ArH), 7.20 (dt,  $J = 9.1, 4.2$  Hz, 1H, ArH), 6.81 (d,  $J = 2.2$  Hz, 2H, ArH), 6.59 (s, 1H, C=CH), 6.30 (d,  $J = 8.2$  Hz, 1H, NH), 6.24 (t,  $J = 2.2$  Hz, 1H, ArH), 4.37 (dd,  $J = 14.1, 7.5$  Hz, 1H, CH), 3.71 (s, 6H, CH<sub>3</sub>, CH<sub>3</sub>), 3.26–3.14 (m, 2H, CH<sub>2</sub>). <sup>13</sup>C NMR (101 MHz, DMSO-*d*<sub>6</sub>)  $\delta$  179.89, 169.77, 160.55, 160.55, 145.26, 140.46, 140.12, 137.17, 133.88, 132.95, 129.23, 129.23, 129.01, 128.45, 128.35, 128.35, 126.68, 125.86, 122.35, 97.89, 97.89, 95.82, 91.41, 57.89, 55.16, 55.16, 37.62. HR-MS ( $m/z$ ) (ESI): calcd for C<sub>27</sub>H<sub>26</sub>N<sub>3</sub>O<sub>5</sub> [M + H]<sup>+</sup>: 472.1867; found: 472.1851. Purity: 99.45%.

(*Z*)-*N*-(4-Bromo-3-fluorophenyl)-2-((4-(hydroxyimino)-1-oxo-1,4-dihydronaphthalen-2-yl)amino)-3-phenylpropanamide (**8v**). Yield: 49.2%, yellow-green solid, mp 122.2–124.2 °C. [ $\alpha$ ]<sub>D</sub><sup>20</sup> = –33 (c 0.1, AcOEt). <sup>1</sup>H NMR (400 MHz, DMSO-*d*<sub>6</sub>)  $\delta$  10.47 (s, 1H, OH), 7.99 (dd,  $J = 7.6, 0.9$  Hz, 1H, NH), 7.90 (dd,  $J = 7.6, 1.0$  Hz, 1H, ArH), 7.82 (td,  $J = 7.5, 1.3$  Hz, 1H, ArH), 7.76–7.62 (m, 3H, ArH), 7.36–7.15 (m, 7H, ArH), 5.67 (s, 1H, C=CH), 4.44 (q,  $J = 7.0$  Hz, 1H, CH), 3.27 (d,  $J = 6.8$  Hz, 2H, CH<sub>2</sub>). <sup>13</sup>C NMR (101 MHz, DMSO-*d*<sub>6</sub>)  $\delta$  181.89, 181.00, 169.19, 147.63, 139.47, 139.37, 136.85, 135.01, 133.50, 132.66, 132.59, 130.22, 129.25, 128.34, 126.75, 126.06, 125.42, 117.05, 107.82, 107.55, 101.64, 101.44, 101.06, 57.64, 36.96. HR-MS ( $m/z$ ) (ESI): calcd for C<sub>25</sub>H<sub>19</sub>BrFN<sub>3</sub>O<sub>3</sub>Na [M + Na]<sup>+</sup>: 530.0486; found: 530.0471. Purity: 99.16%.

(*Z*)-*N*-(3,5-Difluorophenyl)-2-((4-(hydroxyimino)-1-oxo-1,4-dihydronaphthalen-2-yl)amino)-3-phenylpropanamide (**8w**). Yield: 43.5%, yellow-green solid, mp 166.0–167.6 °C. [ $\alpha$ ]<sub>D</sub><sup>20</sup> = –31 (c 0.1, AcOEt). <sup>1</sup>H NMR (400 MHz, DMSO-*d*<sub>6</sub>)  $\delta$  12.35 (s, 1H, OH), 10.57 (s, 1H, NH), 8.20–8.15 (m, 1H, ArH), 8.05 (dd,  $J = 7.9, 1.0$  Hz, 1H, ArH), 7.68 (td,  $J = 7.8, 1.4$  Hz, 1H, ArH), 7.61–7.53 (m, 1H, ArH), 7.37–7.26 (m, 6H, ArH), 7.21 (dd,  $J = 5.9, 2.8$  Hz, 1H, ArH), 6.93 (tt,  $J = 9.3, 2.3$  Hz, 1H, ArH), 6.57 (s, 1H, C=CH), 6.34 (d,  $J = 8.1$  Hz, 1H, NH), 4.38 (dd,  $J = 14.5, 7.0$  Hz, 1H, CH) 3.23 (d,  $J = 6.8$  Hz, 2H, CH<sub>2</sub>). <sup>13</sup>C NMR (101 MHz, DMSO-*d*<sub>6</sub>)  $\delta$  179.82, 170.43, 163.72, 161.30, 145.21, 140.87, 140.43, 136.93, 133.83, 132.95, 129.20, 129.20, 129.01, 128.42, 128.36, 128.36, 126.73, 125.84, 122.32, 102.59, 102.30, 98.96, 91.46, 57.95, 37.40. HR-MS ( $m/z$ ) (ESI): calcd for C<sub>25</sub>H<sub>19</sub>F<sub>2</sub>N<sub>3</sub>O<sub>3</sub>Na [M + Na]<sup>+</sup>: 470.1287; found: 470.1270. Purity: 98.14%.

(*Z*)-*N*-(2-Fluoro-4-methylphenyl)-2-((4-(hydroxyimino)-1-oxo-1,4-dihydronaphthalen-2-yl)amino)-3-phenylpropanamide (**8x**). Yield: 60.2%, yellow-green solid, mp 218.5–220.4 °C. [ $\alpha$ ]<sub>D</sub><sup>20</sup> = –36 (c 0.1, AcOEt). <sup>1</sup>H NMR (400 MHz, DMSO-*d*<sub>6</sub>)  $\delta$  9.96 (s, 1H, NH), 8.16 (dd,  $J = 8.0, 0.6$  Hz, 1H, ArH), 8.05 (dd,  $J = 7.9, 1.0$  Hz, 1H, ArH), 7.72–7.65 (m, 1H, ArH), 7.58 (dt,  $J = 8.3, 4.7$  Hz, 2H, ArH), 7.30 (dt,  $J = 14.9, 4.6$  Hz, 4H, ArH), 7.23–7.17 (m, 1H, ArH), 7.08 (dd,  $J = 11.8, 1.1$  Hz, 1H, ArH), 6.96 (d,  $J = 8.2$  Hz, 1H, ArH), 6.63 (s, 1H, C=CH), 6.32 (d,  $J = 8.3$  Hz, 1H, NH), 4.55 (q,  $J = 6.9$  Hz, 1H, CH), 3.21 (d,  $J = 6.7$  Hz, 2H, CH<sub>2</sub>), 2.27 (s, 3H, CH<sub>3</sub>). <sup>13</sup>C NMR (101 MHz, DMSO-*d*<sub>6</sub>)  $\delta$  179.91, 170.03, 155.08, 152.64, 145.27, 140.44, 137.15, 136.01, 133.91, 132.94, 129.30, 128.99, 128.45, 128.30, 126.65, 125.84, 124.83, 124.80, 124.38, 122.63, 116.05, 115.86, 91.49, 57.24, 37.63, 20.41. HR-MS ( $m/z$ ) (ESI): calcd for C<sub>26</sub>H<sub>23</sub>FN<sub>3</sub>O<sub>3</sub> [M + H]<sup>+</sup>: 444.1718; found: 444.1704. Purity: 99.34%.

(*Z*)-*N*-(3-Chloro-4-methylphenyl)-2-((4-(hydroxyimino)-1-oxo-1,4-dihydronaphthalen-2-yl)amino)-3-phenylpropanamide (**8y**). Yield: 51.2%, yellow-green solid, mp 172.6–174.5 °C.  $[\alpha]_D^{20} = -67$  (c 0.1, AcOEt).  $^1\text{H NMR}$  (400 MHz, DMSO- $d_6$ )  $\delta$  12.28 (s, 1H, OH), 10.30 (s, 1H, NH), 8.16 (d,  $J = 7.5$  Hz, 1H, ArH), 8.05 (dd,  $J = 7.9, 1.0$  Hz, 1H, ArH), 7.72 (d,  $J = 2.0$  Hz, 1H, ArH), 7.70–7.65 (m, 1H, ArH), 7.60–7.54 (m, 1H, ArH), 7.33 (dd,  $J = 8.3, 2.1$  Hz, 1H, ArH), 7.30–7.26 (m, 4H, ArH), 7.20 (td,  $J = 5.7, 2.6$  Hz, 1H, ArH), 6.65–6.64 (m, 1H, ArH), 6.58 (s, 1H, C=CH), 6.31 (d,  $J = 8.1$  Hz, 1H, NH), 4.36 (dd,  $J = 14.5, 7.0$  Hz, 1H, CH), 3.21 (d,  $J = 6.7$  Hz, 2H, CH<sub>2</sub>), 2.26 (s, 3H, CH<sub>3</sub>).  $^{13}\text{C NMR}$  (101 MHz, DMSO- $d_6$ )  $\delta$  179.85, 169.80, 145.22, 140.42, 137.52, 137.06, 133.86, 133.02, 132.94, 131.27, 130.49, 129.21, 129.21, 129.00, 128.43, 128.34, 128.34, 126.69, 125.84, 122.33, 119.59, 118.25, 91.40, 57.81, 37.52, 18.96. HR-MS ( $m/z$ ) (ESI): calcd for C<sub>26</sub>H<sub>23</sub>ClN<sub>3</sub>O<sub>3</sub> [M + H]<sup>+</sup>: 460.1422; found: 460.1405. Purity: 96.83%.

(*Z*)-*N*-(4-Bromo-2-methylphenyl)-2-((4-(hydroxyimino)-1-oxo-1,4-dihydronaphthalen-2-yl)amino)-3-phenylpropanamide (**8z**). Yield: 52.8%, yellow-green solid, mp 234.5–236.0 °C.  $[\alpha]_D^{20} = -83$  (c 0.1, AcOEt).  $^1\text{H NMR}$  (400 MHz, DMSO- $d_6$ )  $\delta$  9.66 (s, 1H, NH), 8.18 (d,  $J = 8.0$  Hz, 1H, ArH), 8.05 (d,  $J = 7.3$  Hz, 1H, ArH), 7.73–7.63 (m, 1H, ArH), 7.61–7.52 (m, 1H, ArH), 7.41 (d,  $J = 2.0$  Hz, 1H, ArH), 7.35–7.28 (m, 4H, ArH), 7.27–7.20 (m, 2H, ArH), 6.69 (s, 1H, C=CH), 6.30 (d,  $J = 7.9$  Hz, 1H, NH), 4.49 (q,  $J = 7.2$  Hz, 1H, CH), 3.27–3.17 (m, 2H, CH<sub>2</sub>), 2.08 (s, 3H, CH<sub>3</sub>).  $^{13}\text{C NMR}$  (101 MHz, DMSO- $d_6$ )  $\delta$  179.91, 169.88, 145.28, 140.51, 137.17, 135.14, 134.91, 133.92, 132.94, 132.80, 129.34, 129.34, 129.01, 128.82, 128.48, 128.40, 128.40, 127.06, 126.73, 125.86, 122.38, 117.80, 91.77, 57.44, 37.72, 17.46. HR-MS ( $m/z$ ) (ESI): calcd for C<sub>26</sub>H<sub>23</sub>BrN<sub>3</sub>O<sub>3</sub> [M + H]<sup>+</sup>: 504.0917; found: 504.0903. Purity: 96.23%.

#### General Procedure for the Preparation of Compounds 10.

Under argon protection, a solution of compound **8b**, **8k**, or **8n** (2 mmol) in dichloromethane (10 mL) was treated with 4-*tert*-butylbenzenesulfonyl chloride (3 mmol), and the resulting mixture was stirred for 30 min under an ice bath. Then, triethylamine (4 mmol) was added and the mixture was stirred for 10 min. The reaction was quenched with ice water (20 mL), extracted with dichloromethane (3 × 10 mL), dried (Na<sub>2</sub>SO<sub>4</sub>), filtered, and concentrated. The residue was purified by flash chromatography (light petroleum/ethyl acetate, V/V = 8:1) to give compounds **10** as a yellow solid.

(*E*)-2-((4-(((4-(*tert*-Butyl)phenyl)sulfonyl)oxy)imino)-1-oxo-1,4-dihydronaphthalen-2-yl)amino)-3-phenyl-*N*-(3-(trifluoromethyl)phenyl)propanamide (**10a**). Yield: 80.1%, yellow solid, mp 121.4–122.6 °C.  $[\alpha]_D^{20} = -25$  (c 0.1, AcOEt).  $^1\text{H NMR}$  (400 MHz, DMSO- $d_6$ )  $\delta$  10.71 (s, 1H, NH), 8.07 (s, 1H, NH), 7.98 (dd,  $J = 7.7, 1.3$  Hz, 1H, ArH), 7.95–7.92 (m, 1H, ArH), 7.84 (dd,  $J = 15.3, 8.5$  Hz, 3H, ArH), 7.66–7.53 (m, 5H, ArH), 7.46 (d,  $J = 7.8$  Hz, 1H, ArH), 7.34 (d,  $J = 7.0$  Hz, 2H, ArH), 7.25 (t,  $J = 7.5$  Hz, 2H, ArH), 7.16 (t,  $J = 7.3$  Hz, 2H, ArH), 6.12 (s, 1H, C=CH), 4.56 (dd,  $J = 13.8, 7.7$  Hz, 1H, CH), 3.32–3.18 (m, 2H, CH<sub>2</sub>), 1.22 (d,  $J = 11.2$  Hz, 9H, 3CH<sub>3</sub>).  $^{13}\text{C NMR}$  (101 MHz, DMSO- $d_6$ )  $\delta$  179.14, 169.46, 157.86, 151.72, 143.46, 139.06, 136.92, 134.02, 131.98, 131.12, 130.19, 129.30, 129.30, 129.00, 128.33, 128.33, 128.28, 128.28, 126.73, 126.32, 126.32, 125.34, 124.34, 123.16, 122.69, 120.30, 115.72, 88.16, 57.85, 37.45, 34.97, 31.04, 30.52, 30.52, 30.52, 26.32. HR-MS ( $m/z$ ) (ESI): calcd for C<sub>36</sub>H<sub>33</sub>N<sub>3</sub>O<sub>5</sub>S [M + H]<sup>+</sup>: 676.2088; found: 676.2062. Purity: 97.24%.

(*E*)-*N*-(3-Bromophenyl)-2-((4-(((4-(*tert*-butyl)phenyl)sulfonyl)oxy)imino)-1-oxo-1,4-dihydronaphthalen-2-yl)amino)-3-phenylpropanamide (**10b**). Yield: 85.2%, yellow solid, mp 121.0–122.6 °C.  $[\alpha]_D^{20} = -22$  (c 0.1, AcOEt).  $^1\text{H NMR}$  (400 MHz, DMSO- $d_6$ )  $\delta$  10.54 (s, 1H, NH), 8.01 (dd,  $J = 7.7, 1.3$  Hz, 1H, NH), 7.96–7.92 (m, 2H, ArH), 7.88–7.80 (m, 2H, ArH), 7.69 (td,  $J = 7.6, 1.5$  Hz, 1H, ArH), 7.63 (td,  $J = 7.6, 1.2$  Hz, 1H, ArH), 7.60–7.56 (m, 2H, ArH), 7.49 (dt,  $J = 7.2, 2.0$  Hz, 1H, ArH), 7.35–7.30 (m, 4H, ArH), 7.25 (t,  $J = 7.5$  Hz, 2H, ArH), 7.15 (dd,  $J = 17.3, 7.7$  Hz, 2H, ArH), 6.09 (s, 1H, C=CH), 4.51 (dd,  $J = 14.0, 7.5$  Hz, 1H, CH), 3.32–3.15 (m, 2H, CH<sub>2</sub>), 1.23 (s, 9H, 3CH<sub>3</sub>).  $^{13}\text{C NMR}$  (101 MHz, DMSO- $d_6$ )  $\delta$  179.21, 169.27, 157.98, 151.80, 143.49, 139.86, 136.90, 134.18,

131.98, 131.28, 131.17, 130.98, 129.34, 129.34, 129.07, 128.40, 128.40, 128.33, 126.80, 126.66, 126.44, 126.44, 125.36, 124.39, 123.23, 122.04, 121.70, 118.51, 88.20, 57.85, 37.47, 35.09, 30.65, 30.65, 30.65. HR-MS ( $m/z$ ) (ESI): calcd for C<sub>35</sub>H<sub>32</sub>BrN<sub>3</sub>O<sub>5</sub>S [M + Na]<sup>+</sup>: 708.1138; found: 708.1109. Purity: 99.12%.

(*E*)-2-((4-(((4-(*tert*-Butyl)phenyl)sulfonyl)oxy)imino)-1-oxo-1,4-dihydronaphthalen-2-yl)amino)-*N*-(3-methoxyphenyl)-3-phenylpropanamide (**10c**). Yield: 85.5%, yellow solid, mp 107.4–108.9 °C.  $[\alpha]_D^{20} = -18$  (c 0.1, AcOEt).  $^1\text{H NMR}$  (400 MHz, DMSO- $d_6$ )  $\delta$  10.41 (s, 1H, NH), 7.95 (dd,  $J = 7.6, 1.4$  Hz, 1H, NH), 7.89 (dd,  $J = 13.0, 5.0$  Hz, 3H, ArH), 7.61–7.52 (m, 2H, ArH), 7.36–7.30 (m, 4H, ArH), 7.26 (dt,  $J = 7.7, 6.1$  Hz, 4H, ArH), 7.17 (d,  $J = 7.6$  Hz, 2H, ArH), 7.09 (d,  $J = 8.1$  Hz, 1H, ArH), 6.70 (dd,  $J = 8.2, 1.8$  Hz, 1H, ArH), 6.11 (s, 1H, C=CH), 4.54 (dd,  $J = 14.0, 7.5$  Hz, 1H, CH), 3.74 (s, 3H, CH<sub>3</sub>), 3.30–3.21 (m, 2H, CH<sub>2</sub>), 1.22 (d,  $J = 11.7$  Hz, 9H, 3CH<sub>3</sub>).  $^{13}\text{C NMR}$  (101 MHz, DMSO- $d_6$ )  $\delta$  179.15, 168.88, 159.60, 157.85, 151.76, 143.39, 139.53, 137.00, 133.99, 132.00, 131.13, 131.09, 129.73, 129.32, 129.32, 128.96, 128.31, 128.31, 126.69, 126.62, 126.37, 126.37, 125.35, 124.38, 123.15, 111.88, 109.36, 105.39, 88.10, 57.76, 55.01, 34.99, 31.05, 30.56, 30.56, 30.56. HR-MS ( $m/z$ ) (ESI): calcd for C<sub>36</sub>H<sub>36</sub>N<sub>3</sub>O<sub>6</sub>S [M + H]<sup>+</sup>: 638.2319; found: 638.2294. Purity: 98.14%.

**Enzymatic Assays.** IDO1 inhibition assays were carried out according to the manufacturers' procedures, as described previously.<sup>43</sup> The standard assay mixture (100  $\mu\text{L}$ ) contained 50 mM potassium phosphate buffer (pH = 6.5), 10 mM ascorbate, 10  $\mu\text{M}$  methylene blue, 100  $\mu\text{g}/\text{mL}$  catalase, 1 mM L-tryptophan, and 10  $\mu\text{g}/\text{mL}$  of rhIDO1. The plate was incubated at 37 °C in a dark environment, and reactions were terminated after 60 min by the addition of 50  $\mu\text{L}$  of fluorogenic developer solution and further incubated at 45 °C in the dark for 3 h. The plate was then allowed to cool to room temperature for at least 1 h. After centrifugation at 1500 g for 5 min at 20 °C, the fluorescence intensity (Ex/Em = 402/488 nm) was measured with a Fluoroskan Ascent microplate reader (Infinite M1000 Pro, Tecan US, Morrisville, NC) in endpoint mode. All determinations were carried out in triplicate.

**Cell Viability Assays.** The cell lines Hct-116, HepG2, A549, and SKOV3 were obtained from the Shanghai Cell Bank at the Chinese Academy of Sciences. Hct-116, HepG2, and SKOV3 cell lines were grown on 96-well microtiter plates at a density of 10 × 10<sup>5</sup> cells/well in Dulbecco's modified Eagle's medium (DMEM) with 10% FBS. DMEM and FBS were obtained from Gibco-Thermo (BRL Co. Ltd.). The plates were incubated at 37 °C in a humidified atmosphere of 5% CO<sub>2</sub>/95% air overnight. The cells were then exposed to different concentrations of target compounds and DOX and incubated for another 48 h. The cells were stained with 10  $\mu\text{L}$  of MTT in an incubator for approximately 4 h. The medium was discharged and replaced by 100  $\mu\text{L}$  of dimethyl sulfoxide (DMSO). The O.D. value was read at 570/630 nm with a spectrophotometer.

**Molecular Docking.** All docking studies were carried out in Sybyl-X 2.0 on a Windows workstation. The crystal structure of the IDO1 proteins was retrieved from the RCSB Protein Data Bank (IDO1: 4PK5).<sup>41</sup> The synthetic analogues **7**, **8**, and **10** were selected for the docking studies. The 3D structures of these selected compounds were first built with Sybyl-X 2.0 sketch, and this was followed by energy minimization with the MMFF94 force field and Gasteiger-Marsili charges. We used Powell's method for optimizing the geometry with a distance-dependent dielectric constant and a termination energy gradient of 0.005 kcal/mol. All selected compounds were automatically docked into the binding pocket of IDO1 through an empirical scoring function and a patented search engine in the Surflex docking program. Before the docking process, the natural ligand was extracted, and the water molecules were removed from the crystal structure. Subsequently, the protein was prepared with the Biopolymer module implemented in Sybyl. The polar hydrogen atoms were added, and other parameters were established by default to estimate the binding affinity characterized by the Surflex-Dock scores in the software. The Surflex-Dock total scores, which were expressed in  $-\log_{10}(K_d)$  units to represent binding

affinities, were applied to estimate the ligand–receptor interactions of newly designed molecules.

**SPR Experiments.** Surface plasmon resonance experiments were performed with a Biacore T200 instrument at 25 °C. Sensor chips, buffer stock solutions, and immobilization reagents were from GE Healthcare. Recombinant human IDO1 was Novoprotein. Other reagents were obtained from Sigma. For immobilization, PBS was used as the running buffer. The four flow cells were treated in the same manner to optimize throughput. In summary, by using a CMS chip, spots 1 and 2 were activated with the coupling reagents EDC and NHS for 10 min. IDO1 at a concentration of 20  $\mu\text{g}/\text{mL}$  in 10 mM sodium acetate, pH 5, was injected onto the surface for 10 and 5 min at spots 1 and 2, respectively, to generate surfaces with high and low densities. The immobilization levels ranged from 2302 to 1823 RU at spot 1 and from 948 to 1112 RU at spot 2. The unmodified spot 3 was used as a reference. For kinetics and affinity measurements, PBS (containing 0.05% DMSO) was used as the running buffer and sample dilution buffer. Dose–response relationships were determined with a twofold sample dilution from 0 to 500  $\mu\text{M}$  and an injection time of 60 s. For data processing, binding curves were corrected for variations in DMSO concentration and normalized by molecular weight. The  $K_D$  values reported were derived from steady-state binding responses and therefore correspond to the equilibrium binding affinities of the compounds.

**UV–Visible Spectra.** UV–visible scans (200–700 nm) were performed and recorded on a NanoDrop 2000 spectrophotometer (Thermo Fisher Scientific, Inc.) with 100  $\mu\text{M}$  IDO1 mixed with 2 mM tested compounds.

**Western Blotting.** Total cell lysates from cultured SKOV-3 cells after compound **8u** treatment, as described earlier, were obtained by lysing the cells in ice-cold RIPA buffer with protease and phosphatase inhibitors. Lysates were stored at  $-20$  °C until use. The protein concentrations were quantified by the Bradford method (BIO-RAD) with a Multimode Varioscan instrument (Thermo Fisher Scientific). Equal amounts of protein per lane were applied to a 12% sodium dodecyl sulfate polyacrylamide gel for electrophoresis (SDS-PAGE) and transferred to a poly(vinylidene difluoride) (PVDF) membrane (Amersham Biosciences). After the membrane was blocked at room temperature for 2 h in the blocking solution, primary antibody was added and incubated at 4 °C overnight. Antibodies to STAT3 were purchased from Abcam. After three TBST washes, the membrane was incubated with corresponding horseradish peroxidase-labeled secondary antibody (1:2000) (Santa Cruz Biotechnology) at room temperature for 1 h. Membranes were washed with TBST three times for 15 min, and the protein blots were detected with chemiluminescent reagent (Thermo Fisher Scientific, Ltd.). The X-ray films were developed with a developer and fixed with a fixer solution.

**Immunofluorescence Staining.** Studies were performed as previously described.<sup>64</sup> Briefly, SKOV3 cells were cultured in six-well plates ( $2 \times 10^5$  cells per well) for 24 h, pretreated with compound **8u** at 0.5  $\mu\text{M}$  for 6 h, and then treated with IL-6 for another 30 min. The cells were then washed and fixed with anhydrous methanol for 15 min at room temperature, permeabilized with 0.1% Triton X-100 for 15 min, and blocked with 1% bovine serum albumin (BSA) for 10 min at room temperature. Next, the cells were incubated with primary p-STAT3 antibody in PBS overnight at 4 °C followed by FITC-conjugated antibody secondary antibodies. After being washed with PBS three times, the cells were incubated in 10  $\mu\text{M}$  4',6-diamidino-2-phenylindole (DAPI) for 15 min in the dark. The fluorescence of the p-STAT3 protein and nuclei was red and blue, respectively, and live cell imaging was simultaneously accomplished with a fluorescence microscope (Olympus BX-51, Tokyo, Japan).

**Luciferase Assays.** Cells were seeded in 24-well plates and transiently transfected with STAT reporter plasmid (0.2  $\mu\text{g}$  per well, Addgene) and *Renilla* luciferase control reporter plasmid pRL-CMV (0.1  $\mu\text{g}$  per well, Promega), with Lipofectamine 2000 reagent (Invitrogen). Then, the cells were incubated in complete medium for 24 h with **8u**. After the treatment, the cells were harvested in 100  $\mu\text{L}$  of passive lysis buffer (Promega) per well. A 25  $\mu\text{L}$  aliquot of cell

lysate was subjected to a luciferase assay with a dual-luciferase assay kit (Promega). STAT luciferase activity was measured with an EnVision Multilabel Reader (PerkinElmer). Relative luciferase activity was calculated after the activity of STAT-dependent firefly luciferase had been normalized to that of *Renilla* luciferase.

**In Vivo Antitumor Efficacy in Nude Mice.** The in vivo antitumor activity of compound **8u** was evaluated in the human hepatocellular carcinoma cell line HepG2 in BALB/c nude mice. Five-week-old male BALB/c nude mice were purchased from Shanghai Ling Chang Biotechnology Co. Ltd. (China), and tumors were induced through a subcutaneous injection of  $1 \times 10^7$  cells in 100  $\mu\text{L}$  of sterile PBS into the dorsal region. The animals were divided into four groups, starting on the second day. When the tumors reached a volume of 100–150  $\text{mm}^3$  in all mice on day 15, the first group was injected via the tail vein with an equivalent volume of 5% dextrose as the vehicle control. The second group was treated with doxorubicin at a dose of 5 mg/kg body weight once every 3 days for 3 weeks. The third and fourth groups were treated with complex **8u** at doses of 10 mg/kg or 30 mg/kg body weight once every 3 days for 3 weeks, respectively. All compounds were dissolved in vehicle. Tumor volumes and body weights were recorded every other day after drug treatment. All mice were sacrificed after 3 weeks of treatment, and the tumor volumes were measured with electronic digital calipers and examined by measurement of the length (*A*) and width (*B*) to calculate the volume ( $V = AB^2/2$ ).

B16F10 melanoma was established in C57BL/6 mice through a subcutaneous injection of  $1 \times 10^7$  cultured cells. The animals were divided into four groups starting on the first day. The four groups were subsequently administered 5% dextrose, D-1-MT (200 mg/kg), **8u** (100 mg/kg), and **8u** (150 mg/kg), by tail vein injection once every 2 days for 3 weeks. Tumor volumes and body weights were recorded as described above.

**Statistical Analysis.** All of the results were expressed as mean  $\pm$  SD where applicable. GraphPad Prism 6 software (GraphPad Software) was used for statistical analysis. All of the results are expressed as mean  $\pm$  S.D.

## ■ ASSOCIATED CONTENT

### Supporting Information

The Supporting Information is available free of charge at <https://pubs.acs.org/doi/10.1021/acs.jmedchem.9b01386>.

Binding modes of **8u** in complex with IDO1 (PDB ID: 4PK5); UV spectra of ferric IDO1 without and with compound **8u**; effects of the indicated treatments of **8u** on B16-F10 melanoma tumor xenografts in C57BL/6 mice; inhibition of tumor growth for compound **8u** and doxorubicin (DOX) in nude mice bearing HepG2 xenograft model; inhibitory effects of **8u** on STATs; table of docking scores (kcal/mol) for all studied compounds; table of STAT3 binding affinities of selected 2-amino-1,4-naphthoquinone derivatives; and <sup>1</sup>H NMR, <sup>13</sup>C NMR, HR-MS, and HPLC of target compounds (PDF)

Molecular formula strings and some data (CSV)

## ■ AUTHOR INFORMATION

### Corresponding Authors

Hengshan Wang – State Key Laboratory for the Chemistry and Molecular Engineering of Medicinal Resources (Ministry of Education of China), School of Chemistry and Pharmaceutical Sciences of Guangxi Normal University, Guilin 541004, China; [orcid.org/0000-0001-6474-8323](https://orcid.org/0000-0001-6474-8323); Email: [whengshan@163.com](mailto:whengshan@163.com)

Zhenfeng Chen – State Key Laboratory for the Chemistry and Molecular Engineering of Medicinal Resources (Ministry of Education of China), School of Chemistry and Pharmaceutical

Sciences of Guangxi Normal University, Guilin 541004, China;  
orcid.org/0000-0002-6548-6131; Email: chenzzf@gxnu.edu.cn

**Ye Zhang** – School of Pharmacy, Guilin Medical University, Guilin 541004, China; State Key Laboratory for the Chemistry and Molecular Engineering of Medicinal Resources (Ministry of Education of China), School of Chemistry and Pharmaceutical Sciences of Guangxi Normal University, Guilin 541004, China; orcid.org/0000-0002-6903-5602; Email: zhangye81@126.com

## Authors

**Rizhen Huang** – State Key Laboratory for the Chemistry and Molecular Engineering of Medicinal Resources (Ministry of Education of China), School of Chemistry and Pharmaceutical Sciences of Guangxi Normal University, Guilin 541004, China; School of Pharmacy, Guilin Medical University, Guilin 541004, China; Jiangsu Province Hi-Tech Key Laboratory for Biomedical Research and School of Chemistry and Chemical Engineering, Southeast University, Nanjing 211189, China

**Xiaoteng Jing** – State Key Laboratory for the Chemistry and Molecular Engineering of Medicinal Resources (Ministry of Education of China), School of Chemistry and Pharmaceutical Sciences of Guangxi Normal University, Guilin 541004, China

**Xiaochao Huang** – Jiangsu Province Hi-Tech Key Laboratory for Biomedical Research and School of Chemistry and Chemical Engineering, Southeast University, Nanjing 211189, China

**Yingming Pan** – State Key Laboratory for the Chemistry and Molecular Engineering of Medicinal Resources (Ministry of Education of China), School of Chemistry and Pharmaceutical Sciences of Guangxi Normal University, Guilin 541004, China

**Yilin Fang** – State Key Laboratory for the Chemistry and Molecular Engineering of Medicinal Resources (Ministry of Education of China), School of Chemistry and Pharmaceutical Sciences of Guangxi Normal University, Guilin 541004, China

**Guibin Liang** – State Key Laboratory for the Chemistry and Molecular Engineering of Medicinal Resources (Ministry of Education of China), School of Chemistry and Pharmaceutical Sciences of Guangxi Normal University, Guilin 541004, China

**Zhixin Liao** – Jiangsu Province Hi-Tech Key Laboratory for Biomedical Research and School of Chemistry and Chemical Engineering, Southeast University, Nanjing 211189, China

Complete contact information is available at:  
<https://pubs.acs.org/10.1021/acs.jmedchem.9b01386>

## Author Contributions

<sup>||</sup>R.H. and X.J. contributed equally to this work.

## Notes

The authors declare no competing financial interest.

## ACKNOWLEDGMENTS

The authors are grateful to the National Natural Science Foundation of China (21431001, 21501032, and 81760626), the Ministry of Education Innovation Team Fund (IRT\_16R15 and 2016GXNSFGA380005), the Innovative Team & Outstanding Talent Program of Colleges and Universities in Guangxi (2017-38), Guangxi New Century Ten, Hundred and Thousand Talents Project ([2017]42), Natural Science Foundation of Guangxi Province (2016GXNSFAA380300 and AB17292075), and Guangxi Funds for Distinguished Experts.

## ABBREVIATIONS USED

IDO1, indoleamine-2,3-dioxygenase 1; STAT3, signal transducer and activator of transcription 3; IDO5L, 4-amino-*N*-(3-chloro-4-fluorophenyl)-*N'*-hydroxy-1, 2, 5-oxadiazole-3-carboximidamide; 1-MT, 1-methyl-L-tryptophan; DOX, doxorubicin; PDL1, programmed death ligand 1; PD1, programmed cell death protein 1; CTLA4, cytotoxic T-lymphocyte-associated protein 4; Pt, platinum; TDO, tryptophan 2,3-dioxygenase; HRMS, high-resolution mass spectrometry; NMR, nuclear magnetic resonance; DMEM, Dulbecco's modified Eagle's medium; SDS-PAGE, sodium dodecyl sulfate polyacrylamide gel electrophoresis; SPR, surface plasmon resonance; MTT, 3-(4,5-dimethylthiazol-2-yl)-2,5-diphenyltetrazolium bromide; PVDF, poly(vinylidene difluoride)

## REFERENCES

- (1) Sharma, P.; Allison, J. P. The future of immune checkpoint therapy. *Science* **2015**, *348*, 56–61.
- (2) Muller, A. J.; Scherle, P. A. Targeting the mechanisms of tumoral immune tolerance with small molecule inhibitors. *Nat. Rev. Cancer* **2006**, *6*, 613–625.
- (3) Kane, L. P. T cell Ig and mucin domain proteins and immunity. *J. Immunol.* **2010**, *184*, 2743–2749.
- (4) Couzin-Frankel, J. New highlight of cancer immunotherapy. *Science* **2013**, *342*, 1432–1433.
- (5) Postow, M. A.; Chesney, J.; Pavlick, A. C.; Robert, C.; Grossmann, K.; McDermott, D.; Linette, G. P.; Meyer, N.; Giguere, J. K.; Agarwala, S. S.; Shaheen, M.; Ernstoff, M. S.; Minor, D.; Salama, A. K.; Taylor, M.; Ott, P. A.; Rollin, L. M.; Horak, C.; Gagnier, P.; Wolchok, J. D.; Hodi, F. S. Nivolumab and ipilimumab versus ipilimumab in untreated melanoma. *N. Engl. J. Med.* **2015**, *372*, 2006–2017.
- (6) Vanneman, M.; Dranoff, G. Combining immunotherapy and targeted therapies in cancer treatment. *Nat. Rev. Cancer* **2012**, *12*, 237–251.
- (7) Hughes, P. E.; Caenepeel, S.; Wu, L. C. Targeted therapy and checkpoint immunotherapy combinations for the treatment of cancer. *Trends Immunol.* **2016**, *37*, 462–476.
- (8) Wong, D. Y. Q.; Yeo, C. H. F.; Ang, W. H. Immuno-chemotherapeutic platinum(IV) prodrugs of cisplatin as multimodal anticancer agents. *Angew. Chem., Int. Ed.* **2014**, *53*, 6752–6756.
- (9) Awuah, S. G.; Zheng, Y. R.; Bruno, P. M.; Hemann, M. T.; Lippard, S. J. A Pt(IV) pro-drug preferentially targets indoleamine-2,3-dioxygenase, providing enhanced ovarian cancer immune-chemotherapy. *J. Am. Chem. Soc.* **2015**, *137*, 14854–14857.
- (10) Wang, N.; Wang, Z.; Xu, Z.; Chen, X.; Zhu, G. A cisplatin-loaded immuno-chemotherapeutic nanohybrid bearing immune checkpoint inhibitors for enhanced cervical cancer therapy. *Angew. Chem., Int. Ed.* **2018**, *57*, 3426–3430.
- (11) Röhrig, U. F.; Majjigapu, S. R.; Vogel, P.; Zoete, V.; Michielin, O. Challenges in the discovery of indoleamine 2,3-dioxygenase 1 (IDO1) inhibitors. *J. Med. Chem.* **2015**, *58*, 9421–9437.
- (12) Uyttenhove, C.; Pilotte, L.; Théta, I.; Stroobant, V.; Colau, D.; Parmentier, N.; Boon, T.; Eynde, B. J. V. Evidence for a tumoral immune resistance mechanism based on tryptophan degradation by indoleamine 2,3-dioxygenase. *Nat. Med.* **2003**, *9*, 1269–1274.
- (13) Munn, D. H.; Mellor, A. L. Indoleamine 2,3-dioxygenase and tumor-induced tolerance. *J. Clin. Invest.* **2007**, *117*, 1147–1154.
- (14) Godin-Ethier, J.; Hanafi, L. A.; Piccirillo, C. A.; Lapointe, R. Indoleamine 2,3-dioxygenase expression in human cancers: clinical and immunologic perspectives. *Clin. Cancer Res.* **2011**, *17*, 6985–6991.
- (15) Yang, S.; Li, X.; Hu, F.; Li, Y.; Yang, Y.; Yan, J.; Kuang, C.; Yang, Q. Discovery of tryptanthrin derivatives as potent inhibitors of indoleamine 2,3-dioxygenase with therapeutic activity in Lewis lung cancer (LLC) tumor-bearing mice. *J. Med. Chem.* **2013**, *56*, 8321–8331.

- (16) Mansfield, A. S.; Heikkilä, P. S.; Vaara, A. T.; von Smitten, K. A. J.; Vakkilä, J. M.; Leidenius, M. H. K. Simultaneous Foxp3 and IDO expression is associated with sentinel lymph node metastases in breast cancer. *BMC Cancer* **2009**, *9*, 231–241.
- (17) Muller, A. J.; DuHadaway, J. B.; Jaller, D.; Curtis, P.; Metz, R.; Prendergast, G. C. Immunotherapeutic suppression of indoleamine 2,3-dioxygenase and tumor growth with ethyl pyruvate. *Cancer Res.* **2010**, *70*, 1845–1853.
- (18) Muller, A. J.; DuHadaway, J. B.; Donover, P. S.; Sutanto-Ward, E.; Prendergast, G. C. Inhibition of indoleamine 2,3-dioxygenase, an immunoregulatory target of the cancer suppression gene Bin1, potentiates cancer chemotherapy. *Nat. Med.* **2005**, *11*, 312–319.
- (19) Yue, E. W.; Douty, B.; Wayland, B.; Bower, M.; Liu, X.; Leffet, L.; Wang, Q.; Bowman, K. J.; Hansbury, M. J.; Liu, C.; Wei, M.; Li, Y.; Wynn, R.; Burn, T. C.; Koblisch, H. K.; Fridman, J. S.; Metcalf, B.; Scherle, P. A.; Combs, A. P. Discovery of potent competitive inhibitors of indoleamine 2,3-dioxygenase with in vivo pharmacodynamic activity and efficacy in a mouse melanoma model. *J. Med. Chem.* **2009**, *52*, 7364–7367.
- (20) Coluccia, A.; Passacantilli, S.; Famiglini, V.; Sabatino, M.; Patsilinas, A.; Ragno, R.; Mazzoccoli, C.; Sisinni, L.; Okuno, A.; Takikawa, O.; Silvestri, R.; Regina, G. L. New inhibitors of indoleamine 2,3-dioxygenase 1: molecular modeling studies, synthesis, and biological evaluation. *J. Med. Chem.* **2016**, *59*, 9760–9773.
- (21) Lin, S. Y.; Yeh, T. K.; Kuo, C. C.; Song, J. S.; Cheng, M. F.; Liao, F. Y.; Chao, M. W.; Huang, H. L.; Chen, Y. L.; Yang, C. Y.; Wu, M. H.; Hsieh, C. L.; Hsiao, W.; Peng, Y. H.; Wu, J. S.; Lin, L. M.; Sun, M.; Chao, Y. S.; Shih, C.; Wu, S. Y.; Pan, S. L.; Hung, M. S.; Ueng, S. H. Phenyl benzenesulfonylhydrazides exhibit selective indoleamine 2,3-dioxygenase inhibition with potent in vivo pharmacodynamic activity and antitumor efficacy. *J. Med. Chem.* **2016**, *59*, 419–430.
- (22) Crosignani, S.; Bingham, P.; Bottemanne, P.; Cannellè, H.; Cauwenberghs, S.; Cordonnier, M.; Dalvie, D.; Deroose, F.; Feng, J. L.; Gomes, B.; Greasley, S.; Kaiser, S. E.; Kraus, M.; Negrerie, M.; Maegley, K.; Miller, N.; Murray, B. W.; Schneider, M.; Solowij, J.; Stewart, A. E.; Tumang, J.; Torti, V. R.; Eynde, B. V. D.; Wythes, M. Discovery of a novel and selective indoleamine 2,3-dioxygenase (IDO-1) inhibitor 3-(5-fluoro-1H-indol-3-yl)pyrrolidine-2,5-dione (EOS200271/PF-06840003) and its characterization as a potential clinical candidate. *J. Med. Chem.* **2017**, *60*, 9617–9629.
- (23) Peng, Y. H.; Ueng, S. H.; Tseng, C. T.; Hung, M. S.; Song, J. S.; Wu, J. S.; Liao, F. Y.; Fan, Y. S.; Wu, M. H.; Hsiao, W. C.; Hsueh, C. C.; Lin, S. Y.; Cheng, C. Y.; Tu, C. H.; Lee, L. C.; Cheng, M. F.; Shia, K. S.; Shih, C.; Wu, S. Y. Important hydrogen bond networks in indoleamine 2,3-dioxygenase 1 (IDO1) inhibitor design revealed by crystal structures of imidazoleisindole derivatives with IDO1. *J. Med. Chem.* **2016**, *59*, 282–293.
- (24) Ravi, R.; Noonan, K. A.; Pham, V.; Bedi, R.; Zhavoronkov, A.; Ozerov, I. V.; Makarev, E.; Artemov, A. V.; Wysocki, P. T.; Mehra, R.; Nimmagadda, S.; Marchionni, L.; Sidransky, D.; Borrello, I. M.; Izumchenko, E.; Bedi, A. Bifunctional immune checkpoint-targeted antibodyligand traps that simultaneously disable TGF $\beta$  enhance the efficacy of cancer immunotherapy. *Nat. Commun.* **2018**, *9*, No. 741.
- (25) Zou, W. Immunosuppressive networks in the tumour environment and their therapeutic relevance. *Nat. Rev. Cancer* **2005**, *5*, 263–274.
- (26) Yu, H.; Kortylewski, M.; Pardoll, D. Crosstalk between cancer and immune cells: role of STAT3 in the tumour microenvironment. *Nat. Rev. Immunol.* **2007**, *7*, 41–51.
- (27) Yu, H.; Lee, H.; Herrmann, A.; Buettner, R.; Jove, R. Revisiting STAT3 signalling in cancer: new and unexpected biological functions. *Nat. Rev. Cancer* **2014**, *14*, 736–746.
- (28) Debnath, B.; Xu, S.; Neamati, N. Small molecule inhibitors of signal transducer and activator of transcription 3 (Stat3) protein. *J. Med. Chem.* **2012**, *55*, 6645–6668.
- (29) Hirano, T.; Ishihara, K.; Hibi, M. Roles of STAT3 in mediating the cell growth, differentiation and survival signals relayed through the IL-6 family of cytokine receptors. *Oncogene* **2000**, *19*, 2548–2556.
- (30) Ma, D. L.; Liu, L. J.; Leung, K. H.; Chen, Y. T.; Zhong, H. J.; Chan, D. S. H.; Wang, H. M. D.; Leung, C. H. Antagonizing STAT3 dimerization with a rhodium(III) complex. *Angew. Chem., Int. Ed.* **2014**, *53*, 9178–9182.
- (31) Kortylewski, M.; Kujawski, M.; Wang, T.; Wei, S.; Zhang, S.; Pilon-Thomas, S.; Niu, G.; Kay, H.; Mulé, J.; Kerr, W. G.; Jove, R.; Pardoll, D.; Yu, H. Inhibiting stat3 signaling in the hematopoietic system elicits multicomponent antitumor immunity. *Nat. Med.* **2005**, *11*, 1314–1321.
- (32) Litzenburger, U. M.; Opitz, C. A.; Sahm, F.; Rauschenbach, K. J.; Trump, S.; Winter, M.; Ott, M.; Ochs, K.; Lutz, C.; Liu, X.; Anastasov, N.; Lehmann, I.; Höfer, T.; Deimling, A.; Wick, W.; Platten, M. Constitutive IDO expression in human cancer is sustained by an autocrine signaling loop involving IL-6, STAT3 and the AHR. *Oncotarget* **2014**, *5*, 1038–1051.
- (33) Fujita, Y.; Yagishita, S.; Hagiwara, K.; Yoshioka, Y.; Kosaka, N.; Takeshita, F.; Fujiwara, T.; Tsuta, K.; Nokihara, H.; Tamura, T.; Asamura, H.; Kawaiishi, M.; Kuwano, K.; Ochiya, T. The clinical relevance of the miR-197/CKS1B/STAT3-mediated PD-L1 network in chemoresistant non-smallcell lung cancer. *Mol. Ther.* **2015**, *23*, 717–727.
- (34) Prati, F.; Bergamini, C.; Molina, M. T.; Falchi, F.; Cavalli, A.; Kaiser, M.; Brun, R.; Fato, R.; Bolognesi, M. L. 2-phenoxy-1,4-naphthoquinones: from a multitarget antitrypanosomal to a potential antitumor profile. *J. Med. Chem.* **2015**, *58*, 6422–6434.
- (35) Jiménez-Alonso, S.; Orellana, H. C.; Estévez-Braun, A.; Ravelo, A. G.; Pérez-Sacau, E.; Machín, F. Design and synthesis of a novel series of pyranonaphthoquinones as topoisomerase II catalytic inhibitors. *J. Med. Chem.* **2008**, *51*, 6761–6772.
- (36) Ge, Y.; Kazi, A.; Marsilio, F.; Luo, Y.; Jain, S.; Brooks, W.; Daniel, K. G.; WGuida, C.; Sebti, S. M.; Lawrence, H. R. Discovery and synthesis of hydronaphthoquinones as novel proteasome inhibitors. *J. Med. Chem.* **2012**, *55*, 1978–1998.
- (37) Kumar, S.; Malachowski, W. P.; DuHadaway, J. B.; LaLonde, J. M.; Carroll, P. J.; Jaller, D.; Metz, R.; Prendergast, G. C.; Muller, A. J. Indoleamine 2,3-dioxygenase is the anticancer target for a novel series of potent naphthoquinone-based inhibitors. *J. Med. Chem.* **2008**, *51*, 1706–1718.
- (38) Wu, J. S.; Lin, S. Y.; Liao, F. Y.; Hsiao, W. C.; Lee, L. C.; Peng, Y. H.; Hsieh, C. L.; Wu, M. H.; Song, J. S.; Yueh, A.; Chen, C. H.; Yeh, S. H.; Liu, C. Y.; Lin, S. Y.; Yeh, T. K.; Hsu, J. T. A.; Shih, C.; Ueng, S. H.; Hung, M. S.; Wu, S. Y. Identification of substituted naphthotriazolidiones as novel tryptophan 2,3-dioxygenase (TDO) inhibitors through structure-based virtual screening. *J. Med. Chem.* **2015**, *58*, 7807–7819.
- (39) Yu, W.; Li, C.; Zhang, W.; Xia, Y.; Li, S.; Lin, J.; Yu, K.; Liu, M.; Yang, L.; Luo, J.; Chen, Y.; Sun, H.; Kong, L. Discovery of an orally selective inhibitor of signal transducer and activator of transcription 3 using advanced multiple ligand simultaneous docking. *J. Med. Chem.* **2017**, *60*, 2718–2731.
- (40) Sandur, S. K.; Pandey, M. K.; Sung, B.; Aggarwal, B. B. 5-hydroxy-2-methyl-1,4-naphthoquinone, a vitamin K3 analogue, suppresses STAT3 activation pathway through induction of protein tyrosine phosphatase, SHP-1: potential role in chemosensitization. *Mol. Cancer Res.* **2010**, *8*, 107–118.
- (41) Tojo, S.; Kohno, T.; Tanaka, T.; Kamioka, S.; Ota, Y.; Ishii, T.; Kamimoto, K.; Asano, S.; Isobe, Y. Crystal structures and structure–activity relationships of imidazothiazole derivatives as IDO1 inhibitors. *ACS Med. Chem. Lett.* **2014**, *5*, 1119–1123.
- (42) Al-Hazimi, H. M.; El-Faham, A.; Ghazzali, M.; Al-Farhan, K. Microwave irradiation: a facile, scalable and convenient method for synthesis of N-phthaloylamino acids. *Arab. J. Chem.* **2012**, *5*, 285–289.
- (43) Cheng, M. F.; Hung, M. S.; Song, J. S.; Lin, S. Y.; Liao, F. Y.; Wu, M. H.; Hsiao, W.; Hsieh, C. L.; Wu, J. S.; Chao, Y. S.; Shih, C.; Wu, S. Y.; Ueng, S. H. Discovery and structure-activity relationships of phenyl benzenesulfonylhydrazides as novel indoleamine 2,3-dioxygenase inhibitors. *Bioorg. Med. Chem. Lett.* **2014**, *24*, 3403–3406.

- (44) Liao, R. Z.; Thiel, W. Why is the oxidation state of iron crucial for the activity of heme dependent aldoxime dehydratase? A QM/MM study. *J. Phys. Chem. B* **2012**, *116*, 9396–9408.
- (45) Yue, E. W.; Sparks, R.; Polam, P.; Modi, D.; Douty, B.; Wayland, B.; Glass, B.; Takvorian, A.; Glenn, J.; Zhu, W.; Bower, M.; Liu, X.; Leffert, L.; Wang, Q.; Bowman, K. J.; Hansbury, M. J.; Wei, M.; Li, Y.; Wynn, R.; Burn, T. C.; Koblisch, H. K.; Fridman, J. S.; Emm, T.; Scherle, P. A.; Metcalf, B.; Combs, A. P. INCB24360 (Epacadostat), a highly potent and selective indoleamine-2,3-dioxygenase 1 (IDO1) inhibitor for immuno-oncology. *ACS Med. Chem. Lett.* **2017**, *8*, 486–491.
- (46) Röhrig, U. F.; Majjigapu, S. R.; Grosdidier, A.; Bron, S.; Stroobant, V.; Pilotte, L.; Colau, D.; Vogel, P.; Van den Eynde, B. J.; Zoete, V.; Michielin, O. Rational design of 4-aryl-1,2,3-triazoles for indoleamine 2,3-dioxygenase 1 inhibition. *J. Med. Chem.* **2012**, *55*, 5270–5290.
- (47) Schenkman, J. B.; Sligar, S. G.; Cinti, D. L. Substrate interaction with cytochrome P-450. *Pharmacol. Ther.* **1981**, *12*, 43–71.
- (48) Powell, J.; Mota, F.; Steadman, D.; Soudy, C.; Miyauchi, J. T.; Crosby, S.; Jarvis, A.; Reisinger, T.; Winfield, N.; Evans, G.; Finniear, A.; Yelland, T.; Chou, Y. T.; Chan, A. W. E.; Leary, A. O.; Cheng, L.; Liu, D.; Fotinou, C.; Milagre, C.; Martin, J. F.; Jia, H.; Frankel, P.; Djordjevic, S.; Tsirka, S. E.; Zachary, I. C.; Selwood, D. L. Small molecule neuropilin-1 antagonists combine antiangiogenic and antitumor activity with immune modulation through reduction of transforming growth factor beta (TGF $\beta$ ) production in regulatory T-cells. *J. Med. Chem.* **2018**, *61*, 4135–4154.
- (49) Munn, D. H.; Sharma, M. D.; Hou, D.; et al. Expression of indoleamine 2,3-dioxygenase by plasmacytoid dendritic cells in tumor-draining lymph nodes. *J. Clin. Invest.* **2004**, *114*, 280–290.
- (50) Lamson, D. W.; Plaza, S. M. The anticancer effects of vitamin K. *Altern. Med. Rev.* **2003**, *8*, 303–318.
- (51) Galluzzi, L.; Senovilla, L.; Zitvogel, L.; Kroemer, G. The secret ally: immunostimulation by anticancer drugs. *Nat. Rev. Drug Discovery* **2012**, *11*, 215–233.
- (52) Bracci, L.; Schiavoni, G.; Sistigu, A.; Belardelli, F. Immune-based mechanisms of cytotoxic chemotherapy: implications for the design of novel and rationale-based combined treatments against cancer. *Cell Death Differ.* **2014**, *21*, 15–25.
- (53) Flick, H. E.; LaLonde, J. M.; Malachowski, W. P.; Muller, A. J. The tumor-selective cytotoxic agent  $\beta$ -lapachone is a potent inhibitor of IDO1. *Int. J. Tryptophan Res.* **2013**, *6*, 35–45.
- (54) Bridewell, D. J. A.; Sperry, J.; Smith, J. R.; Kosim-Satyaputra, P.; Ching, L. M.; Jamie, J. F.; Brimble, M. A. Natural product-inspired pyranonaphthoquinone inhibitors of indoleamine 2,3-dioxygenase-1 (IDO-1). *Aust. J. Chem.* **2013**, *66*, 40–49.
- (55) Sperry, J.; Lorenzo-Castrillejo, I.; Brimble, M. A.; Machín, F. Pyranonaphthoquinone derivatives of eleutherin, ventiloquinone L, thysanone and nanaomycin A possessing a diverse topoisomerase II inhibition and cytotoxicity spectrum. *Bioorg. Med. Chem.* **2009**, *17*, 7131–7137.
- (56) Yu, W.; Xiao, H.; Lin, J.; Li, C. Discovery of novel STAT3 small molecule inhibitors via in silico site directed fragment-based drug design. *J. Med. Chem.* **2013**, *56*, 4402–4412.
- (57) Yu, H.; Pardoll, D.; Jove, R. STATs in cancer inflammation and immunity: a leading role for STAT3. *Nat. Rev. Cancer* **2009**, *9*, 798–809.
- (58) Hossain, D. M. S.; Santos, C. D.; Zhang, Q.; Kozłowska, A.; Liu, H.; Gao, C.; Moreira, D.; Swiderski, P.; Jozwiak, A.; Kline, J.; Forman, S.; Bhatia, R.; Kuo, Y. H.; Kortylewski, M. Leukemia cell-targeted STAT3 silencing and TLR9 triggering generate systemic antitumor immunity. *Blood* **2014**, *123*, 15–25.
- (59) Nair, V. S.; Toor, S. M.; Ali, B. R.; Elkord, E. Dual inhibition of STAT1 and STAT3 activation downregulates expression of PD-L1 in human breast cancer cells. *Expert Opin. Ther. Targets* **2018**, *22*, 547–557.
- (60) He, G.; Yu, G. Y.; Temkin, V.; Ogata, H.; Kuntzen, C.; Sakurai, T.; Sieghart, W.; Peck-Radosavljevic, M.; Leffert, H. L.; Karin, M. Hepatocyte IKK $\beta$ /NF- $\kappa$ B inhibits tumor promotion and progression by preventing oxidative stress-driven STAT3 activation. *Cancer Cell* **2010**, *17*, 286–297.
- (61) Lin, L.; Liu, A.; Peng, Z.; Lin, H.-J.; Li, P.-K.; Li, C.; Lin, J. STAT3 is necessary for proliferation and survival in colon cancer-initiating cells. *Cancer Res.* **2011**, *71*, 7226–7237.
- (62) Rosen, D. G.; Mercado-Urbe, I.; Yang, G.; Bast, R. C., Jr.; Amin, H. M.; Lai, R.; Liu, J. The role of constitutively active signal transducer and activator of transcription 3 in ovarian tumorigenesis and prognosis. *Cancer* **2006**, *107*, 2730–2740.
- (63) Zhang, X.; Yue, P.; Fletcher, S.; Zhao, W.; Gunning, P. T.; Turkson, J. A novel small-molecule disrupts stat3 SH2 domain-phosphotyrosine interactions and stat3-dependent tumor processes. *Biochem. Pharmacol.* **2010**, *79*, 1398–1409.
- (64) Zhao, W.; Jaganathan, S.; Turkson, J. A cell-permeable STAT3 SH2 domain mimetic inhibits STAT3 activation and induces antitumor cell effects in vitro. *J. Biol. Chem.* **2010**, *285*, 35855–35865.